



Asphalt Research Consortium

Quarterly Technical Progress Report July 1-September 30, 2011

October 2011

Prepared for
Federal Highway Administration
Contract No. DTFH61-07-H-00009

By
Western Research Institute
Texas A&M University
University of Wisconsin-Madison
University of Nevada-Reno
Advanced Asphalt Technologies

www.westernresearch.org
www.ARC.unr.edu

TABLE OF CONTENTS

INTRODUCTION	1
GENERAL CONSORTIUM ACTIVITIES	3
PROGRAM AREA: MOISTURE DAMAGE.....	5
Category M1: Adhesion.....	5
Category M2: Cohesion.....	11
Category M3: Aggregate Surface	17
Category M4: Modeling.....	17
Category M5: Moisture Damage Prediction System	19
Table of Decision Points and Deliverables for Moisture Damage	20
Gantt Charts for Moisture Damage.....	23
PROGRAM AREA: FATIGUE.....	25
Category F1: Material and Mixture Properties	25
Category F2: Test Method Development.....	42
Category F3: Modeling.....	53
Table of Decision Points and Deliverables for Fatigue	65
Gantt Charts for Fatigue.....	69
PROGRAM AREA: ENGINEERED MATERIALS.....	71
Category E1: Modeling.....	71
Category E2: Design Guidance.....	100
Table of Decision Points and Deliverables for Engineered Materials	116
Gantt Charts for Engineered Materials	121
PROGRAM AREA: VEHICLE-PAVEMENT INTERACTION.....	123
Category VP1: Workshop.....	123
Category VP2: Design Guidance.....	123
Category VP3: Modeling.....	124
Table of Decision Points and Deliverables for Vehicle-Pavement Interaction	127
Gantt Charts for Vehicle-Pavement Interaction.....	128
PROGRAM AREA: VALIDATION.....	131
Category V1: Field Validation.....	131
Category V2: Accelerated Pavement Testing.....	132
Category V3: R&D Validation	133
Table of Decision Points and Deliverables for Validation	147
Gantt Charts for Validation.....	149

TABLE OF CONTENTS (continued)

PROGRAM AREA: TECHNOLOGY DEVELOPMENT	151
PROGRAM AREA: TECHNOLOGY TRANSFER	157
Category TT1: Outreach and Databases	157
Table of Decision Points and Deliverables for Technology Transfer.....	172
Gantt Charts for Technology Transfer	173

INTRODUCTION

This document is the Quarterly Report for the period of July 1 to September 30, 2011 for the Federal Highway Administration (FHWA) Contract DTFH61-07-H-00009, the Asphalt Research Consortium (ARC). The Consortium is coordinated by Western Research Institute with partners Texas A&M University, the University of Wisconsin-Madison, the University of Nevada Reno, and Advanced Asphalt Technologies.

The Quarterly Report is grouped into seven areas, Moisture Damage, Fatigue, Engineered Paving Materials, Vehicle-Pavement Interaction, Validation, Technology Development, and Technology Transfer. The format of the report is based upon the Research Work Plan that is grouped by Work Element and Subtask. At this point in the project, much of the planned work is completed or near completion, therefore, many of the Subtasks and some Work Elements have coalesced into a larger product (as planned) and current activity is reported there.

This Quarterly Report summarizes the work accomplishments, data, and analysis for the various Work Elements and Subtasks. This report is being presented in a summary form. The Quarter of July 1 to September 30, 2011 is second quarter of the Year 5 contract year. Reviewers may want to reference the previous Annual Work Plans and many other documents that are posted on the ARC website, www.ARC.unr.edu. The more detailed information about the research such as approaches to test method development, data collection, and analyses will be reported in research publications as part of the deliverables. This quarterly report contains updates to the Table of Deliverables that was presented in the Year 5 Work Plan.

SUPPORT OF FHWA AND DOT STRATEGIC GOALS

The Asphalt Research Consortium research is responsive to the needs of asphalt engineers and technologists, state DOT's, and supports the FHWA Strategic Goals and the Asphalt Pavement Road Map. More specifically, the research reported here supports the Strategic Goals of safety, mobility, and environmental stewardship. By addressing the causes of pavement failure and thus determining methods to improve asphalt pavement durability and longevity, this research will provide the motoring public with increased safety and mobility. The research directed at improved use of recycled asphalt pavement (RAP), warm mix asphalt, and cold mix asphalt supports the Strategic Goal of environmental stewardship.

GENERAL CONSORTIUM ACTIVITIES

PROGRESS THIS QUARTER

Several ARC members attended and made presentations at the 48th Petersen Asphalt Research Conference and the 2011 Pavement Performance Prediction Symposium in Laramie, Wyoming on July 11 – 15, 2011.

ARC members attended and made presentations at the Binder, Mix & Construction, and Fundamental Properties & Advanced Models ETG meetings in Fall River, Massachusetts during the week of September 19 – 23, 2011. A considerable part of the Fundamental Properties and Advanced Models ETG was for review of the ARC project extension work plan review.

WORK PLANNED FOR NEXT QUARTER

Several ARC members have planned to attend and make presentations at the 2nd Warm-Mix Asphalt Conference in St. Louis, Missouri during the week of October 10, 2011.

ARC members are planning to meet with FHWA personnel on November 9 and 10, 2011 to discuss the ARC 21-Month Extension Work Plan.

PROGRAM AREA: MOISTURE DAMAGE

CATEGORY M1: ADHESION

Work Element M1a: Affinity of Asphalt to Aggregate (UWM)

Work Done This Quarter

In this quarter, the research group focused its efforts in evaluating the interference of the asphalt binder stiffness ($|G^*|$) in the Bitumen Bond Strength (BBS) test results. Testing in the Dynamic Shear Rheometer (DSR) was conducted at three temperatures to determine the iso-stiffness testing temperature of eight binders. This iso-stiffness temperature was then used to perform the BBS test. Results indicate that bond strength of asphalt-aggregate systems is highly dependent on stiffness of the asphalt binder. Pull off Strength results are found to be significantly affected by binder's stiffness and, therefore, temperature needs to be controlled during the BBS test. A single linear model is proposed for correction of bond strength when testing at a single temperature and different stiffness conditions.

Significant Results

Testing in the DSR was conducted at three temperatures: 20, 25 and 30°C. These temperatures are thought to encompass the typical range of ambient temperatures in the laboratory. At each temperature, an oscillatory strain of 1% was applied at 1.59 Hz frequency (10 rad/sec) to obtain a measure of complex modulus $|G^*|$ within the linear viscoelastic range of the asphalt binder. The range in moduli measured is an indicator of the possible range of stiffness experienced when conducting the BBS at ambient room temperature.

The iso-testing temperature of eight asphalt binders was determined by interpolating between the three DSR test temperatures to calculate the temperature at which the $|G^*|$ is equal to 1 MPa (figure M1a.1).

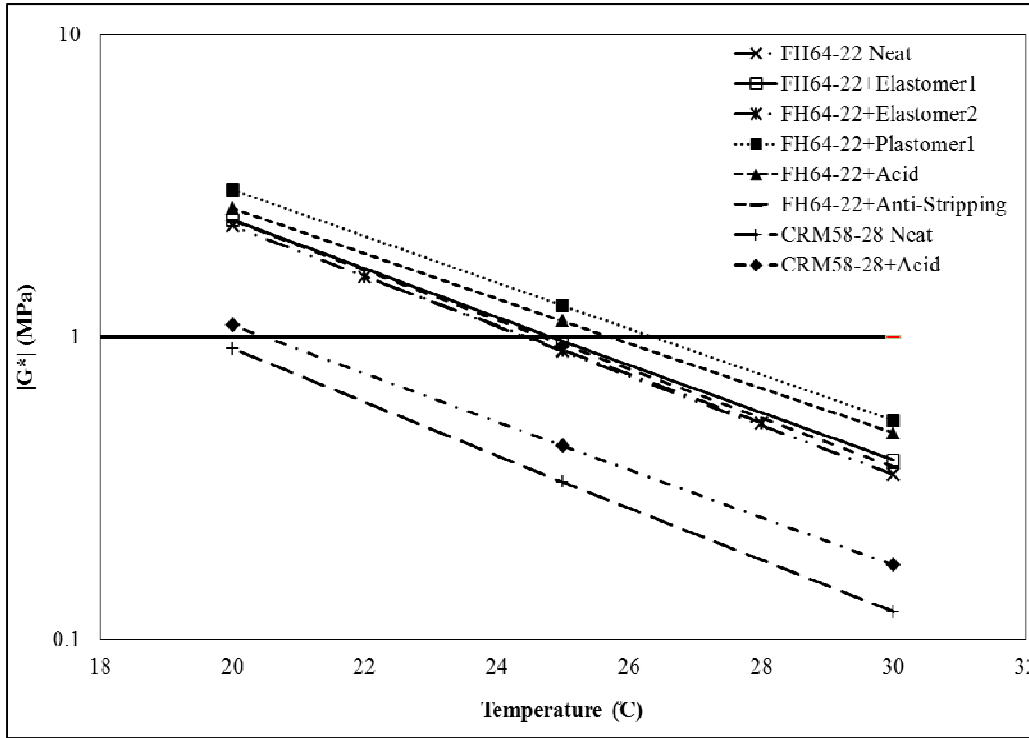


Figure M1a.1. Graph. Determination of the iso-stiffness temperature for each asphalt binder (temperature at which the $|G^*|$ is equal to 1 MPa).

Table M1a.1 shows the determined iso-stiffness temperature of the selected asphalt binders.

Table M1a.1. Asphalt binders iso-stiffness temperature.

Sample	Iso-Stiffness Temperature (°C)
FH64-22 Neat	24.5
FH64-22+Elastomer1	24.9
FH64-22+Elastomer2	24.5
FH64-22+Plastomer1	26.4
FH64-22+Anti-Stripping	24.7
FH64-22+Acid	25.7
CRM58-28 Neat	19.5
CRM58-28+Acid	20.5

For each binder, the BBS test was performed after dry and wet conditioning (i.e., 96 hours of moisture) at the iso-stiffness temperature. During the BBS test, the temperature was controlled in a water bath as shown in figure M1a.2. Table M1a.2 presents the BBS and DSR results.



Figure M1a.2. Photograph. BBS test with controlled temperature.

Table M1a.2. BBS and DSR results at 25°C and at iso-stiffness temperature.

Sample	Dry Conditioning - 24h		Wet Conditioning - 96h		G*	
	POTS at 25°C (MPa)	POTS at Iso-stiffness Temp. (MPa)	POTS at 25°C (MPa)	POTS at Iso-stiffness Temp. (MPa)	G* at 25°C (MPa)	G* at Iso-stiffness Temp. (MPa)
FH64-22 Neat	2.01	2.33	1.47	1.60	0.897	1
FH64-22+Elastomer1	2.36	2.51	1.36	2.27	0.967	1
FH64-22+Elastomer2	2.15	2.69	1.94	1.84	0.906	1
FH64-22+Plastomer1	2.34	2.11	1.88	1.57	1.271	1
FH64-22+Anti-Stripping	2.32	2.32	1.96	1.86	0.945	1
FH64-22+Acid	2.36	2.47	2.01	1.91	1.127	1
CRM58-28 Neat	1.51	2.33	1.37	1.85	0.332	1
CRM58-28+Acid	1.73	2.29	1.43	1.94	0.438	1

It is assumed that the effects of moisture on the asphalt binder stiffness are negligible compared to the accuracy of the parameters measured in this test method. This assumption is based on extensive testing of asphalt binders in the DSR stored under water for more than 7 hours. Thus, binder stiffness is assumed to be independent of moisture conditioning. On the other hand, the significant effect of moisture conditioning on adhesive strength as measured by the BBS is well recognized.

Figure M1a.3 shows the relation between the change in pull-off tensile strength defined as $\Delta POTS = POTS_{Iso-Temp} - POTS_{25^{\circ}C}$, and the change in bitumen stiffness defined as $\Delta G^* = |G^*|_{Iso-Temp} - |G^*|_{25^{\circ}C}$, after dry conditioning. Figure M1a.4 presents same relation after wet conditioning. Note that the BBS results used for the comparison after wet conditioning correspond to asphalt binders that experienced failure through the cohesive mode only.

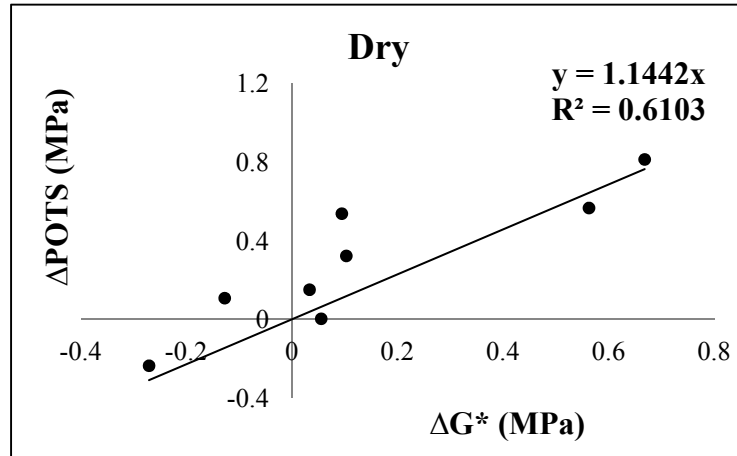


Figure M1a.3. Graph. Correlation between change in pull-off tensile strength ($\Delta POTS$) and change in asphalt binder stiffness (ΔG^*) at dry conditioning.

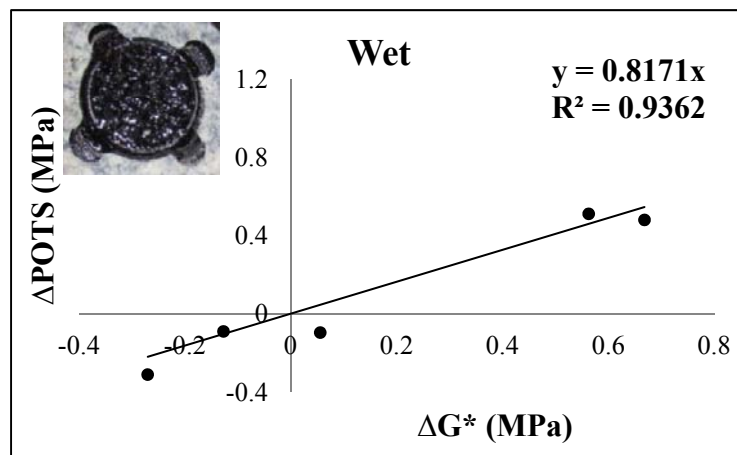


Figure M1a.4. Graph. Correlation between change in pull off tensile strength ($\Delta POTS$) and change in asphalt binder stiffness (ΔG^*) after wet conditioning (for cohesive failures only).

As can be seen, asphalt binder stiffness has a considerable influence on the value of pull-off tensile strength (POTS). Therefore, the BBS test should be conducted in a temperature controlled environment, and at a temperature that reflects field conditions, rather than at ambient room temperature. On the other hand, if one is strictly comparing the moisture sensitivity of different asphalt binders, it is necessary to test at an iso-stiffness condition to eliminate the effect of stiffness variation on POTS. Once the representative temperature for the project is determined, either testing at the selected temperature is conducted or the following equations can be used to adjust the POTS values. Since the change in G^* is required for these equations, the DSR measurements needs to be known.

$$\Delta POTS = 1.14 \Delta G^* \quad (M1a.1)$$

$$\Delta POTS = 0.82 \Delta G^* \quad (M1a.2)$$

where, $\Delta POTS = POTS_{Iso-Temp} - POTS_{Temp}$, and $\Delta G^* = |G^*|_{Iso-Temp} - |G^*|_{Temp}$

Work Planned Next Quarter

The research team will use TSR testing results available from other ARC work elements to continue the validation effort of the BBS test procedure. The research team will work in collaboration with consortium partners to include information related to the development and implementation of the Bitumen Bond Strength (BBS) test as a chapter in a consolidated report for moisture damage work element.

Papers Submitted/Accepted in the Last Quarter

Moraes, R., R. Velasquez, and H. Bahia, *Using Bond Strength and Surface Energy to Estimate Moisture Resistance of Asphalt-Aggregate Systems*. Full paper submitted to AAPT 2012 Annual Meeting and Technical Sessions, Austin, Texas, April 1 - 4, 2012.

Moraes, R., R. Velasquez, and H. Bahia, *The Effect of Bitumen Stiffness on the Adhesive Strength Measured by the Bitumen Bond Strength Test*. Full paper submitted to 5th Eurasphalt and Eurobitume Congress, Istanbul, Turkey, 13th to 15th June, 2012.

Moraes, R., R. Velasquez, and H. Bahia, *Selección de Materiales para Mezclas Asfálticas Resistentes al Daño por Humedad Utilizando el Método de La Gota Sésil*. Paper accepted for XVI CILA – Congresso Ibero-Latino Americano do Asfalto, Rio de Janeiro, Brazil, November 20th - 25th, 2011.

Moraes, R., A. Hanz, G. Andreoni, and H. Bahia, *Verification of Warm Mix Asphalt (WMA) Moisture Susceptibility Using the Bitumen Bond Strength Test (BBS)*. Abstract submitted to ISAP 2nd International Symposium on Asphalt Pavements & Environment, Fortaleza, Brazil, October 1st – 3rd, 2012.

Work Element M1b: Work of Adhesion Based on Surface Energy

Subtask M1b-1: Surface Free Energy and Micro-Calorimeter Based Measurements for Work of Adhesion (TAMU)

Work Done This Quarter

The main goal of this subtask is to provide material property inputs required in other work elements as required. Any data obtained from this subtask will be included in the material properties database. In the last quarter surface free energy of some aggregates and asphalt binders that are being used to develop test methods were measured.

Significant Results

None.

Significant Problems, Issues and Potential Impact on Progress

None.

Work Planned Next Quarter

Work on this subtask will be conducted in conjunction with and as required by other work elements.

Subtask M1b-2: Work of Adhesion at Nano-Scale using AFM (WRI)

Work Done This Quarter

Work reported under subtask M2a-2 (Work of Cohesion) is also directly relevant to this subtask.

Significant Results

See subtask M2a-2.

Subtask M1b-3: Identify Mechanisms of Competition Between Water and Organic Molecules for Aggregate Surface (TAMU)

Work Done This Quarter

This work element was completed and findings were reported in previous quarterly reports. There was no activity this quarter.

Work Planned Next Quarter

None.

Work Element M1c: Quantifying Moisture Damage Using DMA (TAMU)

Work Done This Quarter

This work element was completed and findings were reported in previous quarterly reports. There was no activity this quarter.

Work Planned Next Quarter

None.

CATEGORY M2: COHESION

Work Element M2a: Work of Cohesion Based on Surface Energy

Subtask M2a-1: Methods to Determine Surface Free Energy of Saturated Asphalt Binders (TAMU)

Note about Subtask M2a-1: Per the Year 5 work plan, the objectives of this subtask will be accomplished in other tasks.

Subtask M2a-2: Work of Cohesion Measured at Nano-Scale using AFM (WRI)

Work Done This Quarter

Work conducted this quarter was primarily directed toward beginning to apply the AFM-based nano-mechanical measurement techniques that have been developed over preceding quarters to adhesion measurements on actual aggregate surfaces. Preliminary experiments conducted on model surfaces to evaluate the “adhesive microprobe” technique developed for micro-scale measurements on aggregate surfaces indicate good repeatability and precision for this new method. Pull-off force profiles generated using the technique indicate good sensitivity in discriminating between model low and high energy surfaces. A simple technique to prepare small-scale aggregate samples suitable for mounting on the AFM stage was also demonstrated this quarter.

Quantitative interpretation of conventional nano/micro-scale pull-off-force type measurements, particularly on soft sticky surfaces, is complicated due to difficulties associated with accurately defining the contact area between the probe and the substrate. Understanding this contact has been the subject of a great deal of research ultimately leading to a series of contact models and associated modifying parameters that can be used, provided that some assumptions are accepted and that all of the necessary inputs can actually be measured, to predict the contact area (e.g., Xu et al. 2007) for a variety of adhesive/substrate systems. An adhesive microprobe technique in which the contact is defined in terms of a constant film thickness, constant probe diameter, and constant applied contact loading force, instead of the contact area, has been developed to facilitate adhesion measurements on aggregate surfaces.

The adhesive microprobe technique uses a 10- μm diameter glass bead as the probe tip and AFM feedback electronics to apply a constant loading pressure. For a typical measurement, the tip is first pressed onto a thin film of the test asphalt with a controlled force, held in contact for a few seconds, and then withdrawn. This process leaves a coating of asphalt on the glass bead tip, and a large number of repeated measurements indicate the residual film is quite consistent in thickness. The coated tip is then positioned over the test surface (e.g., bare glass, aggregate surfaces, polymer or wax surfaces, etc.) and an adhesive contact is established by pressing the tip onto the surface with a controlled loading force and holding this force for some specified amount of time. The tip is then withdrawn from the surface and the force profile is recorded as the tip is pulled away and ultimately separates from the test surface.

Aggregate samples were prepared for adhesion testing by core drilling small cylinders from precut aggregate slabs using a diamond drill. The resulting samples are approximately 0.2-inches (0.5-cm) in diameter and 0.25-inches (0.64-cm) in height. The small cores were then split laterally by applying pressure to four sharp points around the circumference of the core. The split core exposes a fresh uncontaminated surface with a texture (roughness) that should be a reasonable representation of an actual aggregate surface. The two planar ends of the original cylinder can be polished to various degrees and pull-off from the polished surface can be compared with that from the broken surface to assess the effect of surface roughness on the asphalt/aggregate adhesive bond. The 10- μm probe tip is similar in size to the particles of filler in asphalt mastic. Therefore, measurements with the adhesive microprobe may help to provide some additional insight into the bonding between particles in the asphalt mastic and realistic aggregate surfaces.

Significant Results

Figures M2a-2.1 and M2a-2.2 show the resultant pull-off force profiles for adhesive microprobe tests conducted on glass and plastic surfaces respectively. The tests were conducted at ambient temperature using SHRP core asphalt AAA-1 as the adhesive. Both tests used the same load (2.25- μN), loading rate ($\sim 25\text{-}\mu\text{N/s}$), hold time (10-s), and pull-off rate ($\sim 25\text{-}\mu\text{N/s}$). For each test, the probe was first pressed onto the asphalt surface and pulled off, using the loading/unloading parameters as listed above, before it was pressed onto the test surface. The test clearly distinguishes between these two types of surface with two significantly different pull-off force profiles. Note that less force is required to separate the probe from the plastic surface, also, that this force acts over a much shorter time indicating (as expected) that much less work (work of adhesion) is required to separate the adhesive probe from the plastic surface compared to the glass. For the testing conducted to date we have seen repeatability of the pull-off force on glass to be within $\sim \pm 0.5\%$ of the measured value. This repeatability with respect to the measured pull-off force strongly indicates good repeatability with respect to the contact area established between the probe tip and the glass surface.

Figure M2a-2.3 shows pull-off force profiles for AAA-1 asphalt on the plastic and glass surfaces plotted together on the same chart. Beginning at the left, the horizontal portion of the traces represents the 2.25- μN contact loading. At about 1.48 seconds the probe tip is pulled away from the surface. The near vertical portion of the trace from the plastic surface is due to an anomaly in the feedback electronics. We are trying to resolve this, but in the testing conducted so far this electronic anomaly does not seem to significantly affect the results. Ignoring this first part of the pull-off, it is evident that the two traces lie very much on top of each other. Both systems maintain the initial contact with the tip firmly attached to the surface until, at the point where the pulling force reaches $\sim 3\text{-}\mu\text{N}$, the tip separates from the plastic surface and the force exerted by the cantilever spring quickly returns to zero.

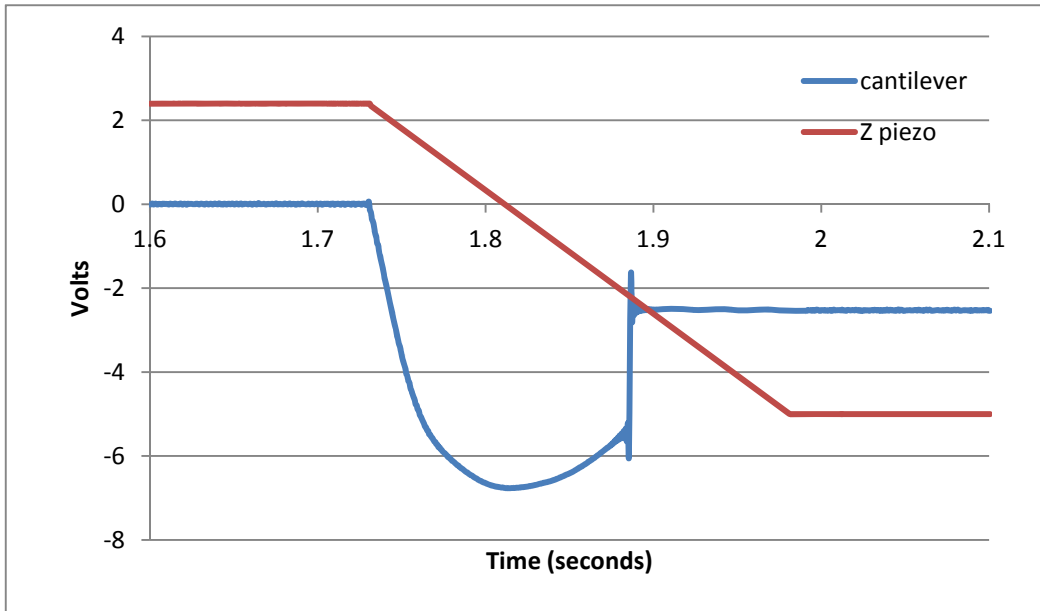


Figure M2a-2.1. Pull-off force profile SHRP core asphalt AAA-1 on glass.

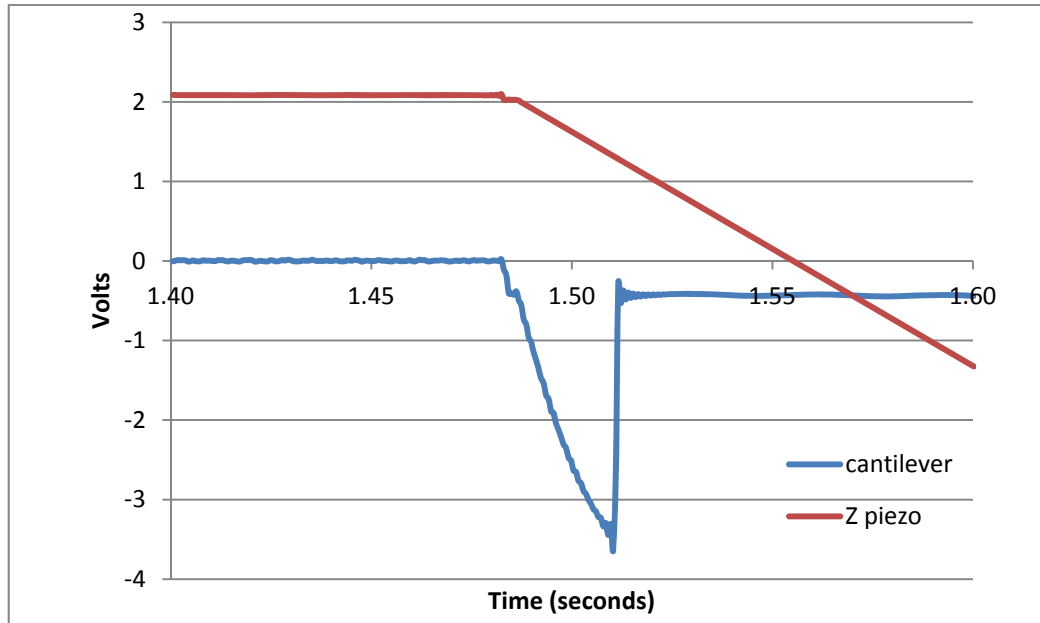


Figure M2a-2.1. Pull-off force profile SHRP core asphalt AAA-1 on plastic.

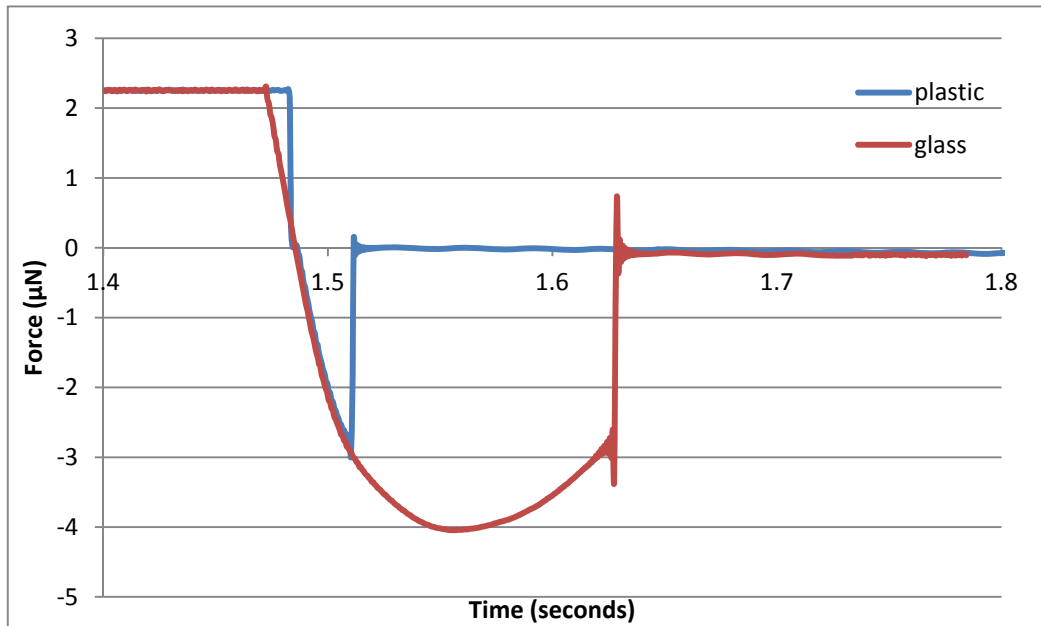


Figure M2a-2.3. Adhesive microprobe pull-off force profiles for glass and plastic surfaces.

The pull-off force profile for the adhesive microprobe on the glass surface exhibits a significantly different behavior. As the pull-off force is increased we see the slope of the force curve begin to change as the tip slowly separates from the surface while forming a “cohesive neck” of diminishing cross-section. As the pull-off force is increased the cross section of the cohesive neck begins to decrease more rapidly until the point where the neck separates and the tip returns to its unloaded position. The maximum force applied before the contact failed was significantly (~33%) greater for the microprobe on glass. However, the force profiles yield a great deal of additional information with respect to the work required to separate the surfaces. If we consider that the work of adhesion is described by the area enclosed by the force lines and the zero-force axis it is quite evident that the difference in work of adhesion for the two systems would be much closer to an order of magnitude than to 33%. Thus, analysis of the pull-off force profile provides for a more sensitive, and we believe more significant, measurement of the work needed to separate (fracture) adhesive/cohesive bonds.

The pull-off force profiles collected for asphalt on both of these surfaces exhibit significant adhesion hysteresis (Perutz et al. 1998). That is, for both systems the force required to separate the contact is greater than the force applied in forming the contact. However, the most significant difference with respect to fracture characteristics of the two systems is the dramatic difference in the area under the respective force curves.

We also note a final point. The force profile for AAA-1 on plastic could be interpreted as representing adhesive failure, whereas the profile for the same asphalt at the same temperature and loading/unloading-rate on glass is more consistent with cohesive failure. Or, we could note that the asphalt/plastic system exhibits essentially brittle behavior (i.e. the contact breaks without significant deformation) while the asphalt/glass system exhibits ductile behavior (i.e. significant

deformation prior to breaking). Or, in terms of strain energy, the asphalt plastic system exhibits lower strain energy compared to the asphalt/glass system. All of these interpretations are consistent with the observation that on the plastic surface when the applied stress exceeded the strength of the contact separation was almost instantaneous with no indication (in the force profile) of significant deformation. On the glass surface the recorded force profile shows a dissipative mechanism associated with deformation of the contact that adsorbs additional energy well past the point where the applied stress exceeded the initial strength of the contact. The asphalt research community seems to focus largely on the concept that oxidative aging appears to lead to embrittlement of the asphalt binder. The results of these preliminary experiments indicate that it is also important to look at embrittlement (and aging) of the asphalt/aggregate matrix as a system with several significant components.

Figure M2a-2.4 shows miniature aggregate cores, of a size to fit on the AFM stage, with a razor blade to show the relative scale. Barely visible in the foreground is a glass slide with a hole bored in the center. The core on the left has been split normal to its axis to obtain an uncontaminated aggregate surface with representative surface texture. An asphalt film will be spin cast in a ring surrounding the hole in the slide. The hole locates the mounting position of the small aggregate cores and the combined pieces provide a convenient arrangement for microprobe testing. This arrangement provides easy access to the three types of surface (asphalt, glass, and aggregate) used for the AFM microprobe technique while maintaining a controlled environment around the test surface.

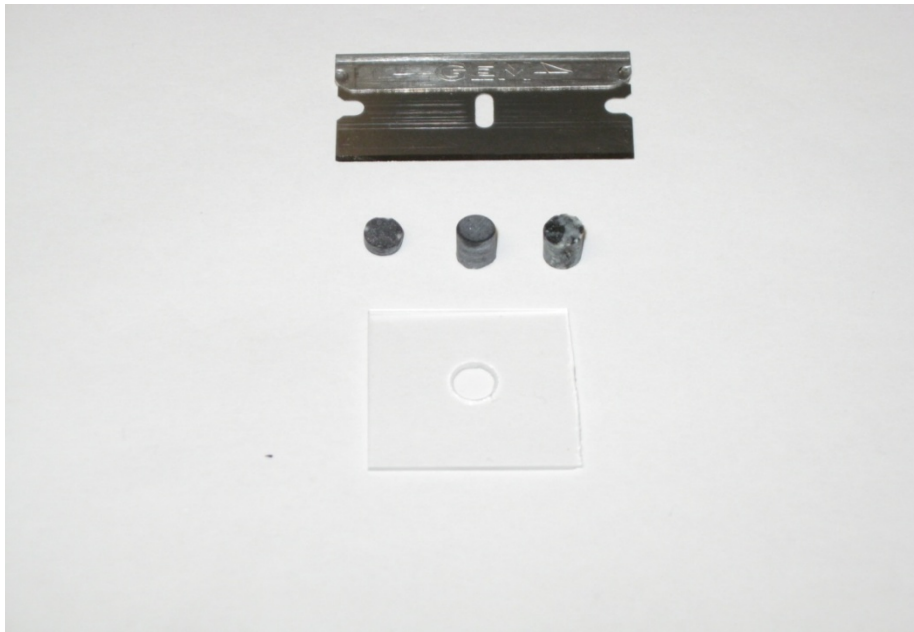


Figure M2a-2.4. Miniature aggregate cores and glass slide prepared for core mounting.

Significant Problems, Issues and Potential Impact on Progress

None.

Work Planned Next Quarter

For the next quarter tests are planned in which the adhesive microprobe technique will be applied to aggregate surfaces. Pull-off force profiles will be collected for asphalt on aggregate surfaces of identical composition but with differing degrees of surface roughness. We will begin a test series that will investigate the effects of variable lengths of bonding time and contact loading/unloading rates.

Cited References

Perutz, S., E.J. Kramer, J. Baney, C.-Y. Hui, and C. Cohen, 1998, Investigation of Adhesion Hysteresis in Poly (dimethylsiloxane) Networks Using the JKR Technique. *Journal of Polymer Science: Part B: Polymer Physics*, 36, 2129-2139.

Xu, Dewei, K.M. Liechti, and K. Ravi-Chandar, 2007, On the modified Tabor parameter for the JKR-DMT transition in the presence of a liquid meniscus. *Journal of Colloid and Interface Science*, 315, 772-785.

Work Element M2b: Impact of Moisture Diffusion in Asphalt Mixtures

Subtask M2b-1: Measurements of Diffusion in Asphalt Binders and Mixtures (TAMU)

Subtask M2b-2: Kinetics of Debonding at the Binder-Aggregate Interface (TAMU)

Work Done This Quarter

There was no activity this quarter.

Work Planned Next Quarter

We have accomplished significant portions of this work element including measurement of diffusion through binders and fine aggregate matrix. Further work will be conducted if prioritized based on the requirements from other work elements.

Work Element M2c: Measuring Thin Film Cohesion and Adhesion Using the PATTI Test and the DSR (UWM)

The remaining activity is reported under Work Element M1a.

CATEGORY M3: AGGREGATE SURFACE

Work Element M3a: Aggregate Surface Characterization (TAMU)

This work element was completed and findings were reported in previous quarterly reports. There was no activity this quarter.

CATEGORY M4: MODELING

Work Element M4a: Micromechanics Model (TAMU)

Subtask M4a-1: Model Development

Work Done This Quarter

In the last quarter, we presented microstructure modeling of asphalt mixtures with moisture damage at the Models Expert Task Group (ETG) meeting held in Fall River, MA. We presented all key components in the modeling efforts including the constitutive theory, modeling methodology, testing protocols developed, resulting test data, and various model simulations for calibration, validation, and application. Model simulation results strongly confirms that our computational microstructure model incorporated with moisture damage has been well developed as a tool to examine the influence of the different physical, mechanical, and geometrical material properties of the asphalt mixture ingredients on the overall moisture-related mechanical performance of asphaltic composites. With the research outcomes, we wrote a journal article and submitted it to the *International Journal for Numerical and Analytical Methods in Geomechanics*. We have also written a final report. The report is currently 85% completed.

Significant Problems, Issues and Potential Impact on Progress

None.

Work Planned Next Quarter

In the next quarter we will finish the final report and submit it to Texas A&M University.

Work Element M4b: Analytical Fatigue Model for Mixture Design (TAMU)

This work element is addressed under Work Element F1b-1 and E1a.

Work Element M4c: Unified Continuum Model (TAMU)

Work Done This Quarter

The work done this quarter concentrated on completing the development of a thermodynamic-based moisture-induced damage model that takes into consideration the effects of the presence and the flow of the moisture. Emphasis is placed on the consideration of the pore-water pressure that accelerates crack evolution and propagation due to presence of moisture. In addition, the flow of moisture washes away the mastic material causing erosion. It is also emphasized to take into account the effect of this erosion damage caused by moisture flow through the asphalt mixtures. Both energetic and dissipative processes are clearly distinguished through this thermodynamic framework. This model is going to be calibrated and validated with the results of ARC 2x2 experimental data which its moisture conditioning protocol and tests types are assigned to be done.

Moreover, three-dimensional (3D) micromechanical moisture-damage simulations have been done. Several simulations on the 3D micromechanical model have been done in order to investigate the effect of moisture conditioning time, moisture content, material properties parameters, strain rate, and temperature at both tension and compression. The results completely show the crack propagation and damage concentration after moisture conditioning the specimens. These simulations can be used to conduct virtual moisture-damage simulation experiments.

Significant Results

None

Significant Problems, Issues and Potential Impact on Progress

The ARC 2x2 experimental data for validating the moisture-induced damage modeling is not available yet.

Work Planned Next Quarter

The next quarter work will be focused on completing the thermodynamic framework that is taking into consideration the different degradation mechanisms due to presence of moisture. This thermodynamic framework is necessary in order to correctly consider the different moisture-induced damage mechanisms and the coupling between them. Moreover, work will continue on conducting three-dimensional micromechanical moisture-damage simulations. Virtual specimens based on the ARC mixtures will be generated using X-ray CT and the finite element method.

CATEGORY M5: MOISTURE DAMAGE PREDICTION SYSTEM (All, TAMU lead)

Work on individual components such as test methods and micromechanics models required in the system is complete. The components will be put together in the form of a methodology towards the end of this project.

TABLE OF DECISION POINTS AND DELIVERABLES FOR MOISTURE DAMAGE

Name of Deliverable	Type of Deliverable	Description of Deliverable	Original Delivery Date	Revised Delivery Date	Reason for changes in delivery date
M1a-5: Propose a novel testing protocol (UWM)	Draft Report	Development and Implementation of the Bitumen Bond Strength test for Moisture Damage Characterization	1/10	8/11 Complete	Additional analysis/verification on the BBS test is included: operator sensitivity data, validation with TSR mixture testing and comparison with contact angle measurements. Report has been consolidated as one chapter and suggested to be included in TAMU report for moisture damage.
	Final Report	Report in 508 format on the use of the Bitumen Bond Strength test for Moisture Damage Characterization	1/11	4/12	First round of revisions by FHWA being implemented. (Report "L")
M1b-2: Work of Adhesion at Nano-Scale using AFM (WRI)	Test Method	A method to determine surface roughness of aggregate and fines based on AFM	12/30/11		N/A
M1b-3: Identify mechanisms of competition between water and organic molecules for aggregate surface (TAMU)	Draft Report	Final report documenting the testing protocol and findings of experiments on asphalt-aggregate interactions	10/31/10	Complete	To be included in the comprehensive report on moisture damage from Texas A&M University.
	Final Report		4/30/12		
M1c: Quantifying Moisture Damage Using DMA (TAMU)	AASHTO procedure	AASHTO procedure for preparing Fine Aggregate Matrix (FAM) specimens for the DMA testing	9/30/10	Complete	N/A
	Draft Report	Use of the method to characterize various mixtures with comparison to field performance	12/31/10	Complete	
	Final Report		3/31/11	6/30/11	Report to be made 508 compliant
M2a-2: Work of Cohesion at Nano-Scale using AFM (WRI)	Test Method	A method to determine ductile-brittle properties via AFM measurements	12/30/11		N/A

Name of Deliverable	Type of Deliverable	Description of Deliverable	Original Delivery Date	Revised Delivery Date	Reason for changes in delivery date
M2b-1: Measurement of diffusion of water through thin films of asphalt binders and FAM (TAMU)	Draft Report	Mechanism and model for the diffusion of moisture through films of asphalt binder, methods to measure diffusivity in binders and mortars, and the influence of wet-dry cycles on the cumulative moisture induced damage.	6/30/10	Complete	The dissertation was completed at TAMU and needs editing for 508 format
	Final Report		9/30/11	12/31/11	
M3a: Aggregate Surface Characteristics (TAMU)	Research report	Report on methods and experimental findings and utility of methodology and findings	6/30/10	Complete	To be included in the comprehensive report on moisture damage from Texas A&M University.
	Research report	Describes implementation of findings into PANDA and expands experiments to characterization for four aggregates used for validation experiments	6/30/11		
M4a: Micro-mechanics Model (TAMU)	Draft Report	Numerical micromechanical model of moisture-induced damage in asphalt mixtures. This report will include the algorithm and modeling method.	Sep-11	Complete	
	Final Report		Sep-11	Mar-12	
M4a: Micromechanics Model Development (Moisture Damage) (UNL)	Models and Algorithm	Cohesive zone modeling with moisture damage of asphalt mixtures considering mixture microstructure: modeling methodology, constitutive theory, testing protocols, test data, model simulation/calibration/validation, and user-friendly manuals.	3/31/11	Complete	Models will be included in final report.
	Draft report		06/30/11	12/11	More time needed to finish extra simulations and documenting final report
	Final report		12/31/11	8/14/12	
M4a: Lattice Micromechanics Model (NCSU)	Draft Report	Documenting development of lattice micromechanical model	2/14/12		N/A
	Final Report	Documenting development of lattice micromechanical model	8/14/12		
M4a: Model to Bridge Continuum Damage and Fracture (NCSU)	Draft Report	Documenting development of continuum damage-to-fracture model	N/A	2/14/12	N/A
	Final Report	Documenting development of continuum damage-to-fracture model	2/14/12	8/14/12	




Name of Deliverable	Type of Deliverable	Description of Deliverable	Original Delivery Date	Revised Delivery Date	Reason for changes in delivery date
M4c: Unified Continuum Model (TAMU)	Models and Algorithm	Algorithm for including moisture damage in the model	6/30/11	12/31/12	Model needs to be updated based on calibration with experimental measurements
	Draft Report	Draft Report on the moisture-damage modeling	9/30/11	12/31/12	
	Final Report (M5, M4c, F1b-1, F1c, F1d-8, F3c, and V3c)	Report in 508 format that describes a comprehensive and integrated approach to assessing moisture damage on three scales; binder and aggregate components, fine aggregate matrix with DMA and in the full mix – Alternative to more sophisticated PANDA approach	03/31/12	3/31/13	Work is progressing in the validation based on ARC experiments.
M5: Moisture Damage Prediction System (All)	Protocol	Protocol for implementation of component selection	6/30/11	Complete	To be included in the comprehensive report on moisture damage from Texas A&M University.
	Experimental method	Experimental method for measuring moisture damage resistance of full mixture	9/30/11	Complete	
	Draft Report (M5, M4c, F1b-1, F1c, F1d-8, F3c, and V3c)	Report in 508 format that describes a comprehensive and integrated approach to assessing moisture damage on three scales; binder and aggregate components, fine aggregate matrix with DMA and in the full mix – Alternative to more sophisticated PANDA approach	12/31/11		
	Final Report (M5, M4c, F1b-1, F1c, F1d-8, F3c, and V3c)		3/31/12	3/31/13	Preparation of a comprehensive report.

Moisture Damage Year 5		Year 5 (4/11-3/12)												Team	Remarks	% Complete	
		4	5	6	7	8	9	10	11	12	1	2	3				
Adhesion																	
M1a	Affinity of Asphalt to Aggregate - Mechanical Tests																
M1a-1	Select Materials															UWM	
M1a-2	Conduct PATTI and modified DSR tests																
M1a-3	Evaluate the moisture damage of asphalt mixtures																
M1a-4	Correlate moisture damage between DSR, PATTI, and mix tests																
M1a-5	Propose a Novel Testing Protocol																
M1a-6	Standard Testing Procedure and Recommendation for Specifications									D					F		
M1b	Work of Adhesion																
M1b-1	Adhesion using Micro calorimeter and SFE															TAMU	
M1b-2	Evaluating adhesion at nano scale using AFM															WRI	
M1b-3	Mechanisms of water-organic molecule competition															TAMU	
M1c	Quantifying Moisture Damage Using DMA															TAMU	
Cohesion																	
M2a	Work of Cohesion Based on Surface Energy																
M2a-1	Methods to determine SFE of saturated binders								JP							TAMU	
M2a-2	Evaluating cohesion at nano scale using AFM															WRI	
M2b	Impact of Moisture Diffusion in Asphalt																
M2b-1	Diffusion of moisture through asphalt/mastic films								F							TAMU	
M2b-2	Kinetics of debonding at binder-aggregate interface																
M2c	Thin Film Rheology and Cohesion																
M2c-1	Evaluate load and deflection measurements using the modified PATTI test															UWM	
M2c-2	Evaluate effectiveness of the modified PATTI test for Detecting Modification																
M2c-3	Conduct Testing																
M2c-4	Analysis & Interpretation																
M2c-5	Standard Testing Procedure and Recommendation for Specifications															see Subtask M1a-6	
Aggregate Surface																	
M3a	Impact of Surface Structure of Aggregate																
M3a-1	Aggregate surface characterization															TAMU	Ongoing effort. Results will be in
Modeling																	
M4a	Micromechanics model development				D			DP				F,SW			JP	TAMU	
M4b	Analytical fatigue model for use during mixture design											M&A, D			F	TAMU	
M4c	Unified continuum model				D			DP				F,SW				TAMU	
M5	Moisture Damage Prediction System															ALL	

LEGEND

Deliverable codes

- D: Draft Report
- F: Final Report
- M&A: Model and algorithm
- SW: Software
- JP: Journal paper
- P: Presentation
- DP: Decision Point
- [x]

-  Work planned
-  Work completed
-  Parallel topic

Deliverable Description




- Report delivered to FHWA for 3 week review period.
- Final report delivered in compliance with FHWA publication standards
- Mathematical model and sample code
- Executable software, code and user manual
- Paper submitted to conference or journal
- Presentation for symposium, conference or other
- Time to make a decision on two parallel paths as to which is most promising to follow through
- Indicates completion of deliverable x

Moisture Damage Year 2 - 5		Year 2 (4/08-3/09)				Year 3 (4/09-3/10)				Year 4 (04/10-03/11)				Year 5 (04/11-03/12)				Team
		Q1	Q2	Q3	Q4	Q1	Q2	Q3	Q4	Q1	Q2	Q3	Q4	Q1	Q2	Q3	Q4	
Adhesion																		
M1a	Affinity of Asphalt to Aggregate - Mechanical Tests																	
M1a-1	Select Materials		DP														UWM	
M1a-2	Conduct PATTI and modified DSR tests		P		P													
M1a-3	Evaluate the moisture damage of asphalt mixtures				DP		P			P	JP		P					
M1a-4	Correlate moisture damage between DSR, PATTI, and mix tests						P			P								
M1a-5	Propose a Novel Testing Protocol				P					P			JP					
M1a-6	Standard Testing Procedure and Recommendation for Specifications											P				D	F	
M1b	Work of Adhesion																	
M1b-1	Adhesion using Micro calorimeter and SFE						JP										TAMU	
M1b-2	Evaluating adhesion at nano scale using AFM							JP									JP, F	
M1b-3	Mechanisms of water-organic molecule competition				JP												TAMU	
M1c	Quantifying Moisture Damage Using DMA											JP	D	F			TAMU	
Cohesion																		
M2a	Work of Cohesion Based on Surface Energy																	
M2a-1	Methods to determine SFE of saturated binders													JP			TAMU	
M2a-2	Evaluating cohesion at nano scale using AFM							JP								JP, F	WRI	
M2b	Impact of Moisture Diffusion in Asphalt																	
M2b-1	Diffusion of moisture through asphalt/mastic films						JP	D	F	D	F				F		TAMU	
M2b-2	Kinetics of debonding at binder-aggregate interface																	
M2c	Thin Film Rheology and Cohesion																	
M2c-1	Evaluate load and deflection measurements using the modified PATTI test	DP	JP	D	F												UWM	
M2c-2	Evaluate effectiveness of the modified PATTI test for Detecting Modification			D	DP,F													
M2c-3	Conduct Testing						JP											
M2c-4	Analysis & Interpretation				P				D									
M2c-5	Standard Testing Procedure and Recommendation for Specifications					D											see Subtask M1a-6	
Aggregate Surface																		
M3a	Impact of Surface Structure of Aggregate																	
M3a-1	Aggregate surface characterization									JP							TAMU	
Models																		
M4a	Micromechanics model development				JP				JP				M&A	D	DP	F, SW	JP	TAMU
M4b	Analytical fatigue model for use during mixture design															M&A,D	F	TAMU
M4c	Unified continuum model								JP				M&A	D	DP	F, SW		TAMU
M5	Moisture Damage Prediction System																	ALL

LEGEND

Deliverable codes

- D: Draft Report
- F: Final Report
- M&A: Model and algorithm
- SW: Software
- JP: Journal paper
- P: Presentation
- DP: Decision Point
- [x]

-  Work planned
-  Work completed
-  Parallel topic

Deliverable Description

- Report delivered to FHWA for 3 week review period.
- Final report delivered in compliance with FHWA publication standards
- Mathematical model and sample code
- Executable software, code and user manual
- Paper submitted to conference or journal
- Presentation for symposium, conference or other
- Time to make a decision on two parallel paths as to which is most promising to follow through
- Indicates completion of deliverable x

PROGRAM AREA: FATIGUE

CATEGORY F1: MATERIAL AND MIXTURE PROPERTIES

Work Element F1a: Cohesive and Adhesive Properties (TAMU)

Work Done This Quarter

This task was completed in the last quarter.

Significant Results

The results demonstrated that a multiplicative relationship exists between the ideal and practical work of fracture. The relationship between these two quantities depends on binder compliance, loading rate, and temperature. This work has validated that the ideal work of fracture, which is calculated from surface energy, is a fundamental property than can be used to rank asphalt-aggregate systems based on their resistance to fracture under dry and wet conditions.

Significant Problems, Issues and Potential Impact on Progress

None

Work Planned Next Quarter

This subtask is completed.

Work Element F1b: Viscoelastic Properties (Year 1 start)

Subtask F1b-1: Viscoelastic Properties under Cyclic Loading (UT and TAMU)

Work Done This Quarter

In the previous quarters, the UT team had investigated the influence of interaction or a combination of shear and normal stresses on the viscoelastic shear properties of the asphalt binder. This effect was modeled and the efficacy of the model was demonstrated using load histories other than the ones used to calibrate the model. Incorporating these effects can significantly improve the accuracy of the computational models currently being employed at different length scales. Two other material properties that are very important in computational models are the bulk modulus and Poisson's ratio. Most models currently assume a time independent Poisson's ratio with typical values ranging from 0.3 to 0.45 for different materials (binders, mastics etc.).

In this quarter we investigated the time dependency of bulk modulus in asphalt binders. The bulk modulus of an asphalt binder was obtained by measuring the change in axial stress, $\sigma_z(t)$, in the poker-chip geometry specimen under step strain load in compression, ε_0 . Solving the boundary value problem, it can be shown that the stress in the poker-chip test changes as a function of bulk modulus and shear modulus:

$$\sigma_z(t) = \left[\frac{4}{3} \mu(t) + K(t) \right] \varepsilon_0 \quad (\text{F1b-1.1})$$

where $K(t)$ is the bulk modulus and $\mu(t)$ is the shear relaxation modulus. Therefore, to obtain the bulk modulus from the poker-chip test, the shear modulus of the asphalt binder was also measured at the same temperature. This was done using a Dynamic Shear Rheometer (DSR) with a cone and plate geometry. Figure F1b-1.1 shows the measured bulk and shear relaxation modulus for asphalt binder PG 76-22 at 28°C. These preliminary test results were obtained by conducting the compression test using the squeeze test procedure in DSR. Although the results clearly showed the change in bulk modulus with time, it did not measure the glassy behavior due to the low rate of loading. To resolve this problem, the poker chip test is being carried out using Instron ElectroPuls E1000 test instrument. This instrument has a linear motor that is capable of applying step loads with a very small raising time.

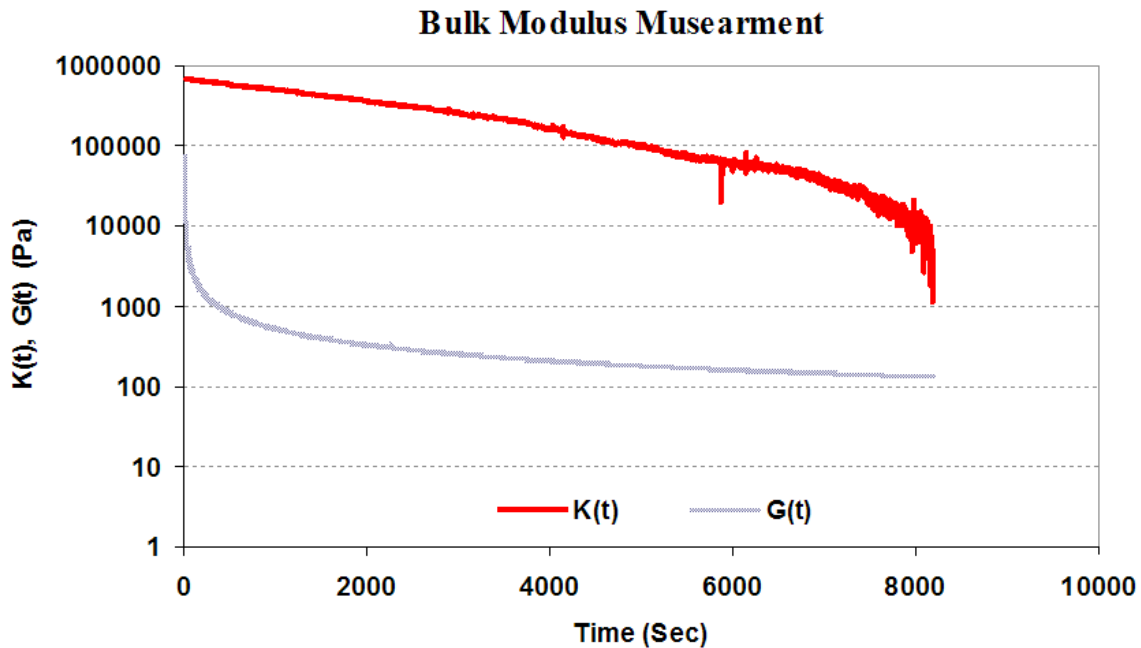


Figure F1b-1.1. Laboratory measurement of the bulk and shear relaxation modulus for asphalt binder PG 76-22, at 28°C.

The aforementioned model allows for a more accurate constitutive model for implementing in a computational framework. In addition, a thermodynamics based nonlinear model was also investigated.

At TAMU, the new nonlinear, viscoelastic model for asphalt binders based on the stress relaxation data that has been developed under this subtask is being validated with the two binders selected for validation of all testing protocols. The model is a purely mechanical model and does not take into account the thermal and aging effect of asphalt binders. Therefore, we fit the model to experimental data developed by Narayan et al. (2011) at each temperature and age condition separately.

Significant Results

The preliminary test results from the UT team show that the bulk modulus of asphalt binders change with time and is not constant. It was also observed that the rate of change in bulk modulus does not follow the rate of change in shear relaxation modulus. Considering the relation between shear and bulk modulus implies that the Poisson's ratio is not constant and changes with time.

$$K = \frac{2\mu(1+\nu)}{3(1-2\nu)}, \quad (\text{F1b-1.2})$$

We expect that this understanding of the bulk response combined with the nonlinear viscoelastic model will significantly improve the accuracy of computational micromechanics models. In addition to validating Schapery's model the thermodynamic model was also validated. The model was found to fit the experimental results quite well. The agreement with the experimental data obtained with this model was much better than those obtained with the models used by Krishnan and Rajagopal (2005) and Narayan et al. (2010) with the error measures of the fits several times smaller.

Since the model captures the response of asphalt binders quite well, we believe it has the potential to distinguish and characterize asphalt binders. However, this model has been evaluated for only one set of experimental data - the stress relaxation data recorded by Narayan et al. (2011). It is necessary to test this model against experimental data from other types of tests such as creep, oscillatory tests, etc. It should also be noted that this model does not capture certain features of the nonlinear viscoelastic behavior of asphalt binders such as shear thickening/ shear thinning behavior, stress overshoots in steady shear flows, etc. However, the model can be extended to include these complexities.

The model can be expressed as:

$$(\{\tau - \eta D\} \cdot \{\tau - \eta D\})^n \{\tau - \eta D\} + \lambda \overset{\nabla}{\tau} = \mu (D \cdot D)^n D + \lambda \eta \overset{\nabla}{D}$$

Where τ is the deviatoric part of the Cauchy stress \mathbf{T} . The torque and the normal force relaxation curves of this model in torsion asymptotically approach straight lines of slope $\frac{1}{2n}$ in the log-log

scale as $t \rightarrow \infty$. Due to the presence of ηD , the model exhibits a jump in stress shear corresponding to a jump in rate of shear in shear flow.

Significant Problems, Issues and Potential Impact on Progress

None.

Work Planned Next Quarter

In the next quarter we plan to continue the tests and analysis related to the measurement of bulk modulus. The poker-chip tests will be conducted with different aspect ratios to find the aspect ratio that eliminates the effect of singular point at the edge of the specimen. The linearity of the response will also be investigated by measuring the bulk modulus at different strain levels.

We will also continue the validation of the thermodynamics based model with the two binders being used for all product validation and add a set of additional polymer modified binders to the validation protocol. These binders will be selected with the help of the University of Wisconsin at Madison.

References

Krishnan, J.M., and K.R. Rajagopal, 2005, On the mechanical behavior of asphalt. *Mechanics of Materials*, 37(11), 1085-1100.

Narayan, S.P.A., K.A. Venkata Nag, J. Murali Krishnan, A. Deshpande, and K.R. Rajagopal. On the transient response of asphalt binders. *Submitted for publication*. 2010.

Subtask F1b-2: Separation of Nonlinear Viscoelastic Deformation from Fracture Energy under Repeated and Monotonic Loading (TAMU)

Work Done This Quarter

The reader is referred to Work Elements F2c and E1a.

Work Planned Next Quarter

The reader is referred to Work Elements F2c and E1a.

Work Element F1c: Aging

Subtask F1c-1: Critical Review of Binder Oxidative Aging and Its Impact on Mixtures (TAMU)

Work Done This Quarter

No work this quarter.

Significant Results

N/A

Significant Problems, Issues and Potential Impact on Progress

There are no problems or issues.

Work Planned Next Quarter

Review of the literature and work on other research projects is ongoing.

Subtask F1c-2: Develop Experimental Design (TAMU)

Work Done This Quarter

No work this quarter.

Significant Results

None.

Significant Problems, Issues and Potential Impact on Progress

The planned experiments using ARC core binders is underway, as well as measurements on mixtures fabricated using other binders.

Work Planned Next Quarter

Measurements of mixture rheology and fatigue continue. Also, rheological measurements of binders extracted and recovered from these mixtures will be made as part of the effort to link binder oxidation to changes in mixture properties.

Subtask F1c-3: Develop a Transport Model of Binder Oxidation in Pavements (TAMU)

Work Done This Quarter

Work on developing a transport model of binder oxidation in pavements continues. The methodology of air void analysis with respect to asphalt oxidation was improved. And a new concept of diffusion depth was proposed to define the oxygen diffusion boundary in mastic for asphalt oxidation in pavement modeling.

Previously, the air voids responsible for asphalt oxidation were considered to be interconnected air voids, voids that connect from the top of a pavement core all the way to the bottom (Prapaitrakul et al. 2009). However, for the surface course, there are a significant number of air void channels that are open only to the top, ending somewhere inside the field core but not connecting to the bottom. These air voids also should be recognized as channels that supply oxygen for asphalt oxidation. These air voids plus the interconnected air voids are termed accessible air voids.

The characterization of accessible air voids depends on the position of the asphalt layer in the pavement structure. When the asphalt layer is the surface course, all air voids channels connecting to the top surface might be considered to be accessible air voids. When the asphalt layer is a rich bottom layer, the situation is more complicated and oxidation depends on the availability of air from the top and/or the bottom of the asphalt layer. Furthermore, the accessibility of air from the horizontal direction is not considered in this methodology.

The diffusion depth from an air void channel into the surrounding binder is another issue and one that we have considered in more detail during this quarter. Diffusion depth is calculated as the volume of asphalt surrounding the accessible air voids by the binder-air interfacial area of these voids. This simple calculation amounts to assuming that binder surrounds the accessible air voids to a uniform depth, a reasonable assumption for the purpose of approximate asphalt oxidation calculations. This calculation also is different from the previous model that characterizes the diffusion distance by an average distance between pores, instead of one that is related to contact area between the air voids and the binder. This assumption also lends itself better to a rectangular Cartesian oxygen transport-reaction model rather than the cylindrical system that was used before. The concept of diffusion depth is similar to the concept of asphalt film thickness, except that the asphalt volume is divided by the air void interfacial surface area instead of the aggregate interfacial area. Because the exposed surface area of asphalt to accessible air voids is much less than aggregate surface area, the magnitude of diffusion depth is usually significantly greater than the conventional film thickness.

The exposed surface area is obtained from the analysis of X-ray CT images of total air voids in the mixture. First, the image processing toolbox in MATLAB is used to identify objects of connected air voids. Parts of these objects are accessible air voids. After accessible air voids in each image are identified, the total perimeter of accessible air voids is obtained. Assuming the same total perimeter for the X-ray CT interval (1 mm), the exposed surface area of binder to accessible air voids in that 1-mm interval is this perimeter times the interval. By applying this procedure to all images, the exposed surface area is obtained for every image.

Figure F1c-3.1 shows the comparison of total perimeter for each image from accessible air voids and from interconnected air voids. In general, the total perimeter of accessible air voids is greater than that of interconnected air voids, because interconnected air voids are a subset of accessible air voids. Furthermore, the main difference resides in the images close to the surface and less difference close to the bottom.

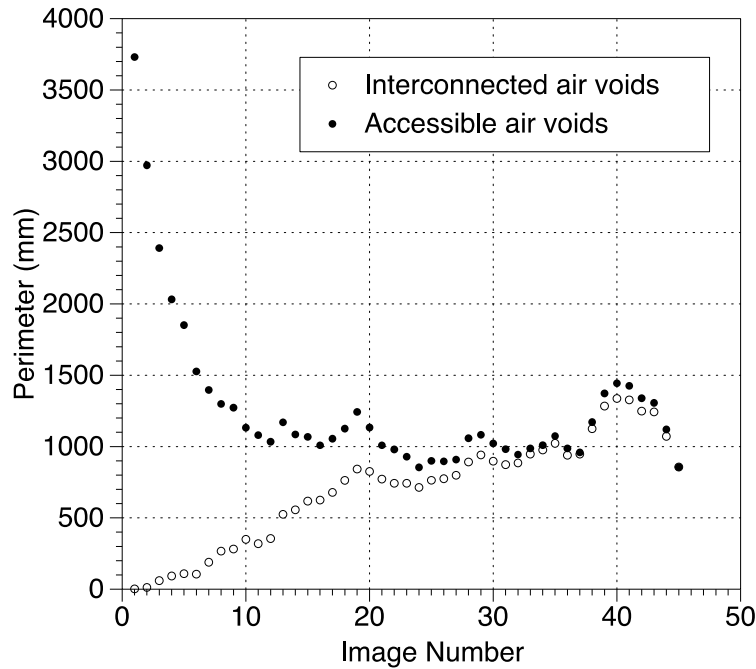


Figure F1c-3.1. Comparison of total perimeters from top image (Image Number 1) to the bottom image (Image Number 45).

Significant Results

N/A

Significant Problems, Issues and Potential Impact on Progress

There are no problems or issues.

Work Planned Next Quarter

Two SHRP asphalts (AAD-1 and AAM-1) are being aged in POV according to the experimental design in the previous work plan. Kinetics data will be obtained and analyzed for model parameters. Results will be reported in the next quarter.

The concept of diffusion depth is being incorporated into the pavement oxidation model for model predictions.

Publications

Han, Rongbin, Jin, Xin., and Glover, C. J., “Modeling Pavement Temperature for Use in Binder Oxidation Models and Pavement Performance Prediction,” *Journal of Materials in Civil Engineering*, 23(4), 351-359 (2011).

Han, R., Jin, X., and Glover, C.J., “Oxygen Diffusivity in Asphalts and Mastics,” *Petroleum Sci. and Technol.*, in press.

Presentations

Han, Rongbin, Yuanchen Cui, Xin Jin, and Charles J. Glover. “A Comprehensive Model of Binder Oxidation in Pavements,” presented at the 48th Annual Petersen Asphalt Research Conference, July 13, 2011.

Yuanchen Cui, Xin Jin, Rongbin Han, and Charles J. Glover. “Introduction to a New, Fast, Binder Aging Test,” presented at the 48th Annual Petersen Asphalt Research Conference, July 13, 2011.

Subtask F1c-4: The Effects of Binder Aging on Mixture Viscoelastic, Fracture, and Permanent Deformation Properties (TAMU)

Work Done This Quarter

The reader is referred to Work Elements F2c and E1a.

Work Planned Next Quarter

The reader is referred to Work Elements F2c and E1a.

Subtask F1c-5: Polymer Modified Asphalt Materials (TAMU)

Work Done This Quarter

No additional work on this subtask was conducted this quarter.

Work Planned Next Quarter

The effort to establish polymer degradation kinetics due to oxidation is being reviewed and appears to be an intractable problem.

Work Element F1d: Healing (TAMU)

Subtask F1d-1: Critical review of the literature

Subtask F1d-2: Material selection

Subtask F1d-3: Experiment design

Subtask F1d-4: Test methods to measure properties related to healing

Subtask F1d-5a: Testing of materials and validating healing model

Subtask F1d-5b: Thermodynamic model for healing in asphalt binders

Work Done This Quarter

In the previous quarters, we reported two test procedures to measure inherent healing in asphalt binders and overall healing in asphalt composites (fine aggregate matrix) using a dynamic shear rheometer (DSR). We also designed and executed a series of verification tests to establish that the healing surface developed as function of rest periods and damage level is unique for a given mix, binder type, binder content, duration of rest period and level of damage preceding the rest period. In this quarter we completed the verification tests and analysis of results from these tests. In particular, we ran several tests by interchanging the mode of load from controlled strain to controlled stress and vice versa, between rest periods in the same test sample. Also in this quarter, we have fine-tuned and improved the robustness of the procedure used to quantify healing. The new procedure to quantify healing now includes the number of cycles in the initial apparent healed portion of fatigue, which were previously neglected.

Currently, we are working on three aspects of related to the healing properties of the FAM:

1. A procedure to back calculate gain in number of load cycles from the percentage drop in S (damage parameter) or percent healed measured earlier is being developed. The translation of healing to gain in number of load cycles for a given test condition will allow the users of this procedure to couple it with the fatigue damage process and assess the impact of healing and cracking on the fatigue cracking life of mixtures.
2. The procedure used with the FAM mixes will be up scaled and applied to full asphalt mixtures or extended to FAM specimens in the tension-compression mode of loading. This task will be coordinated with other research agencies involved with similar testing.
3. A modification of the current procedure is being investigated in order to reduce the number of tests required to generate the healing function. This is done by modifying the test procedure such that multiple measurements of percentage healing at different damage levels and for different rest periods can be made using only one specimen. The objective of this task is to expedite and standardize the procedure for measuring healing characteristics for an asphalt mix

Significant Results

Based on the verification tests done so far we have been successful in demonstrating the healing potential surface to be artifact free and largely dependent on the material and not the test procedure. Also the healing potential functions were developed for the four FAM mixes tested earlier and the functional form were verified using the results from different verification tests.

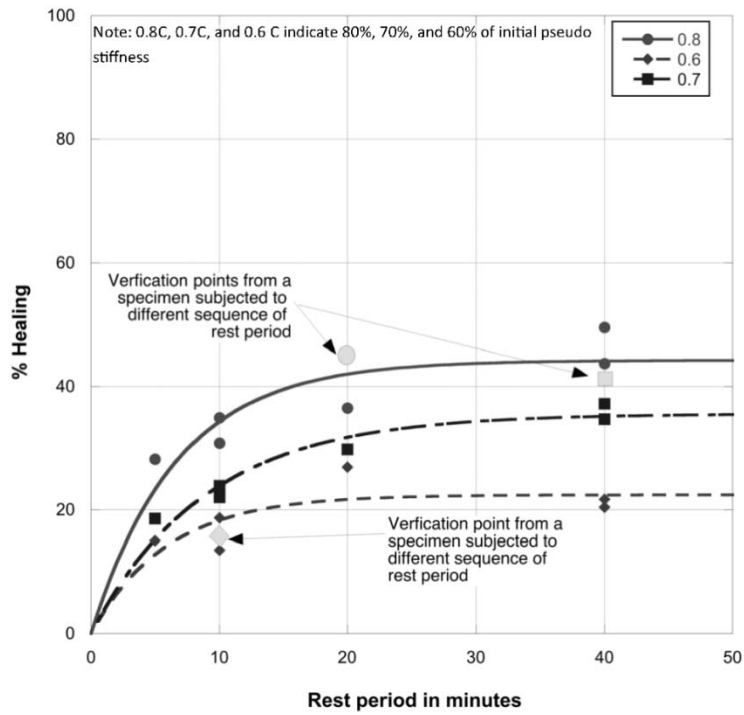


Figure F1d.1. Percentage healing in FAM mix with ARC binder B002 and verification tests.

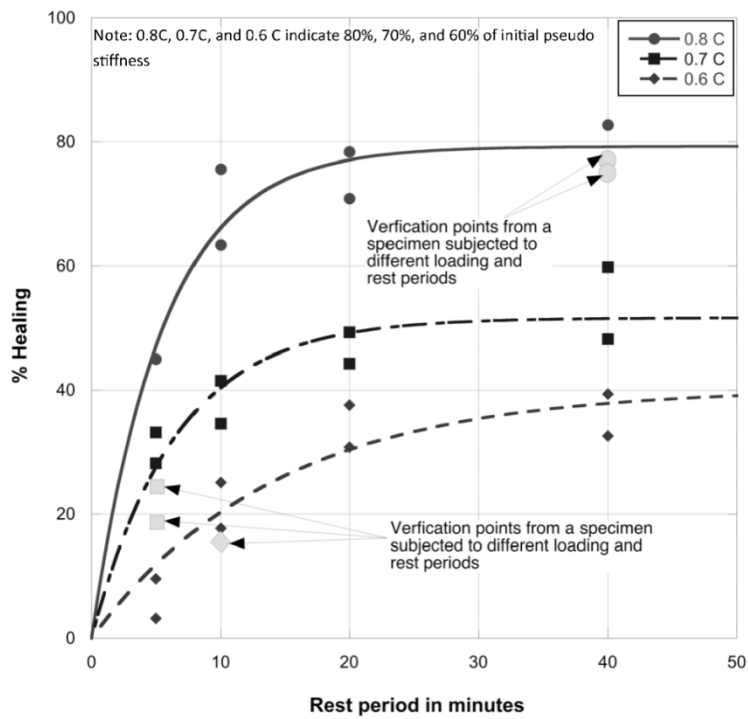


Figure F1d.2. Percentage healing in FAM mix with ARC binder B001 and verification tests.

Significant Problems, Issues and Potential Impact on Progress

None.

Work Planned Next Quarter

We plan to investigate the possibility of a more efficient experimental method to determine the healing surface for a particular mix along with a method to back calculate the gain in terms of load cycles for given loading-rest period combination.

Subtask F1d-6: Evaluate Relationship Between Healing and Endurance Limit of Asphalt Binders (UWM)

Work Done This Quarter

In the past quarter, the research team focused on investigating the effect of healing on the relationship between strain and fatigue (i.e., $N_f = A \cdot \gamma^B$). Studying the effect of rest on this relationship is thought to provide a more useful insight into the healing capabilities of asphalt binders than healing indices alone. Two base binders and one modifier, styrene-butadiene-styrene (SBS), with cross linking were used. For one base binder, two levels of the modification were applied. This set of binders also served to determine the effect of modification on healing and the relative importance of healing in comparison to binder modification. All binders were RTFO aged prior to testing.

To eliminate the effect of initial stiffness on fatigue response, binders were tested at an iso-stiffness condition, $|G^*| \cdot \sin \delta = 6.5$ MPa. All binders were tested at three strain levels to allow for determination of fatigue law coefficients. For all binders, strain amplitudes of 2% and 3% were used. The third strain amplitude was selected such that it would produce failure in roughly one to two hours. For all binders, a single rest period of 30 minutes inserted at 35% reduction in $|G^*| \cdot \sin \delta$ was used. A summary of the materials and test conditions is provided in table F1d-6.1. Additionally, to determine the effect of rest period duration on the relationship between strain and fatigue life, binder *B* was tested at additional rest period durations of one and two hours. Binder *B* was also tested using 10 rest periods to determine the effect of having multiple rest periods. To establish when rest periods should be inserted in tests conducted with multiple rest periods, the number of loading cycles after the rest period required to reach the $|G^*| \cdot \sin \delta$ value before the rest period, N , was determined. Also, to determine the effect of temperature on healing during rest period, binder *B* was tested at the three strain levels with a rest period in which the temperature was increased to 40°C at a controlled rate during the first 20 minutes of the rest period, held constant for 20 minutes, and brought back to the original testing temperature, and allowed to thermally equilibrate, over the last 20 minutes.

Table F1d-6.1. Experimental plan.

Binder	Modification	PG Grade	Test Temperature (°C)	Test Strain Amplitudes (%)	Rest Period Duration (min)	Number of Rest Periods
A	none	64-22	23.5	2, 3, 3.5	30	1
A	2% SBS	70-22	24.5	2, 3	30	1
B	none	64-22	20.0	2, 3, 3.5	30, 60, 120	1,10
B	2% SBS	70-22	23.0	2, 3, 4	30	1
B	4% SBS	76-22	23.5	2, 3, 5	30	1

Additionally, a draft final report has been completed. Results of the F1d-6 work element are included in the F2e final report.

Significant Results

Results of testing for base binder “A” are provided in figure F1d-6.1. Results demonstrate healing effects are minimal and that the effect of modification is much greater than the effect of rest.

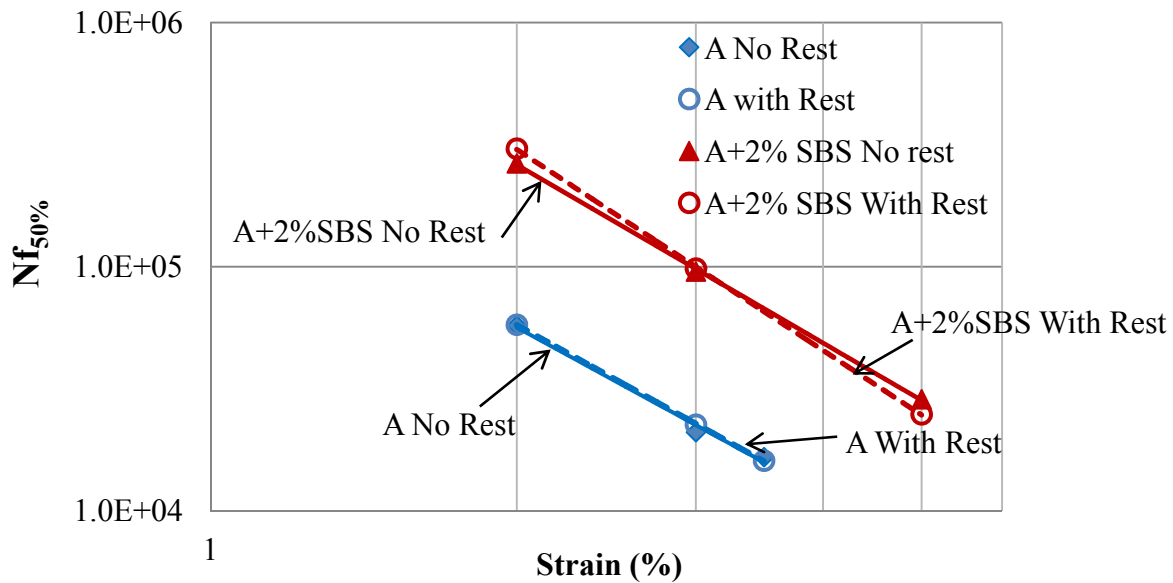


Figure F1d-6.1. Graph. Results of base binder A.

Results for base binder B are presented in figures F1d-6.2 and F1d-6.3. Results show that a single rest period, regardless of duration does not have a significant effect on the fatigue life. However, inclusion of 10 rest periods leads to a vertical shift in the fatigue law. Furthermore,

increasing the temperature during the rest period shifts the fatigue curve to that of the 2% SBS modified binder. Thus, while a single rest period shows little healing affect, and thus lacks the ability to capture the effect of healing, multiple rest periods and increasing temperature during the rest period lead to significant healing effects. Further analysis with additional binders and testing to determine the effect of number of rest periods and temperature during rest period on the relationship between fatigue life and strain is needed.

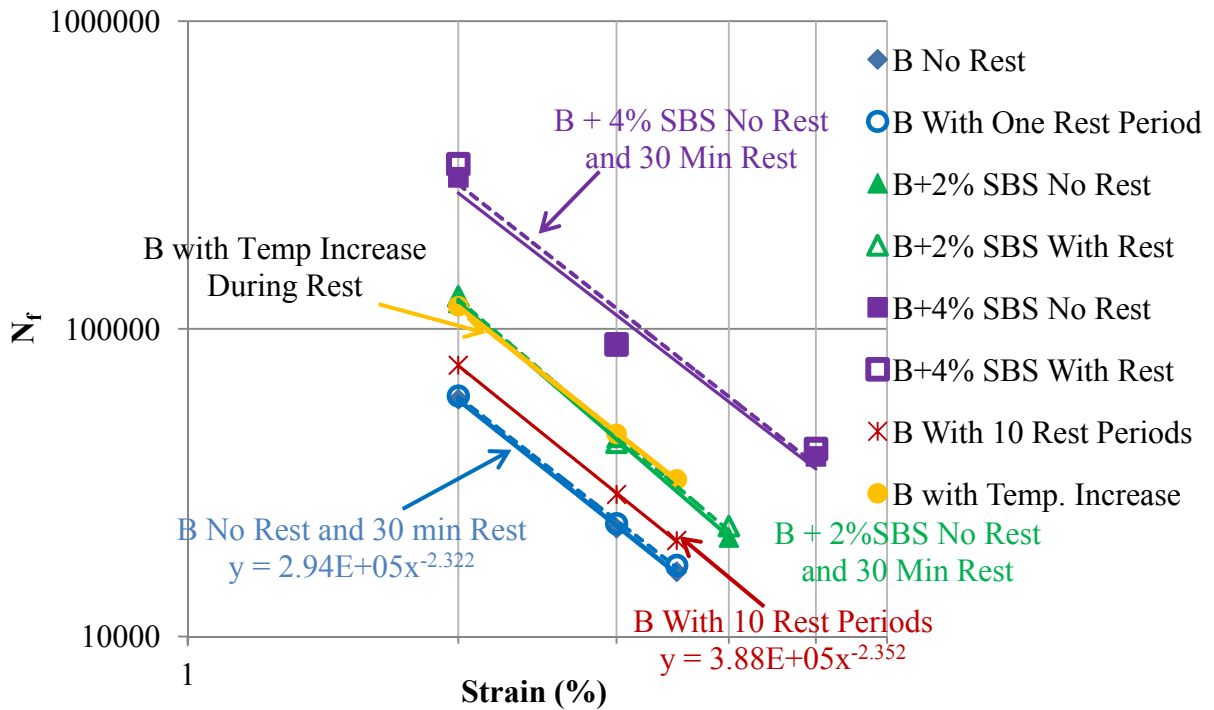


Figure F1d-6.2. Graph. Results of base binder B.

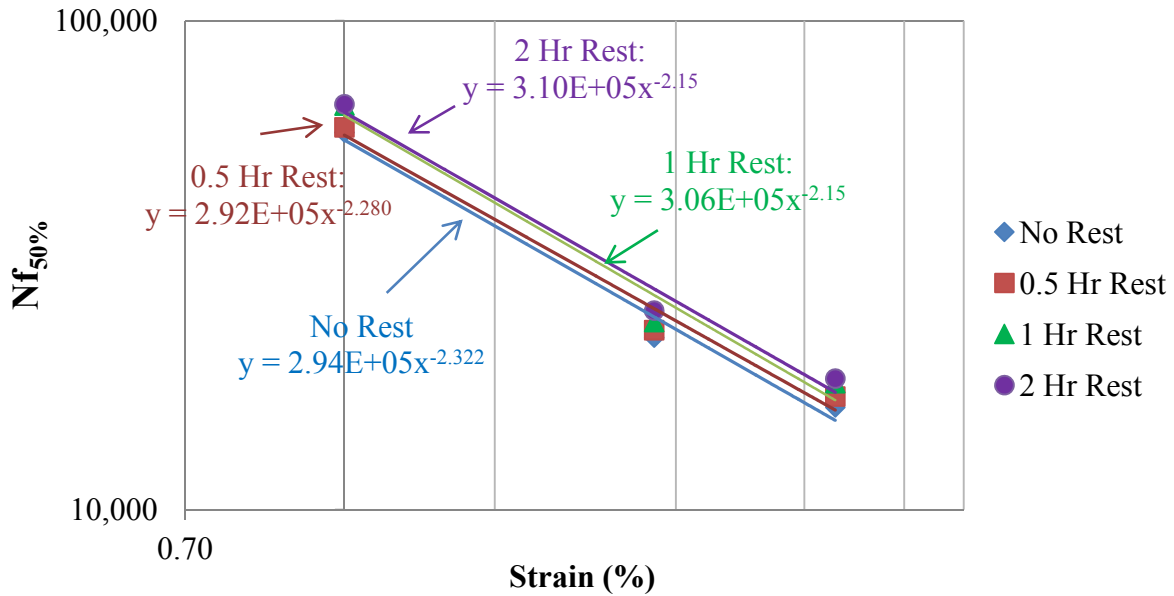


Figure F1d-6.3. Graph. Results of base binder B for tests with varying rest period duration.

Significant Problems, Issues and Potential Impact on Progress

None.

Work Planned Next Quarter

The research team will test a subset of the binders tested using the time sweep with rest procedure using the procedure proposed by Texas A&M, which consists of placing two samples in the dynamic shear rheometer (one on the spindle and one on the bottom plate) and bring the samples into contact. The increase in complex modulus with time is used to measure healing. Results will be compared with the time sweep with rest results.

Papers Submitted

Stimilli, A., Hintz, C., Li, Z., Velasquez, R. and Bahia, H. Effect of Healing on Fatigue Law Parameters of Asphalt Binders. Submitted for presentation and publication to Transportation Research Record, Journal of the Transportation Research Board, August 2011.

Subtask F1d-7: Coordinate with Atomic Force Microscopic (AFM) Analysis (WRI)

Work Done This Quarter

The emphasis of this subtask is to integrate the results from Subtasks M1b-2 and M2a-2, and other pertinent past experimental work where physico-chemical properties including chemical potentials and phase separation phenomena can be used in the asphalt microstructure model

discussed in Work Element F3a. The data generated from these analyses is discussed and incorporated into the chemo-mechanical models of asphalt and asphalt mastic structures in Work Element F3a.

Significant Results

See Work Element F3a.

Significant Problems, Issues and Potential Impact on Progress

None

Work Planned Next Quarter

Activity in Subtask is included in the discussion in Work Element F3a.

Subtask F1d-8: Coordinate Form of Healing Parameter with Micromechanics and Continuum Damage Models (TAMU)

Work Done This Quarter

In this quarter, a general thermodynamic framework for coupling damage and micro-damage healing has been proposed (Abu Al-Rub et al. 2010; Abu Al-Rub and Darabi 2011; Darabi et al. 2011a, b, c). Special attention has been placed on the proper estimation of the energy recovered during the healing process. The thermodynamic framework is formulated by proposing a healing natural configuration which enhances the continuum damage mechanics theories in modeling the micro-damage healing phenomenon in asphalt mixes. This thermodynamic framework is also formulated in a consistent way to capture the effect of the healing process and its associated changes in the temperature to accurately estimate the recovered energy during the healing process. The micro-damage healing model that has been derived based on this thermodynamic framework has been verified against many of the ALF experimental data including cyclic stress- and displacement-controlled tests. It has been shown that the micro-damage healing effect should also be considered during the cyclic strain controlled tests in tension due to the fading memory effect of the viscoelastic materials. During the unloading stage in the cyclic displacement controlled test (when the displacement rate is negative) the stress decreases such that at some point it becomes negative. At this point, the material feels compression although the total strain is still in tension. Therefore the crack faces tend to attract each other and create a bond. As a result, the crack length decreases and micro-damage healing occurs. Figures F1d-8.1-3 clearly show that the micro-damage healing model predicts the experimental measurements on cyclic displacement controlled tests very well.

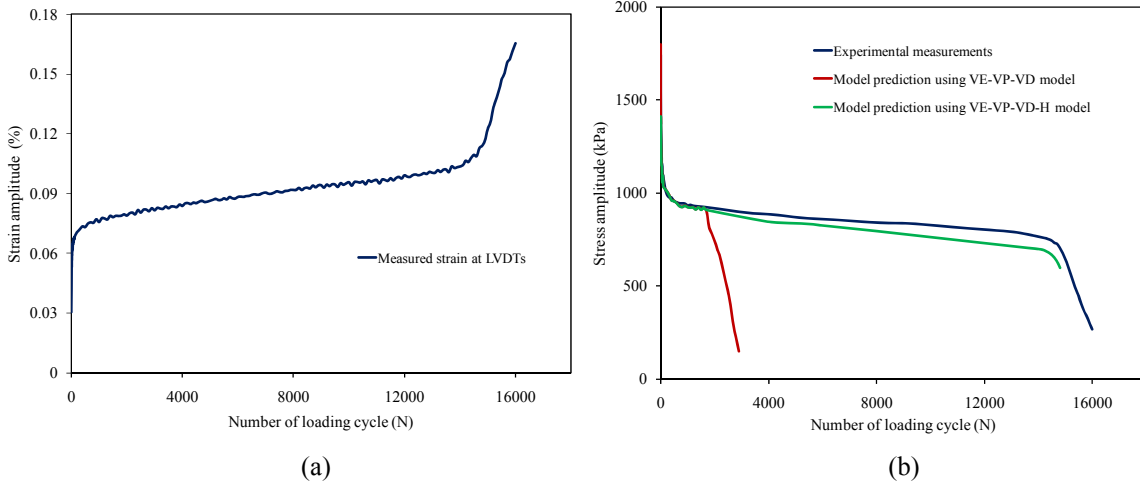


Figure F1d-8.1. Experimental measurements and model predictions for the cyclic strain controlled test at 19°C when the applied strain amplitude at the end plates is 1200 $\mu\epsilon$.
 (a) The amplitude of the measured strains at LVDTs versus the number of loading cycles;
 (b) The tensile stress amplitude versus number of loading cycles.

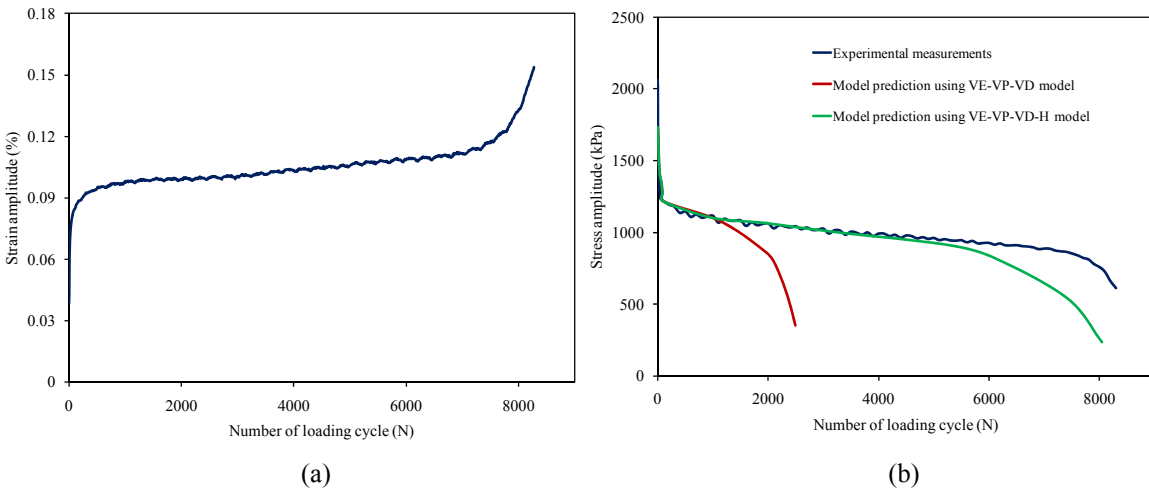


Figure F1d-8.2. Experimental measurements and model predictions for the cyclic strain controlled test at 19°C when the applied strain amplitude at the end plates is 1500 $\mu\epsilon$.
 (a) The amplitude of the measured strains at LVDTs versus the number of loading cycles;
 (b) The tensile stress amplitude versus number of loading cycles.

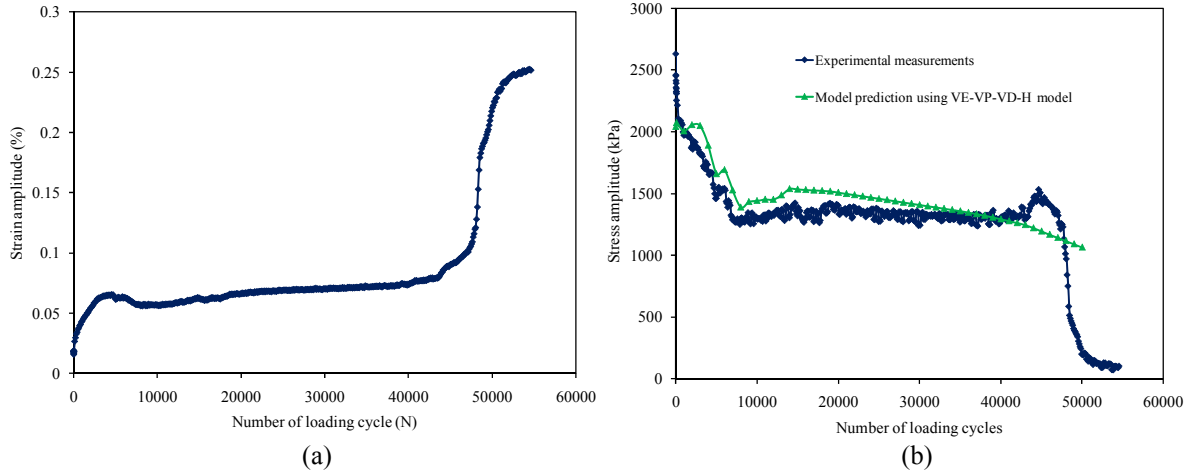


Figure F1d-8.3. Experimental measurements and model predictions for the cyclic strain controlled test at 5°C when the applied strain amplitude at the end plates is 1750 $\mu\epsilon$.
 (a) The amplitude of the measured strains at LVDTs versus the number of loading cycles;
 (b) The tensile stress amplitude versus number of loading cycles.

Significant Results

The proposed thermodynamic framework can be effectively used in deriving various forms of constitutive models for bituminous materials by only assuming mathematical expressions for the stored energy and the rate of energy dissipation. It is anticipated that this thermodynamic framework will be widely used by researchers to derive robust constitutive models for different materials.

Significant Problems, Issues and Potential Impact on Progress

None

Work Planned Next Quarter

The main focus of the coming quarter is on further validation of the micro-damage healing model against available experimental data. Moreover, special emphasis will be placed on the development of a simplified approach for calibrating the micro-damage healing model based on simple experimental procedure.

Cited References

Abu Al-Rub, R.K., **M.K. Darabi**, D.N. Little, and E.A. Masad, “A micro-damage healing model that improves prediction of fatigue life in asphalt mixes,” *International Journal of Engineering Science*, Vol. 48, No. 11, 966-990, 2010, (**Among Top 25 Hottest Articles, IJES**).

Darabi, M.K., R.K. Abu Al-Rub, and D.N. Little, “A Continuum damage mechanics-based framework for modeling micro-damage healing,” *International Journal of Solids and Structures*, 2011a (under review).

Abu Al-Rub, R.K., and **M.K. Darabi**, “A thermodynamic framework for constitutive modeling of time- and rate-dependent materials, Part I: Theory,” *International Journal of Plasticity*, 2011 (under review).

Darabi, M.K., R.K. Abu Al-Rub, E.A. Masad, and D.N. Little, “A thermodynamic framework for constitutive modeling of time- and rate-dependent materials, Part II: Numerical aspects and application to asphalt concrete,” *International Journal of Plasticity*, 2011b (under review).

Darabi, M.K., R.K. Abu Al-Rub, E.A. Masad, and D.N. Little, “A continuum-based micro-damage healing model for asphalt concrete,” In. Engineering Mechanics Institute (EMI), Northeastern University, Boston, MA, June 2-4, 2011c.

CATEGORY F2: TEST METHOD DEVELOPMENT

Work Element F2a: Binder Tests and Effect of Composition (UWM)

Work Done This Quarter

The final draft report was completed and the will be submitted early October.

Work Planned Next Quarter

None.

Work Element F2b: Mastic Testing Protocol (TAMU)

This work element is completed and the reader is referred to work element M1c.

Work Element F2c: Mixture Testing Protocol (TAMU)

Work Done This Quarter

A technical paper entitled “Characterizing Permanent Deformation and Fracture of Asphalt Mixtures Using Compressive Dynamic Modulus Tests” was submitted for publication to the American Society of Civil Engineers' (ASCE) *Journal of Materials in Civil Engineering*. A presentation entitled “Characterization of Permanent Deformation and Cracking of Asphalt Mixtures in Compression” was made at the 48th Petersen Asphalt Research Conference in Laramie, Wyoming, July 11.

Two major achievements were made in this quarter: 1) the mechanistic viscoelastic fracture model was improved to comprehensively and accurately characterize the fracture properties of asphalt mixtures in the tertiary deformation stage; reasonable values for the true stress, the axial damage density and the material constants in Paris' law were obtained based on the laboratory testing results; and 2) a bracelet-based radial deformation measuring system was modified and additional tests were conducted on 8 samples using the modified bracelet. The radial deformation was successfully captured in both creep tests and the dynamic modulus tests, which provided data for the calculation of radial damage density in charactering anisotropic fracture in compression. Details of the achievements made in this quarter are summarized as follows.

1) Improved Mechanistic Viscoelastic Fracture Model in Compression

Significant high values were found for true stress and axial damage density in the previous quarter, which are not reasonable since the asphalt mixture may fail in the tertiary stage at a relatively low lost area that indicates a low damage density. In order to address this issue, the dissipated pseudo-fracture strain energy (DPFSE) balance equation should be formulated as an incremental expression. The following details the new DPFSE formulations and calculations of the true stress, and the damage density as well as the determination of material constants in the Paris' law.

1.1) Model for True Stress and Damage Density

First, the apparent total DPFSE is calculated by integrating the apparent stress with respect to the viscofracture strain, which is obtained by strain decomposition, over the integration interval from the flow number to the current load cycle:

$$DPFSE^A = \int_{\frac{2\pi N_f}{\omega}}^{\frac{2\pi N}{\omega}} \sigma^A(t) \frac{d\varepsilon^{vf}(t)}{dt} dt \quad (F2c.1)$$

where $\sigma^A(t) = \sigma_1 \left[1 - \frac{\sigma_0}{\sigma_1} \cos(\omega t) \right]$, $\varepsilon^{vf}(N) = \varepsilon_0^{vf} \left[e^{\theta(N-N_f)} - 1 \right]$ and $N = \frac{\omega}{2\pi} t$. Using these in equation F2c.1 gives the apparent total DPFSE, which is derived to be $DPFSE^A = \sigma_1 \varepsilon^{vf}(N)$. Thus the incremental DPFSE is:

$$\Delta DPFSE^A = \sigma_1 \left[\varepsilon^{vf}(N) - \varepsilon^{vf}(N-1) \right] \quad (F2c.2)$$

Second, the true incremental DPFSE can be obtained by integrating the true stress with the incremental pseudo true strain within one cycle:

$$\Delta DPFSE^T = \int_{\frac{2\pi(N-1)}{\omega}}^{\frac{2\pi N}{\omega}} \sigma^T(t) \frac{d\Delta\varepsilon^{TR}(t)}{dt} dt \quad (F2c.3)$$

where $\sigma^T(t) = (\sigma_1 + \Delta\sigma) \left[1 - \frac{\sigma_0}{\sigma_1} \cos(\omega t) \right]$ and $\Delta\varepsilon^{TR}(t) = \frac{\Delta\sigma}{E_R} \left[1 - \frac{\sigma_0}{\sigma_1} \frac{|E_{II}^*|}{|E^*|} \cos(\omega t - \delta + \varphi_{II}) \right]$, in

which, $\Delta\sigma$ is the increment of amplitude of the true stress; $|E_{II}^*|$ and φ_{II} are the average dynamic modulus and average phase angle of the secondary stage in the destructive dynamic modulus test, respectively. Thus,

$$\Delta DPFSE^T = \frac{(\sigma_1 + \Delta\sigma)\Delta\sigma}{E_R} \left(\frac{\sigma_0}{\sigma_1} \right)^2 \frac{|E_{II}^*|}{|E^*|} \pi \sin(\delta - \varphi_{II}) \quad (\text{F2c.4})$$

Third, if $K = \frac{1}{E_R} \left(\frac{\sigma_0}{\sigma_1} \right)^2 \frac{|E_{II}^*|}{|E^*|} \pi \sin(\delta - \varphi_{II})$ and equation F2c.2 is set equal to equation F2c.4, the amplitude of the true stress is solved as:

$$\sigma^T(N) = \sigma_1 + \Delta\sigma = \frac{1}{2} \left\{ \sigma_1 + \sqrt{(\sigma_1)^2 + 4 \frac{\sigma_1}{K} [\varepsilon^{vf}(N) - \varepsilon^{vf}(N-1)]} \right\} \quad (\text{F2c.5})$$

Finally, the axial damage density is:

$$\xi(N) = 1 - \frac{\sigma^A}{\sigma^T} = 1 - 2\sigma_1 \left\{ \sigma_1 + \sqrt{(\sigma_1)^2 + 4 \frac{\sigma_1}{K} [\varepsilon^{vf}(N) - \varepsilon^{vf}(N-1)]} \right\}^{-1} \quad (\text{F2c.6})$$

Figure F2c.1 shows an example of the true stress and the axial damage density. The fitted damage density is predicted with the model in equation F2c.9 that is derived in next section. Figure F2c.1 indicates that both the true stress and the axial damage density increase due to the growth of cracks in the tertiary stage. The asphalt mixture was compressed in the primary and secondary stages in which the air void content decreases from the original air void content to a lower value that is the initial point for the axial damage density.

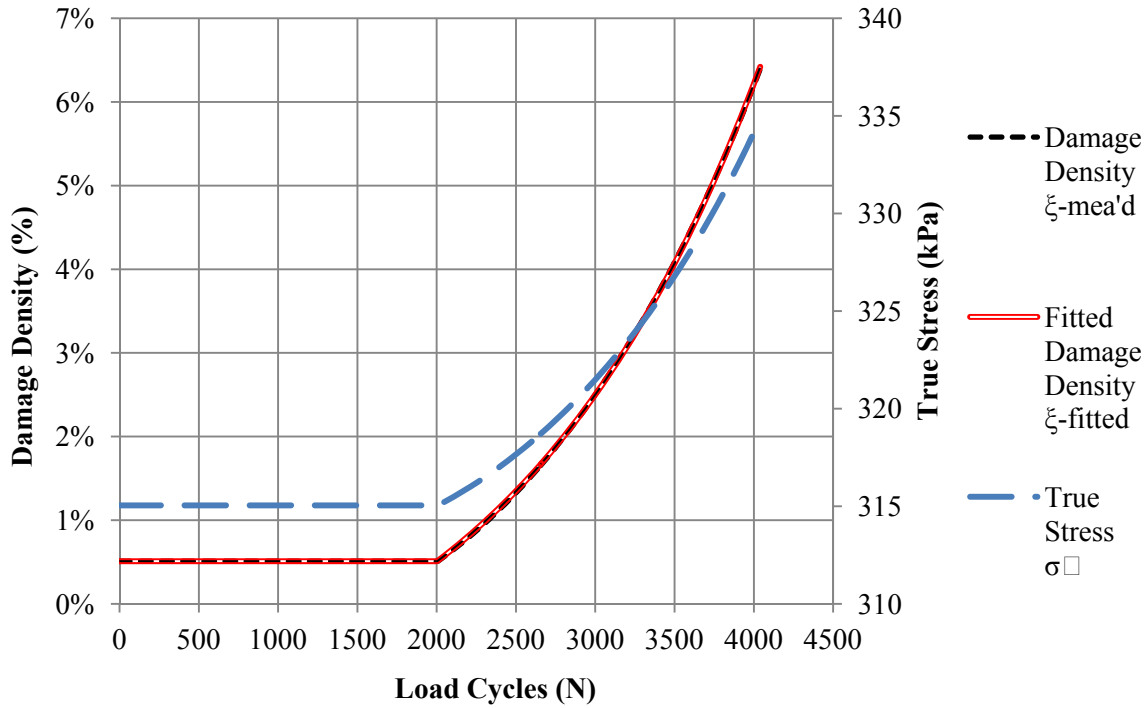


Figure F2c.1. True stress and axial damage density.

1.2) Paris' Law for Compressive Fracture

The pseudo J-integral based on the Paris' law is widely employed to characterize the fatigue damage of asphalt mixtures in tension and has been proved to be capable of capturing the fracture properties of the materials. The same model is used for compressive fracture in the tertiary deformation stage. However, instead of using the average crack size, the damage density which represents the global fracture properties is used in the pseudo J-integral based on the Paris' law. The model is expressed as:

$$\frac{d\xi}{dN} = A_1 (J_R)^{n_1} \quad (\text{F2c.7})$$

where A_1 and n_1 are coefficients of the Paris' law that are material constants and J_R is the pseudo J-integral that can be written as:

$$J_R = \frac{\partial DPFSE^A}{\partial c.s.a.} = \frac{\partial DPFSE^A / \partial N}{\partial c.s.a. / \partial N} = \frac{\partial [\sigma_1 \varepsilon^{vf}(N)] / \partial N}{\partial [2A_0 \xi(N)] / \partial N} \quad (\text{F2c.8})$$

where $c.s.a.$ is crack surface area that is two times the lost area in the asphalt mixture. Equations F2c.7 and F2c.8 yield:

$$\xi(N) = \xi_0 + C \left[e^{D(N-N_f)} - 1 \right] \quad (\text{F2c.9})$$

where ξ_0 is the initial damage density, and C and D are model parameters that can be expressed as:

$$\begin{cases} C = A_1^{\frac{1}{1+n_1}} \left(\frac{\theta \sigma_1 \varepsilon_0^{vf}}{2A_0} \right)^{\frac{n_1}{1+n_1}} \left(\frac{1+n_1}{\theta n_1} \right) \\ D = \frac{\theta n_1}{1+n_1} \end{cases} \quad (\text{F2c.10})$$

Figure F2c.1 shows one example for the predicted damage density with equation F2c.9, which indicates that the model for the damage density in that equation can fit the measured damage density very well. Once the model fitting parameters (C and D) are determined, the material constants in the Paris' law are determined as follows:

$$\begin{cases} A_1 = \left(\frac{2A_0}{\theta \sigma_1 \varepsilon_0^{vf}} \right)^{n_1} (CD)^{1+n_1} \\ n_1 = \frac{D}{\theta - D} \end{cases} \quad (\text{F2c.11})$$

By applying the above fracture theories to the testing data of asphalt mixtures with different binders, air void contents and aging periods, the axial damage density curves are obtained and the material constants in the Paris' law as well as the initial damage density are determined and summarized in table F2c.1.

Table F2c.1 indicates that the air voids in an asphalt mixture will be squeezed under a compressive load and will reduce to a lower value than the initial damage density. The asphalt mixture with a higher original air void content will have a relatively larger initial damage density. Table F2c.1 also shows that a stiffer asphalt mixture, such as a mixture that has a 6-month aging period or a low air void content, yields a larger n_1 value and a smaller A_1 value, which are reasonable because a stiffer asphalt mixture has a smaller slope of creep compliance and the n_1 is inversely proportional to the slope of creep compliance based on Schapery's fracture theory. Thus a stiffer asphalt mixture should have a relatively larger n_1 value. In addition, equation F2c.11 shows that A_1 is strongly related to n_1 . Based on the data in table F2c.1, a relationship is found between $\log(A_1)$ and n_1 with a high coefficient of determination (R^2), which is shown in figure F2c.2.

Table F2c.1. Initial damage density and material constants in Paris' Law for different asphalt mixtures.

Asphalt Mixtures	Binder	Aging Period	Air Void (%)	ξ_0 (%)	A_1 (%/cycle)	n_1
	AAD	0-month	4	0.25	$2.5 \cdot 10^{-10}$	0.80
			7	1.95	$1.05 \cdot 10^{-4}$	0.06
		6-month	4	0.34	$2.65 \cdot 10^{-20}$	3.36
			7	0.51	$1.01 \cdot 10^{-12}$	1.32
	AAM	0-month	4	0.51	$2.88 \cdot 10^{-9}$	0.71
			7	3.44	$1.07 \cdot 10^{-5}$	0.54
		6-month	4	0.42	$3.20 \cdot 10^{-24}$	4.02
			7	2.98	$3.56 \cdot 10^{-23}$	3.41

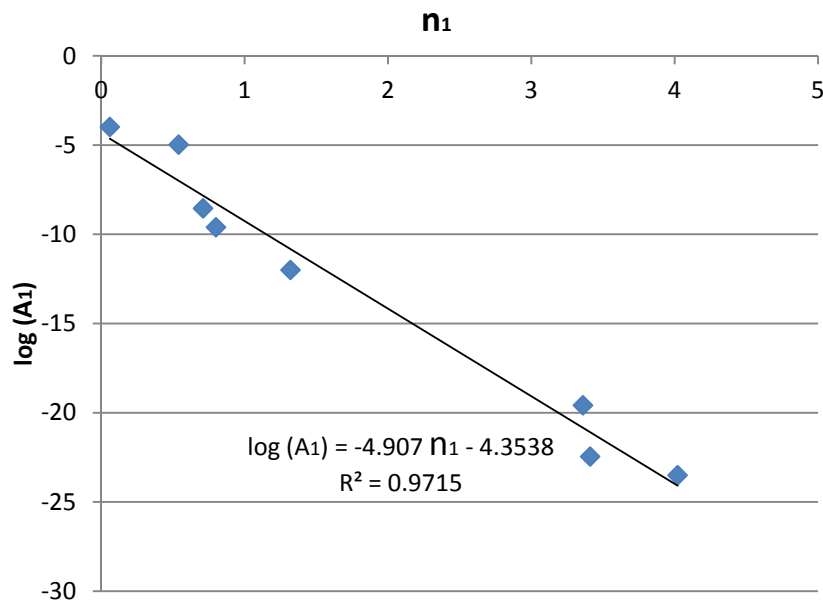


Figure F2c.2. Relationship between A_1 and n_1 .

2) Modified Radial Deformation Measuring System

In previous quarterly reports, the radial deformation measuring system was proposed using one linear variable differential transformer (LVDT) fitted on a bracelet that surrounds the specimen to record the change of the specimen's circumference. The two ends of the bracelet were connected by two rubber rings as shown in figure F2c.3 (a). The disadvantages with this measuring system include: 1) the rubber rings are viscoelastic materials that will relax under a

tensile load, which bring errors to the measured data; and 2) the radial deformation cannot be accurately captured under a dynamic load since the rubber rings are viscoelastic materials that have a damping effect on the responses to the dynamic load. To address the two problems, the rubber rings are replaced by two metallic springs as shown in figure F2c.3 (b). Since the springs are made of stainless steel that is an elastic material, the springs do not relax with time and can respond to the dynamic load instantaneously.



(a) Previous configuration

(b) Modified configuration

Figure F2c.3. Previous and modified radial deformation measuring system using bracelet.

Using the modified radial deformation measuring system, laboratory tests are conducted on eight asphalt mixture specimens that vary with the binder type, air void content and aging period. These tests include the nondestructive creep test, nondestructive dynamic modulus test and destructive dynamic modulus test, all of which were developed in previous quarters and were documented in previous quarterly reports. Figure F2c.4 shows the first 60 sec data for the axial strain and radial strain recorded by the LVDTs in a dynamic modulus test, which indicates that the dynamic response of the radial strain is successfully captured by the modified radial deformation measuring system when the asphalt mixture is subjected to a dynamic load. Based on the radial strain measured in the tests, the time-dependent Poisson's ratio, complex Poisson's ratio including its magnitude and phase angle, as well as the Poisson's ratio in a destructive test can be determined, all of which provide a basis for the strain decomposition in the radial direction and the calculation of the radial damage density for the anisotropic fracture characterization.

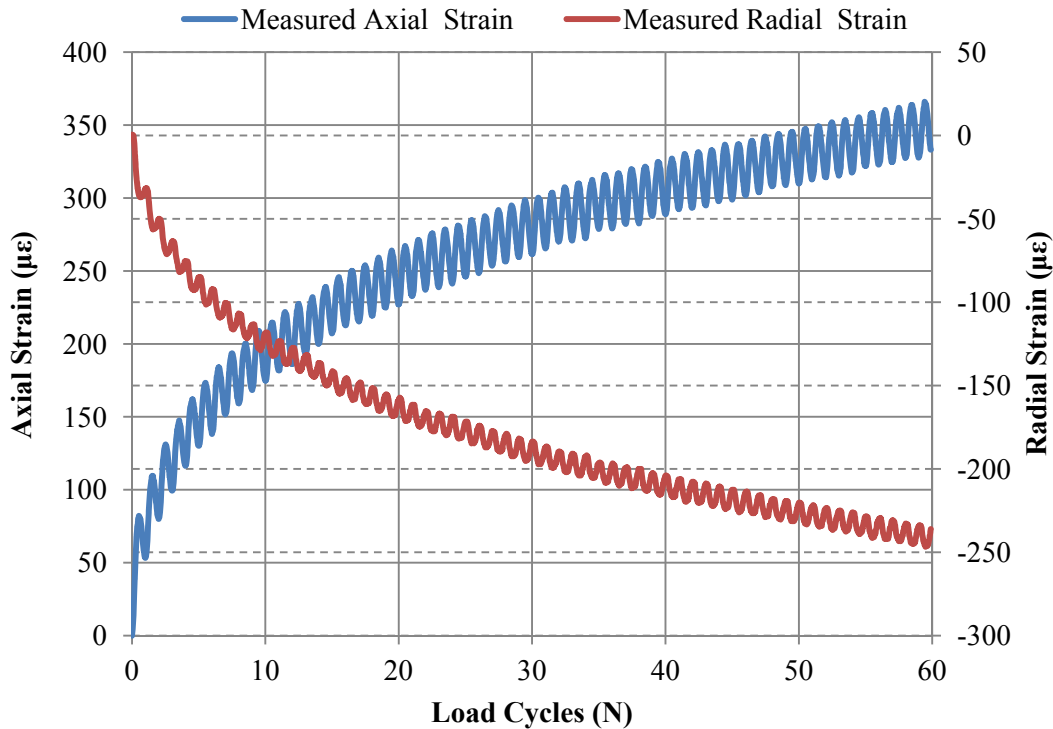


Figure F2c.4. Measured axial and radial strains in first 60 sec testing period in dynamic modulus test.

Significant Results

The mechanistic viscoelastic fracture model was improved to comprehensively and accurately characterize the fracture properties of asphalt mixtures in the tertiary deformation stage. Reasonable values were obtained for the true stress, the axial damage density and the material constants in Paris' law based on the laboratory testing results. In addition, a bracelet-based radial deformation measuring system was modified and additional tests were conducted on 8 samples using the modified bracelet. The radial deformation was successfully captured in both creep tests and the dynamic modulus tests, which provide data for the calculation of the radial damage density in charactering anisotropic fracture in compression.

Significant Problems, Issues and Potential Impact on Progress

None.

Work Planned in Next Quarter

- Strain decomposition in the radial direction and calculation of the radial damage density needs to be continued in the next quarter so that the anisotropic fracture properties of asphalt mixtures can be fully characterized; and

- The unconfined and confined strength tests need to be conducted on a variety of asphalt mixtures with different binders, air void contents and aging periods.

Work Element F2d: Structural Characterization of Micromechanical Properties in Bitumen using Atomic Force Microscopy (TAMU)

Work Done This Quarter

Statistical analysis of the AFM creep presented in previous quarterly reports, and summarized in the year 5 work plan under work element F2d: Structural Characterization of Micromechanical Properties in Bitumen using Atomic Force Microscope (AFM) was performed in order to make inferences about the populations of asphalt phases in which the data were collected. Included in the statistical analysis were relative frequency histograms and q-q plots to test for normality of the data, t-tests and ANOVA f-tests to compare the means of two or more asphalt phases, individual comparisons based on Fisher's LSD to identify specifically where differences occur amongst three or more phases, Matched Pairs analysis to compare means of individual phases (continuous or dispersed) before and after aging, and Contingency analysis of categorical variables for making inferences based on proportions of measurements falling within specified asphalt stiffness ranges.

The relative frequency histograms and q-q plots revealed that some non-normality and outliers were present in most of the data sets, which indicated the need for a more robust statistical method, such as the Wilcoxon/Kruskal Wallis Sum Rank test to verify the results of the more powerful t-tests and f-tests. The t-tests and ANOVA f-tests (accompanied by the Wilcoxon/Kruskal Wallis Sum Rank test) provided at least 95% confidence that differences in phase properties existed in five of the six asphalt binders that were tested. There was a lack of statistical evidence to find a difference between the phase properties of Aged Asphalt AAB. Fisher's LSD analysis revealed with 95% confidence that each of the three phases in Aged Asphalt AAD had distinctively different properties. Matched pairs analysis provided at least 95% confidence that 11 of 12 continuous and dispersed asphalt phases that were studied reveal a decrease in maximum creep deflection (increase in stiffness) due to aging; this finding strongly supports the notion presented by Allen et al. (2011) that observed increases in asphalt stiffness during aging are not only due to the presence of higher percentages of the stiffest phase after aging but also due to increased stiffness of the continuous and dispersed phases due to aging. For Asphalts AAD and ABD, the contingency analysis resulted in rejection of the null hypothesis that asphalt stiffness is independent of both asphalt phase and asphalt age at the $\alpha = 0.0001$ level (99.99% confidence level); however, there was a lack of statistical evidence to reject the null hypothesis for Asphalt AAB.

Significant Problems, Issues and Potential Impact on Progress

None.

Work Planned Next Quarter

Tomography will be carried out as needed for the models development.

Work Element F2e: Verification of the Relationship between DSR Binder Fatigue Tests and Mixture Fatigue Performance (UWM)

Work Done This Quarter

The research team has completed a draft of the final report for work element F2e. Additionally, an experimental plan for ruggedness testing of the linear amplitude sweep (LAS) test has been constructed.

Significant Results

The experimental plan for ruggedness testing of the LAS test is based on ASTM E 1169-07 "Standard Practice for Conducting Ruggedness Tests" and ruggedness testing of the dynamic shear rheometer (DSR) (Shashidhar and Chollar 1995). The intent of a ruggedness test is to identify factors which strongly influence measurements in a specific test.

The procedure outlined in ASTM E 1169-07 is based on a factorial design and therefore allows for only two levels per factor. ASTM 1169-07 does not recommend including multiple laboratories in ruggedness testing. However, in the ruggedness testing of the DSR, four laboratories were included and four materials were included to allow for inter-laboratory comparison. Therefore, multiple laboratories and materials are included in the ruggedness testing plan of the LAS to allow for inter-laboratory comparison and comparison of the influence of factors on different materials. It is recommended that at least two laboratories participate to allow for comparison of results between laboratories. Additionally, two materials will be tested, one unmodified asphalt binder and one polymer modified asphalt binder.

The LAS test consists of two procedures: a frequency sweep to obtain an undamaged material response and a strain amplitude sweep to evaluate damage resistance. Thus, factors affecting both procedures need to be considered. Factors were selected based on results of DSR ruggedness testing and LAS test parameters which could potentially affect results. It was concluded in the ruggedness testing of the DSR that temperature variance greater than $\pm 0.1^\circ\text{C}$ that sample placement method (i.e., pouring hot sample directly onto DSR plate versus placing a pre-formed sample from a silicon mold) significantly affect results (Shashidhar and Chollar 1995). The experimental factors to be considered in ruggedness testing of the LAS test are as follows:

- A. Test Temperature ($T-0.1^\circ\text{C}$ versus $T+0.1^\circ\text{C}$)
- B. Sample Placement Method (Pellet from silicon mold versus pouring hot binder directly onto plate)
- C. Number of frequencies used in frequency sweep (8 versus 12)
- D. Range of frequencies used in frequency sweep (0.1 to 10 Hz versus 1 to 30 Hz)
- E. Strain during frequency sweep (0.05% versus 0.15%)
- F. Strain sequence during amplitude sweep (0.1%, 0.8%, 1.8%, 2.8%, 3.8%...29.8% versus 0.3%, 1.2%, 2.2%, 3.2%...30.2%)
- G. Number of loading cycles per strain step (80 versus 120)

Each factor will have two levels (i.e., +1 and -1). Assignment of levels is shown in table F2e.1.

Table F2e.1. Level assignments.

Variable	-1	1
A	T-0.1°C	T+0.1°C
B	Pellet	Pouring
C	8	12
D	0.1 to 10 Hz	1 to 30 Hz
E	0.05%	0.15%
F	0.1%, 0.8%, 1.8%...	0.3%, 1.2%, 2.2%, ...
G	80	120

Table F2e.2 provides the experimental plan per ASTM E 1169-07. Each run shall be replicated.

Table F2e.2. Experimental plan.

Variable	Determination Number							
	1	2	3	4	5	6	7	8
A	-1	-1	-1	-1	1	1	1	1
B	-1	-1	1	1	-1	-1	1	1
C	1	-1	1	-1	1	-1	1	-1
D	1	1	-1	-1	-1	-1	1	1
E	-1	1	-1	1	1	-1	1	-1
F	1	-1	-1	1	1	-1	-1	1
G	1	-1	-1	1	-1	1	1	-1

VECD analysis will be conducted to determine the relationship between fatigue life and strain (i.e., $N_f = A\gamma^B$). Effects of factors on both A and B as response variables will be evaluated. A statistical analysis will be conducted to determine significant effects.

Significant Problems, Issues and Potential Impact on Progress

None.

Work Planned Next Quarter

The research team will finalize experimental plan and begin ruggedness testing.

Cited References

ASTM E 1169-07. Standard Practice for Conducting Ruggedness Tests.

Shashidhar, N. and B.H. Chollar. *Ruggedness Testing of the Dynamic Shear Rheometer and Bending Beam Rheometer, Final Report*, FHWA-RD-95-079, 1995.

CATEGORY F3: MODELING

Work Element F3a: Asphalt Microstructural Model

Work Done This Quarter

Subtask F3a-1. ab initio Theories, Molecular Mechanics/Dynamics and Density Functional Theory Simulations of Asphalt Molecular Structure Interactions (URI)

Nothing to report.

Subtask F3a-2. Develop algorithms and methods for directly linking molecular simulation outputs and phase field inputs (URI, VT)

Sub-subtask F3a-2.2. Phase-field parameter determination (VT-WRI)

Work Done

We identified a strategic plan for phase-field simulation of asphalt binders. The first step is to perform a coupled simulation of phase separation and thermal stress. With this work, we will be able to obtain the distribution of wax as well as stresses. Then will we perform another series of phase-field simulations on cracking under certain stress or strain conditions. By comparing the cracks with experiments, we can refine the model to provide better predictions. Both approaches have been previously applied in the research of alloys and brittle cracks. For the first step, we only need to incorporate the specific free energy that describes the asphalt binder. This free energy can be obtained from phase diagrams or molecular dynamics simulations. From the literature review, the phase-field simulation of cracking is still at a relative primitive stage. At this stage, a Matlab code has been refined and improved to tackle the target problems. Example runs are currently being analyzed.

Significant Problems, Issues and Potential Impact on Progress

Identification of software packages to perform phase-field simulations.

Work Planned Next Quarter

We investigated different sources to get a running code that performs the coupled simulation of phase transition and thermal stress. MICRESS (MICRostructure Evolution Simulation Software)

developed by a group in Germany is capable of multi-phase-field and elastic stresses, which suits our research goal reasonably well. However this software is very expensive which poses a budget issue. COMSOL Multiphysics (the former FEMLAB), which already has a phase-field module and a structural analysis module built in can be used to build a working code in a short time frame. This general purpose software solves customizable partial differential equations by finite element methods. The license of COMOSL is much cheaper and a lot of departments already have it, (e.g., the VT math department). This should be the approach we follow in the near future.

AFM images of different binders will be acquired as input into the existing code to evaluate stress concentration effects of different binders. We anticipate an independent running code to be developed in the next quarter.

Subtask F3a-3. Obtain temperature-dependent dynamics results for model asphalts that represent asphalts of different crude oil sources (URI)

Results for the model AAA-1 system were presented at the Petersen Asphalt Research Conference. The molecule types in the new AAA-1 model system were well-received by the conference attendees. Compared to past model systems, the new system is of higher molecular weight and yet more similar chemistry to the characterizations that have been measured for asphalts of interest in the ARC. Predictions of viscosity span a range comparable to those that have been reported from experiments on asphalts.

Significant Problems, Issues and Potential Impact on Progress

None

Work Planned Next Quarter

Molecular dynamics simulations have been initiated at the highest typical model temperature (433 K) in order to equilibrate the positions of molecules within model AAK-1 and AAM-1 asphalts. New undergraduate researchers have been conducting the simulations, so progress was slowed as they began to learn the simulation methods. The chemical compounds within the models are the same as in the new model AAA-1. Different numbers of each molecule are chosen compared to AAA-1, which introduces chemical differences among the model asphalts.

Paper drafts that describe the new asphalts are being completed. Submissions to peer-reviewed journals are anticipated during the fourth quarter.

Subtask F3a-4. Simulate changes in asphalt dynamics after inducing representations of chemical and/or physical changes to a model asphalt (URI)

Subtask F3a-5. Molecular mechanics simulations of asphalt-aggregate interfaces (VT)

Subtask F3a-6. Modeling of fatigue behavior at atomic scale (VT)

Subtask F3a-7. Modeling of moisture damage (VT)

Subtask F3a-8. ab initio Calculations of Asphalt Molecular Structures and Correlation to Experimental Physico-Chemical Properties of SHRP Asphalts (WRI-TUDeft)

Nothing to report.

Work Element F3b: Micromechanics Model

Subtask F3b-1: Model Development (TAMU, NCSU, UNL)

Work Done This Quarter

One of our primary progresses during this quarter is the validation of our computational microstructure model with rate-dependent fracture. To that effort, rate-dependent cohesive zone fracture properties were first obtained using a procedure that combines laboratory tests of semi-circular bending specimens of a fine aggregate matrix (FAM) mixture and their numerical simulations based on the ABAQUS-UEL rate-dependent cohesive zone model that we have developed. Model parameters were then used to simulate three-point bending beam tests of asphalt concrete mixtures subjected to different loading rates. Microstructure model simulations were in good agreement with experimental test results, which confirms that our computational microstructure model incorporated with the rate-dependent cohesive zone fracture has been well developed. The model, as a tool, can enhance materials selection, mixture design and structural design of pavements, since it can provide better insights into the linkage between components, mixture, and structure. In addition, our cohesive zone model can be integrated with PANDA by providing a fracture engine so that nonlinear damage with viscoelastic fracture of asphaltic mixtures and pavement structures can be effectively simulated.

We presented our work progresses at the Models Expert Task Group (ETG) meeting held in Fall River, MA. In the meeting, we presented all key components in this subtask including the constitutive theory, modeling methodology, testing protocols developed, resulting test data, and various model simulations for calibration, validation, and application through some parametric analyses.

Regarding technology transfer, we have written two journal articles and submitted during the last quarter. We have also written a final report summarizing the two modeling subtasks (M4a-1 and F3b-1) together. The report is currently 85% completed.

Significant Problems, Issues and Potential Impact on Progress

None.

Work Planned Next Quarter

In the next quarter we will finish the final report and submit it to Texas A&M University.

Lattice Micromechanical Model (NCSU)

Work Done in This Quarter

Lattice Micromechanical Model

In the recent past, air void shape characterization has been completed based on X-ray tomography images. Observations had revealed that air void shape is dependent on the surrounding aggregate structure. A procedure has been developed to generate air void particles in an existing aggregate structure based on these observations.

The effort in the current quarter has been focused on further verification of the air void generation algorithm. The algorithm relates the radius of the air void particle to the distance to its centroid from the closest aggregate. The relationship between these parameters can be defined using an appropriate function. While the general algorithm remains the same, choice of the function may change the shape of generated air voids drastically. After several trials, the functional form has been chosen based on the similarity of the generated shapes to the actual shapes that has been observed in X-ray images.

The effectiveness of the algorithm is shown in figure F3b-1.1 by visually comparing the results with actual microstructure. Given that the visual resemblance is good, the next step is to investigate the effect of air voids on mechanical properties of the microstructures. To this end, the lattice analysis has been performed on a scanned image of a real microstructure with different levels of virtually fabricated air voids. The resulting reduction in stiffness is compared with the experimental observations. The scanned microstructure is obtained from a cut surface of a cylindrical specimen fabricated from a Superpave 9.5 mm mixture (NCDOT S9.5B). The virtually fabricated air void levels are varied from 0% to 12% (an example microstructure with virtually generated air voids is shown in figure F3b-1.2). The stiffness values from the virtual specimens are normalized and compared with the stiffness reduction obtained from laboratory experiments (see figure F3b-1.3). As seen from the figure, the algorithm is able to capture the trend of reduction in stiffness due to increase in air void content.

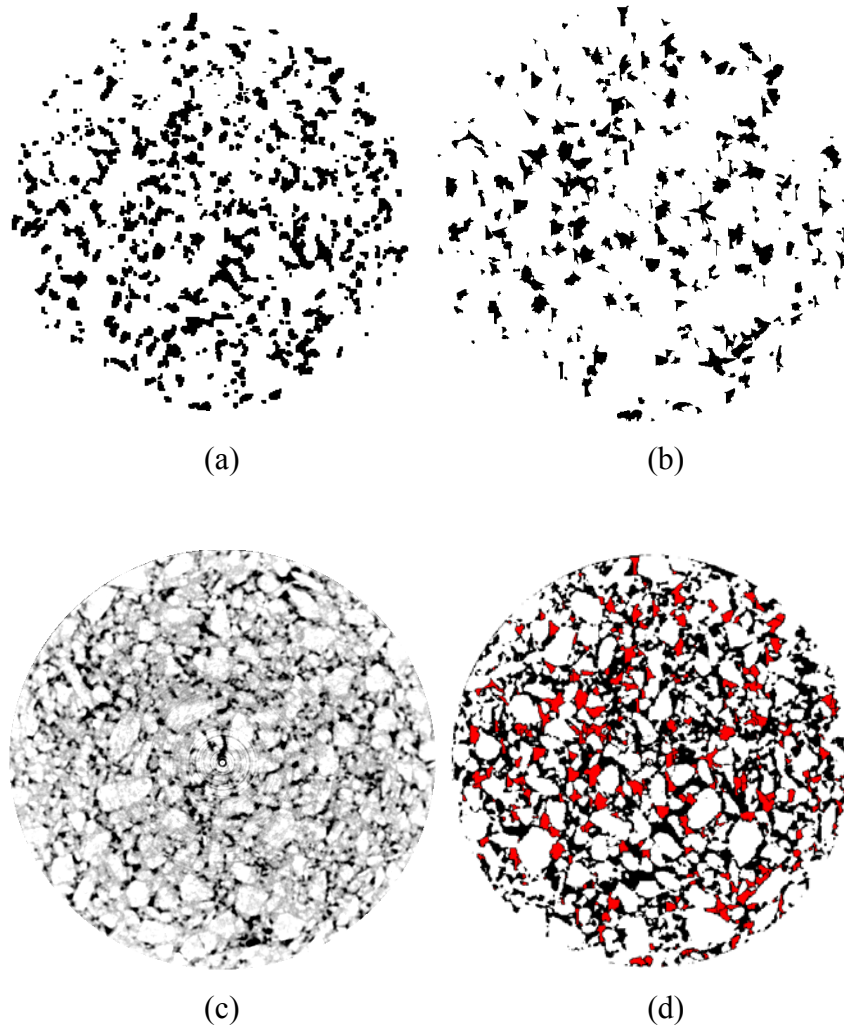


Figure F3b-1.1. Virtual air void fabrication of a real microstructure: (a) real air voids, (b) virtually fabricated voids, (c) real image with air voids, and (d) virtually fabricated voids on a real aggregate structure.

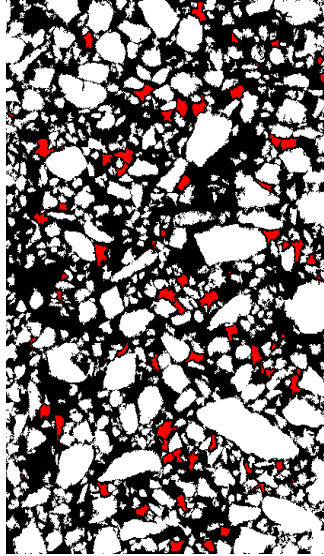


Figure F3b-1.2. Virtually generated air voids (air void content = 4%).

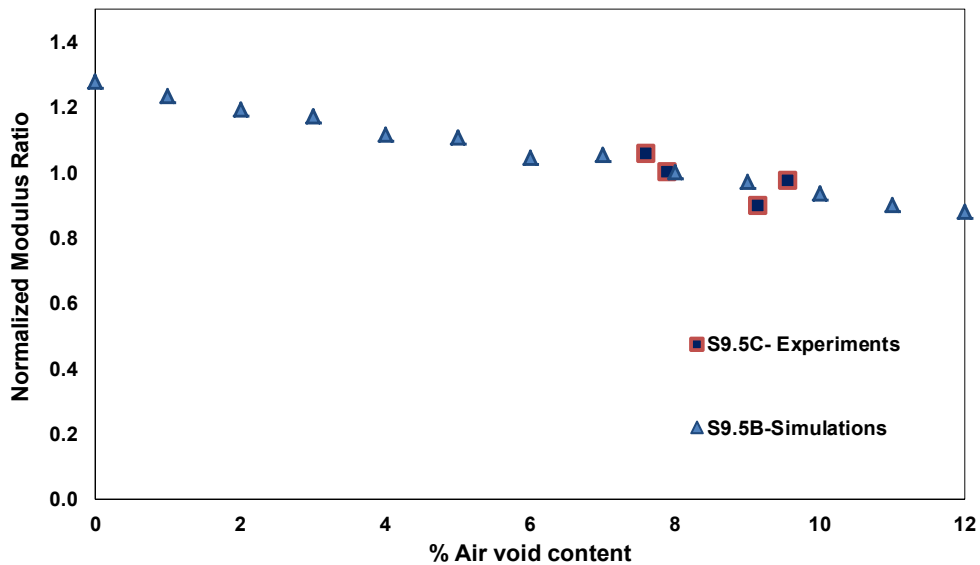


Figure F3b-1.3. Effect of air void content on initial stiffness: comparison between virtual testing and experimental observations.

Continuum Damage to Fracture

The drop of phase angle is widely used as an indicator of fracture of asphalt concrete under fatigue loading. In this quarter, investigation continued on the reason associated with the phase angle drop. The nonlinearity appears to result in the distortion of the material response (stress history in cross-head control test, see e.g. figure F3b-1.4), which in turn appears to result in

apparent phase angle drop. Various approaches are being investigated to quantify this nonlinearity.

Given the high level of nonlinearity, the traditional method to calculate the phase angle will cause significant error. To further study this, four other methods are also applied to obtain the phase shift between the stress and strain, both before and after the phase angle drop. These four methods define the phase angle as the time lag between the stress and strain at their maximum, minimum, increasing zero and decreasing zero, respectively. It is found that before the phase angle drops, all these methods result in almost the same phase angle. However, after the phase angle drops, because of the irregularity in the signal shape, the four time lags are not consistent, indicating that the “phase angle” cannot be accurately defined after fracture. Further work is needed to gain better insight into this phenomenon, which is currently underway.

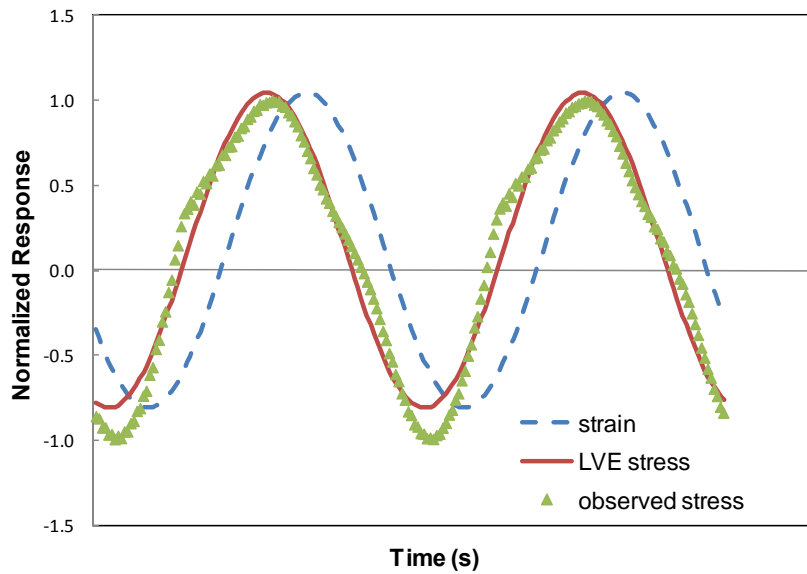


Figure F3b-1.4. Schematic representation of nonlinear viscoelastic response.

Significant Results

Lattice Micromechanical Model

From the results obtained in this quarter the following paper has been submitted to TRB conference 2012 for presentation.

Banadaki, A., M. Guudati, Y . Kim, “An Algorithm for Virtually Fabricating Air Voids in Asphalt Concrete”.

Continuum Damage to Fracture

It is found that the reason for apparent phase angle drop is highly related to the nonlinearity resulting in significant distortion in stress history. Further work is underway in characterizing this nonlinearity.

Significant Problems, Issues and Potential Impact on Progress

None

Work Planned Next Quarter

Lattice Micromechanical Model

- Calibration of the air void fabrication algorithm on virtually generated microstructure.
- Evaluating the fatigue performance of the specimen with virtually fabricated air voids and comparing with experimental results.

Continuum Damage to Fracture

- In the next quarter, we will continue to investigate the nonlinearity and the mechanism of localization and fracture.

Work Element F3c: Development of Unified Continuum Model (TAMU)

Work Done This Quarter

See M4c for details on the progress in the development of the continuum-based moisture-induced damage mode. Also see F1d-8 on the development of the continuum-based micro-damage healing model. We have completed the calibration and validation of the nonlinear viscoelastic and viscoplastic constitutive models in PANDA using the ALF laboratory data based on compression and tension data under different temperatures. However, most of the emphasis in this quarter was placed on the development of a three-dimensional multi-axial thermo-viscoplastic hardening/softening model based on a new novel concept which is the “memory viscoplastic softening surface” (Darabi et al. 2011a, b; Huang et al. 2011). This memory surface takes into consideration the change in the viscoplastic properties during the recovery period (or unloading time) within the cyclic loading history. When subjected to cyclic loading with rest periods between the loading cycles, the viscoplastic behavior of asphalt mixes changes such the rate of accumulation of the viscoplastic strain at the beginning of the subsequent loading cycle increases comparing to that at the end of the preceding loading cycle. This phenomenon is referred to as the viscoplastic-softening (Masad et al. 2005) and is a key element in predicting the permanent deformation (i.e. rutting) of asphalt pavements which is one of the most important distresses in asphalt pavements. It has been shown that the classical hardening plasticity/viscoplasticity theories fail to capture this distinct behavior of asphalt mixes (Darabi et

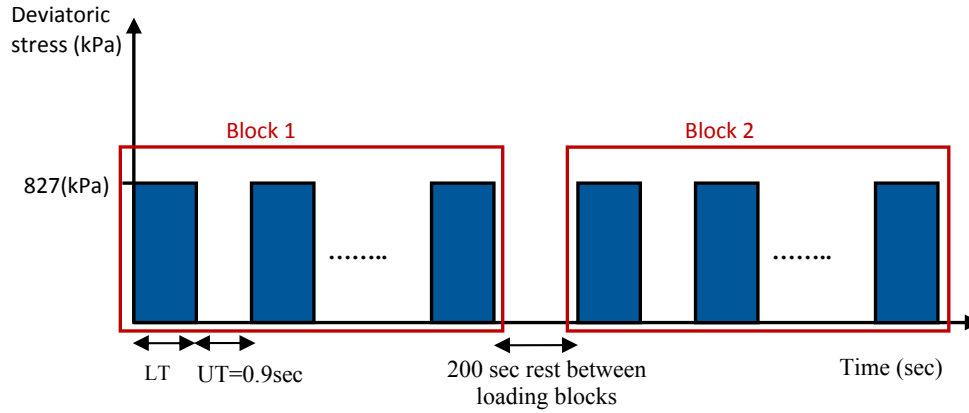
al. 2011a, b). The viscoplastic-softening behavior of asphalt mixes are related to the changes in the microstructure of asphalt mixes during the rest period.

A physically-based rate-dependent viscoplastic-softening model is proposed to significantly enhance the prediction of the permanent deformation in asphaltic materials subjected to cyclic loadings at high temperatures. A viscoplastic-softening memory surface is defined in the viscoplastic strain space as the general condition for the initiation and evolution of the viscoplastic-softening. The memory surface is formulated to be a function of an internal state variable memorizing the maximum viscoplastic strain for which the softening has been occurred during the deformation history. The evolution function for the viscoplastic-softening model is then defined as a function of the viscoplastic-softening internal state variable.

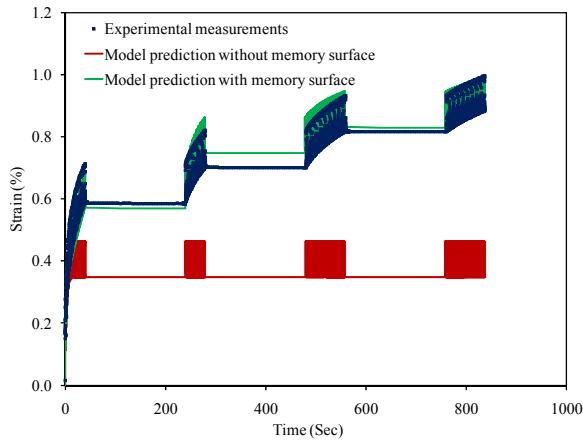
Finally, work has been started on applying realistic loading conditions from a wheel such that normal and shear stresses are taken into consideration. This is crucial for the accurate prediction of rutting and fatigue damage in asphalt pavements.

Significant Results

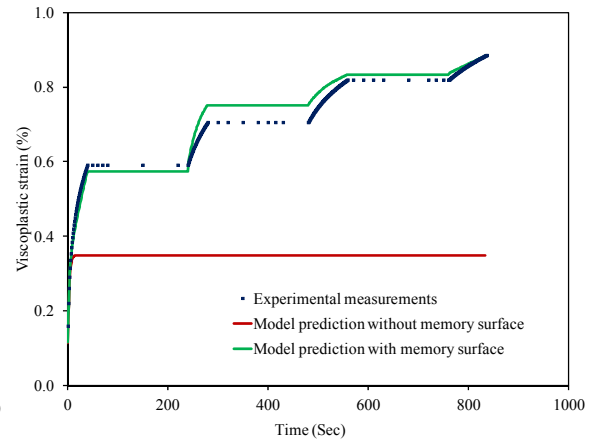
We have developed a model to account for the softening behavior of asphalt mixtures under repeated loading. This model was proven to be essential for predicting accumulation of permanent deformation. The viscoplastic-softening model is validated against the ALF experimental tests for different loading histories. Figures F3c.1 and F3c.2 show examples for the validation of the viscoplastic-softening model. These figures clearly show that the viscoplastic-softening model significantly improves the prediction of permanent deformation in asphalt mixes. The viscoplastic-softening model is believed to be the key element in predicting the rutting performance of asphalt pavements.



(a)

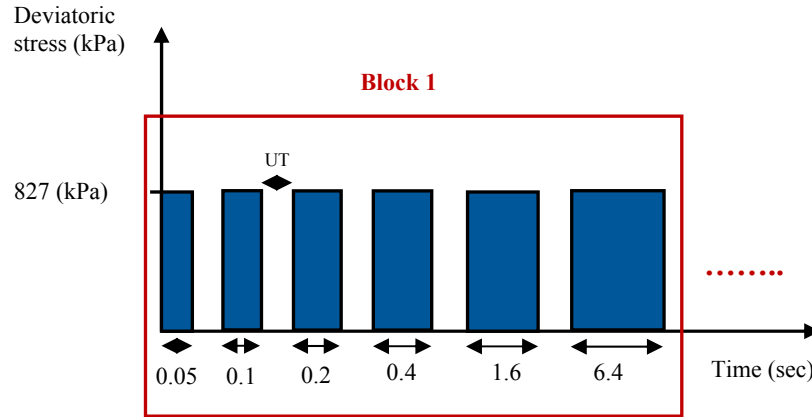


(b)

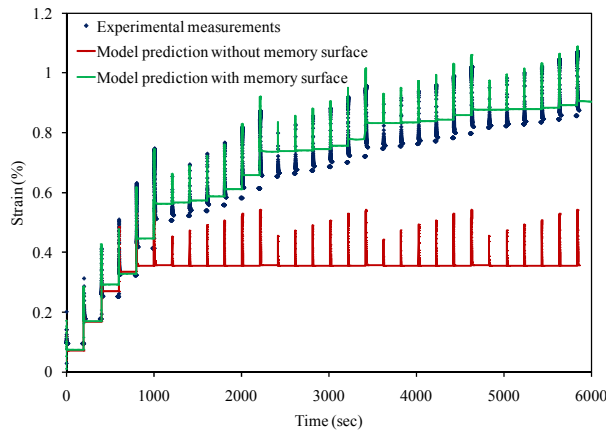


(c)

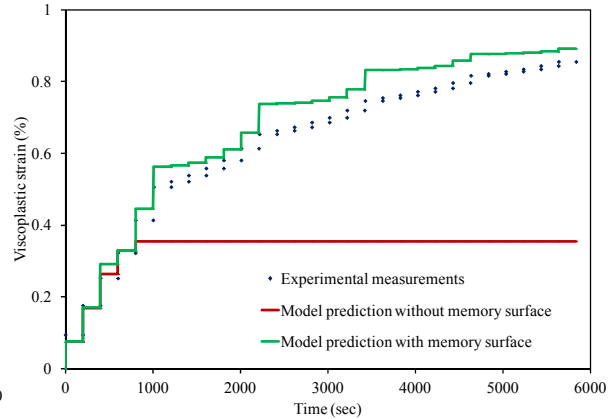
Figure F3c.1. (a) Schematic representation of the stress input for the constant loading time test (CLT). Both loading time (LT) and unloading time (UT) are constant through the entire test. CLT test data is available for four different loading times (LT) of 0.1, 0.4, 1.6, and 6.4 sec. Experimental measurements and model prediction with and without the viscoplastic memory surface for the constant loading and time test (CLT) at 55°C in compression when the loading time is 0.1 sec. This test consists of four loading blocks and 240 loading cycles. (a) total strain response; (b) viscoplastic strain response.



(a)



(b)



(c)

Figure F3c.2. (a) Schematic representation of stress input for variable loading time test (VT). The unloading time (UT) is constant through the test. However, this test is conducted for different unloading times of 0.05, 1, and 200 sec; Experimental measurements and model predictions with and without viscoplastic-softening memory surface for variable loading time test (VT) at 55°C in compression when rest period is 200 sec. (b) total strain response; (c) viscoplastic strain response.

Significant Problems, Issues and Potential Impact on Progress

None

Work Planned Next Quarter

We will work on the simulations of the structural response of the ALF pavements. Also, a parametric study will be conducted to see the effect of viscoplastic hardening/softening model on the rutting predictions under different loading conditions. Wheel realistic loading conditions due

to normal and shear stresses will be taken into consideration and their effect will be investigated thoroughly.

Continuum-based Model for Aging

Work Done This Quarter

This task was temporarily suspended in this quarter and resources were diverted to the task on the validation of PANDA against the ALF rutting tests. We expect to resume work on this task as soon as we complete the validation of PANDA against the ALF rutting performance data.

Significant Results

There are no significant results for this quarter.

Significant Problems, Issues and Potential Impact on Progress

Although this task is temporarily suspended, this task will be resumed this coming quarter.

Work Planned Next Quarter

The mechanistic oxidation aging model that has been developed will be fully calibrated and validated based on the ARC testing plan. Aging data are available now to accomplish this task. The dynamic modulus data at different aging times (0, 3, and 6 months) will be used in the calibration and validation process.

Cited References

Darabi, M.K., K. Abu Al-Rub, E.A. Masad, C.W. Huang, and D.N. Little, "A viscoplastic-softening memory surface that enhances the prediction of permanent deformation of asphaltic materials under cyclic loading," 2011a (In preparation).

Darabi, M.K., "Thermo-Viscoelastic-Viscoplastic-Viscodamage-Healing Modeling of Bituminous Materials: Theory and Computation," Ph.D. dissertation, Texas A&M University, College Station, Texas, 2011b.

Huang, C.W., M.K. Darabi, E.A. Masad, R.K. Abu Al-Rub, and D.N. Little, "Development, Characterization and Validation of the Nonlinear Viscoelastic-Viscoplastic and Softening Model of Asphalt Mixtures," 2011 (In preparation).

Masad, E., L. Tashman, D. Little, and H. Zbib, 2005, Viscoplastic modeling of asphalt mixes with the effects of anisotropy, damage and aggregate characteristics, *Mechanics of Materials*, 37, 1242-1256.

TABLE OF DECISION POINTS AND DELIVERABLES FOR FATIGUE

Name of Deliverable	Type of Deliverable	Description of Deliverable	Original Delivery Date	Revised Delivery Date	Reason for changes in delivery date
F1a: Cohesive and Adhesive Properties (TAMU)	Draft Report	Draft Report on Cohesive and Adhesive Properties, 508 compliant	11/11	N/A	N/A
	Final Report		6/30/12		
F1b-1: Nonlinear viscoelastic response under cyclic loading (TAMU)	Models and Algorithm	A constitutive model that accounts for the nonlinearity and three - dimensional stress state of the material including a method to obtain model constants for asphalt binders.	3/31/09 6/30/10 12/31/11	3/31/13	It is more efficient and informative if the three different final reports, models and algorithms are consolidated into a single final report. The work at UT Austin that will make up the final report is 60% complete.
	Draft report		12/31/08 12/31/11		
	Final report		6/30/08 3/31/12	6/30/13	
F1b-2: Viscoelastic properties under monotonic loading (TAMU)	Draft Report	Documentation of PANDA Models and Validation Including the Method for Analysis of Viscoelastic Properties	11/11	12/31/12	N/A
	Final Report (M5, M4c, F1b-1, F1c, F1d-8, F3c, and V3c)		3/12	3/31/13	N/A
F1c: Aging (Unified Continuum Model for Aging) (TAMU)	Draft Report	Draft Report on the aging modeling	03/12	12/31/12	N/A
	Final Report (M5, M4c, F1b-1, F1c, F1d-8, F3c, and V3c)		3/31/12	3/31/13	Validation of the aging model based on the ARC testing.
F1c-2. Experimental Design (TAMU)	Report	Experimental Design Report	1/09	Complete	N/A

Name of Deliverable	Type of Deliverable	Description of Deliverable	Original Delivery Date	Revised Delivery Date	Reason for changes in delivery date
F1d – 1,2,3,4,5a,5b,8: Healing (TAMU)	Models and Algorithm	A mathematical model for self-healing at the micron scale, partial validation of this model, measurement of properties related to this model, measurement of overall healing as a function of damage and rest period, and micro to nano scale evaluation of properties that influence fracture and self-healing	06/30/11	3/31/13	It is more efficient and informative if the different final reports, models and algorithms are consolidated into a single final report. The final report is based on two theses: the thesis from Texas A&M University is complete and work for the thesis from UT Austin is 70% complete.
	Draft report		06/30/10 06/30/11 12/31/11		
F1d-6: Evaluate relationship between healing and endurance limit of asphalt binders (UWM)	Draft Report	Report summarizing major findings for evaluation of healing of binders by means of cyclic testing with rest periods	12/11	10/11	The reports for F1d-6, F2e and F2a-5 are combined. (report “M”)
	Final Report	Final report in 508 format on healing characterization of binders and its relation to fatigue performance	1/12	4/12	The reports for F1d-6, F2e and F2a-5 are combined. (report “M”)
F1d-8: Coordinate Form of Healing Parameter with Micromechanics and Continuum Damage Models (TAMU)	Draft Report (M5, M4c, F1b-1, F1c, F1d-8, F3c, and V3c)	Draft Report on the self-healing modeling	12/11	12/31/12	Validation based on ARC testing.
	Final Report (M5, M4c, F1b-1, F1c, F1d-8, F3c, and V3c)	Report on the self-healing modeling	3/12	3/31/13	Validation based on ARC testing.

Name of Deliverable	Type of Deliverable	Description of Deliverable	Original Delivery Date	Revised Delivery Date	Reason for changes in delivery date
F2a-5: Analyze data and propose mechanisms (UWM)	Draft Report	Report summarizing major findings for the effect of modification on asphalt binder performance at high and intermediate temperatures.	10/11	Complete	The reports for F1d-6, F2e and F2a-5 are combined. (report "M")
	Final Report	Report in 508 format summarizing major findings for the effect of modification on asphalt binder performance at high and intermediate temperatures	1/12	4/12	
F2d: Structural Characterization of Micromechanical Properties in Bitumen using Atomic Force Microscopy (TAMU)	Protocol for Measuring Viscoelastic Properties Using AFM	Protocol for preparing samples and taking measurements in AASHTO format – Protocol development complete, AASHTO format planned for 5/30/11	7/31/10	Complete	The test protocol was successfully used to measure the micro rheology of aged and unaged asphalt binders. The findings and method are current being reviewed as a journal article.
	Evaluation of Impact of Aging and Moisture Conditioning	Complete	12/15/10	Complete	N/A
	Final Research Report		2/28/12	N/A	N/A
F2e-2: Selection of Testing Protocols (UWM)	Draft Report	Report on the development and implementation of the Binder Yield Energy (BYET) test and the Linear Amplitude Sweep Test (LAS)	4/09	Complete	The reports for F1d-6, F2e and F2a-5 are combined. (report "M")
	Final Report		7/09		
	Draft Report		4/10		
	Final Report		7/10		
F2e-4: Verification of Surrogate Fatigue Test (UWM)	Draft Report	Correspond to reports in F2e-2	10/10	Complete	N/A
	Final Report		1/11		

Name of Deliverable	Type of Deliverable	Description of Deliverable	Original Delivery Date	Revised Delivery Date	Reason for changes in delivery date
F2e-6: Recommendations for Use in Unified Fatigue Damage Model (UWM)	Draft Report	Report summarizing major findings for each subtask. The report includes: evaluation of correlations between binder and mixture fatigue performance, comparison between binder fatigue testing procedures, verification/validation of LAS test	11/11	10/11	The reports for F1d-6, F2e and F2a-5 are combined. (report "M")
	Final Report	Final report in 508 format on the development and implementation of the Linear Amplitude Sweep (LAS) Test. It includes the latest AASHTO standard.	1/12	4/12	
F3b-1: Micromechanics Model Development (Fatigue) (UNL)	Models and Algorithm	Cohesive zone fracture modeling of asphalt mixtures considering inelasticity, nonlinearity, rate-dependent fracture, and mixture microstructure: modeling methodology, constitutive theory, testing protocols, test data, model simulation/calibration/validation, user element (UEL) codes in ABAQUS, and user-friendly manuals. Multiscale modeling of asphaltic mixtures and pavements: modeling methodology, constitutive theory, and parametric analyses of the model.	3/31/11	Complete	Model to be included in final report.
	Draft report		06/30/11	12/31/11	This subtask needs more time for model validation and the final report.
	Final report		12/31/11	8/14/12	
F3c: Development of Unified Continuum Model (TAMU)	PANDA Workshop	Workshop on PANDA Models and Validation Results	8/11	4/13	Waiting for complete validation of PANDA models.
	Draft Report	Documentation of PANDA Models and Validation	11/11	12/31/12	
	Final Report		3/12	3/31/13	
	UMAT Material	PANDA Implemented in Abaqus	3/12	3/31/13	
	PANDA standalone finite element software	Standalone two-dimensional and three-dimensional finite element software for PANDA	3/31/12	3/31/13	Creating the user friendly interface for PANDA

Fatigue Year 5		Year 5 (4/11-3/12)												Team
		4	5	6	7	8	9	10	11	12	1	2	3	
Material Properties														
F1a	Cohesive and Adhesive Properties													
F1a-1	Critical review of literature													TAMU
F1a-2	Develop experiment design													
F1a-3	Thermodynamic work of adhesion and cohesion													
F1a-4	Mechanical work of adhesion and cohesion													
F1a-5	Evaluate acid-base scale for surface energy calculations						JP							
F1b	Viscoelastic Properties													
F1b-1	Separation of nonlinear viscoelastic deformation from fracture energy under cyclic loading									JP	D		M&A,F	TAMU
F1b-2	Separation of nonlinear viscoelastic deformation from fracture energy under monotonic loading						JP	M&A,D					F	
F1c	Aging													
F1c-1	Critical review of binder oxidative aging and its impact on mixtures													TAMU
F1c-2	Develop experiment design													
F1c-3	Develop transport model for binder oxidation in pavements						JP			D	M&A		F	
F1c-4	Effect of binder aging on properties and performance						JP			D			F	
F1c-5	Polymer modified asphalt materials									D			F	
F1d	Healing													
F1d-1	Critical review of literature													TAMU
F1d-2	Select materials with targeted properties													TAMU
F1d-3	Develop experiment design						JP		JP	D		M&A	F	TAMU
F1d-4	Test methods to determine properties relevant to healing													TAMU
F1d-5	Testing of materials													TAMU
F1d-6	Evaluate relationship between healing and endurance limit of asphalt binders						JP			D	F			UWM
F1d-7	Coordinate with AFM analysis												F	WRI
F1d-8	Coordinate form of healing parameter with micromechanics and continuum damage models								JP	D			F	TAMU
Test Methods														
F2a	Binder tests and effect of composition													
F2a-1	Analyze Existing Fatigue Data on PMA													UWM
F2a-2	Select Virgin Binders and Modifiers and Prepare Modified Binder													
F2a-3	Laboratory Aging Procedures													
F2a-4	Collect Fatigue Test Data													
F2a-5	Analyze data and propose mechanisms					P			D			F		
F2b	Mastic testing protocol													
F2b-1	Develop specimen preparation procedures													TAMU
F2b-2	Document test and analysis procedures in AASHTO format													
F2c	Mixture testing protocol													
F2c-1	Develop specimen preparation procedures		P	P	P(2)		P(2)							
F2d	Tomography and microstructural characterization													
F2d-1	Micro scale physicochemical and morphological changes in asphalt binders													TAMU
F2e	Verify relationship between DSR binder fatigue tests and mixture fatigue performance													
F2e-1	Evaluate Binder Fatigue Correlation to Mixture Fatigue Data													UWM
F2e-2	Selection of Testing Protocols													
F2e-3	Binder and Mixture Fatigue Testing													
F2e-4	Verification of Surrogate Fatigue Test													
F2e-5	Interpretation and Modeling of Data													
F2e-6	Recommendations for Use in Unified Fatigue Damage Model								D			F		
Models														
F3a	Asphalt microstructural model										M&A		F	WRI
F3b	Micromechanics model													
F3b-1	Model development				D		JP	DP			F, SW		P	TAMU
F3b-2	Account for material microstructure and fundamental material properties													
F3c	Develop unified continuum model													
F3c-1	Analytical fatigue model for mixture design							M&A,D					F	TAMU
F3c-2	Unified continuum model				D			DP			F, SW			
F3c-3	Multi-scale modeling				D						F			
	Lattice Model							JP			JP		F	NCSU
	Continuum Damage to Fracture							JP			JP			

LEGEND

Deliverable codes

- D: Draft Report
- F: Final Report
- M&A: Model and algorithm
- SW: Software
- JP: Journal paper
- P: Presentation
- DP: Decision Point
- [x]
- Work planned
- Work completed
- Parallel topic

Deliverable Description

- Report delivered to FHWA for 3 week review period.
- Final report delivered in compliance with FHWA publication standards
- Mathematical model and sample code
- Executable software, code and user manual
- Paper submitted to conference or journal
- Presentation for symposium, conference or other
- Time to make a decision on two parallel paths as to which is most promising to follow through
- Indicates completion of deliverable x

Fatigue Year 2 - 5		Year 2 (4/08-3/09)				Year 3 (4/09-3/10)				Year 4 (04/10-03/11)				Year 5 (04/11-03/12)				Team	
		Q1	Q2	Q3	Q4	Q1	Q2	Q3	Q4	Q1	Q2	Q3	Q4	Q1	Q2	Q3	Q4		
Material Properties																			
F1a	Cohesive and Adhesive Properties																		
F1a-1	Critical review of literature			JP													TAMU		
F1a-2	Develop experiment design																		
F1a-3	Thermodynamic work of adhesion and cohesion																		
F1a-4	Mechanical work of adhesion and cohesion						JP			D	F								
F1a-5	Evaluate acid-base scale for surface energy calculations													JP					
F1b	Viscoelastic Properties																		
F1b-1	Separation of nonlinear viscoelastic deformation from fracture energy under cyclic loading			D,JP	M&A				JP	M&A,F,J	JP		P			JP,D	F,M&A	TAMU	
F1b-2	Separation of nonlinear viscoelastic deformation from fracture energy under monotonic loading			JP	M&A				JP				JP		JP,M&A	D	F		
F1c	Aging																		
F1c-1	Critical review of binder oxidative aging and its impact on mixtures																	TAMU	
F1c-2	Develop experiment design			D		F													
F1c-3	Develop transport model for binder oxidation in pavements		P		P,JP		P		P,JP		P,JP	JP	JP		JP	D	M&A	F	
F1c-4	Effect of binder aging on properties and performance				JP,P		JP	D	F						JP		D	F	
F1c-5	Polymer modified asphalt materials						P										D	F	
F1d	Healing																		
F1d-1	Critical review of literature																	TAMU	
F1d-2	Select materials with targeted properties																	TAMU	
F1d-3	Develop experiment design															JP	JP,D	F,M&A	TAMU
F1d-4	Test methods to determine properties relevant to healing			JP					JP	D	F							TAMU	
F1d-5	Testing of materials						JP			JP								TAMU	
F1d-6	Evaluate relationship between healing and endurance limit of asphalt binders	DP				DP	JP	DP					JP,P		JP	D	F	UWM	
F1d-7	Coordinate with AFM analysis									JP								F	WRI
F1d-8	Coordinate form of healing parameter with micromechanics and continuum damage models																JP,D	F	TAMU
Test Methods																			
F2a	Binder tests and effect of composition																		
F2a-1	Analyze Existing Fatigue Data on PMA			DP															UWM
F2a-2	Select Virgin Binders and Modifiers and Prepare Modified Binder			DP															
F2a-3	Laboratory Aging Procedures																		
F2a-4	Collect Fatigue Test Data		P		JP		P		P					P,DP,JP					
F2a-5	Analyze data and propose mechanisms				P		P					P			P	D	F		
F2b	Mastic testing protocol																		
F2b-1	Develop specimen preparation procedures		D								F								TAMU
F2b-2	Document test and analysis procedures in AASHTO format		D								F								
F2c	Mixture testing protocol		D,JP	F	P,JP	JP	P	P	JP	P	P	JP	P	P	P(2)	P(4)			
F2d	Tomography and microstructural characterization																		
F2d-1	Micro scale physicochemical and morphological changes in asphalt binders						JP						JP						TAMU
F2e	Verify relationship between DSR binder fatigue tests and mixture fatigue performance																		
F2e-1	Evaluate Binder Fatigue Correlation to Mixture Fatigue Data																		UWM
F2e-2	Selection of Testing Protocols				DP,D	F				D	F								
F2e-3	Binder and Mixture Fatigue Testing																		
F2e-4	Verification of Surrogate Fatigue Test												D	F,DP					
F2e-5	Interpretation and Modeling of Data		JP		P		JP		P		JP		M&A						
F2e-6	Recommendations for Use in Unified Fatigue Damage Model												P				D	F	
Models																			
F3a	Asphalt microstructural model							JP									M&A	F	WRI
F3b	Micromechanics model																		
F3b-1	Model development				JP				JP			P,JP	P,M&A	D	JP,DP	F,SW	P	TAMU	
F3b-2	Account for material microstructure and fundamental material properties																		
F3c	Develop unified continuum model																		
F3c-1	Analytical fatigue model for mixture design															M&A,D		F	TAMU
F3c-2	Unified continuum model			JP			JP					JP	M&A	D	DP	F,SW			
F3c-3	Multi-scale modeling											JP	M&A	D		F			
	Lattice Model														JP	JP	F		NCSU
	Continuum Damage to Fracture														JP	JP			

LEGEND

Deliverable codes

- D: Draft Report
- F: Final Report
- M&A: Model and algorithm
- SW: Software
- JP: Journal paper
- P: Presentation
- DP: Decision Point
- [x]

- Work planned
- Work completed
- Parallel topic

Deliverable Description

- Report delivered to FHWA for 3 week review period.
- Final report delivered in compliance with FHWA publication standards
- Mathematical model and sample code
- Executable software, code and user manual
- Paper submitted to conference or journal
- Presentation for symposium, conference or other
- Time to make a decision on two parallel paths as to which is most promising to follow through
- Indicates completion of deliverable x

PROGRAM AREA: ENGINEERED MATERIALS

CATEGORY E1: MODELING

Work element E1a: Analytical and Micro-mechanics Models for Mechanical Behavior of Mixtures (TAMU)

Work Done This Quarter

In this quarter, the following technical presentations were made at the 48th Petersen Asphalt Research Conference in Laramie, Wyoming:

1. “Characterization of Permanent Deformation and Cracking of Asphalt Mixtures in Compression”;
2. “Characterization of Fatigue Cracking and Healing of Asphalt Mixtures”;
3. “Characterizing Fatigue Crack Growth of Fine Asphalt Mixture Conditioned at Different Relative Humidity Using Dynamical Mechanical Analyzer”; and
4. “Complex Stiffness Gradient Estimation of Field-Aged Asphalt Concrete Layers Using the Direct Tension Test.”

Investigation is continued on healing properties of laboratory-mixed-laboratory-compacted (LMLC) asphalt mixtures, fracture and healing properties of field cores and fine aggregate mixture testing.

1. Healing Properties of LMLC Asphalt Mixtures

The development work on characterization of healing properties of asphalt mixtures continues in this quarter. In the last quarter, the driven forces for the healing process and the material properties required to conduct the mechanistic analysis for the healing process were studied. The driven forces for the healing process are used to calculate the true stresses that drive healing, which are further used with the determined material properties to derive the true strains in the healing process. The true stresses and true strains are then used to construct the energy balance equation to determine the damage density of a damaged asphalt mixture in the healing process. The change of the damage density from the beginning of the recovery phase to any time during the recovery phase thus represents the extent of healing that occurs during that period. In order to determine the change of the damage density, the initial damage density in the healing process has to be determined first since it is the starting point based on which the change can be quantified.

In the revised creep and recovery test, the initial damage density of the healing process is the damage density at the end of the creep phase. Determination of the initial damage density involves four steps, including 1) determination of the apparent and true material properties, which was elaborated in the last quarterly report; 2) calculation of the pseudo strain and reference modulus; 3) determination of the true creep strain and true creep stress of the damaged asphalt mixtures; and 4) determination of the damage density. Steps 2 to 4 are discussed in sequence in the following section of this report.

The pseudo strain and reference modulus are needed to separate the viscoelastic effect from the damage for asphalt mixtures. The pseudo strain is calculated using equation E1a.1:

$$\varepsilon_R = \frac{\sigma_{VE}(t)}{E_R} \quad (\text{E1a.1})$$

where ε_R is the pseudo strain; $\sigma_{VE}(t)$ is the viscoelastic stress of the undamaged asphalt mixture; t is the loading time; and E_R is the reference modulus and is used to achieve dimensionless variables. The viscoelastic stress is calculated using the hereditary integral for viscoelastic materials as follows:

$$\sigma_{VE}(t) = \int_0^t E(t-\xi) \frac{d\varepsilon_c(\xi)}{d\xi} d\xi \quad (\text{E1a.2})$$

where ξ is any arbitrary time between 0 and t ; the lower integration limit 0 is 0^- to allow for a discontinuous change in stress at $t=0$; $\varepsilon_c(t)$ is the creep strain in the creep phase; and $E(t-\xi)$ is the relaxation modulus of undamaged asphalt mixture that was determined in Step 1. In the creep phase at $t=0$, there is a jump discontinuity so equation E1a.2 is expressed in the following way (Wineman and Rajagopal 2000):

$$\sigma_{VE}(t) = \varepsilon_c(0)E(t) + \int_0^t E(t-\xi) \frac{d\varepsilon_c(\xi)}{d\xi} d\xi \quad (\text{E1a.3})$$

in which the lower integration limit 0 now implies 0^+ . The reference modulus is selected as the magnitude of the complex modulus because assigning E_R a concrete physical meaning makes the pseudo strain comparable to the measured strain. The complex modulus is inferred from the relaxation modulus since they have the following relationship:

$$E^*(\omega) = i\omega \mathcal{L}\{E(t)\}_{s=i\omega} \quad (\text{E1a.4})$$

where $E^*(\omega)$ is the complex modulus; ω is the frequency; and $\mathcal{L}\{E(t)\}$ is the Laplace transform of $E(t)$. Substituting equation E1a.3 into equation E1a.1 with E_R determined as the magnitude of $E^*(\omega)$, the expression of ε_R can be obtained.

The true creep stress and true creep strain are needed to calculate the damage density of the damaged asphalt mixture in the creep phase. The true creep stress is the stress in the intact material of an asphalt mixture, so it can be calculated using the same formula as equation E1a.3:

$$\sigma_c^T(t) = \varepsilon_c^T(0)E^T(t) + \int_0^t E^T(t-\xi) \frac{d\varepsilon_c^T(\xi)}{d\xi} d\xi \quad (\text{E1a.5})$$

where $\sigma_c^T(t)$ is the true creep stress in an damaged asphalt mixture; $\varepsilon_c^T(t)$ is the true creep strain in an damaged asphalt mixture; and $E^T(t-\xi)$ is the true relaxation modulus of the undamaged asphalt mixture that was determined in Step 1. As a result, $\sigma_c^T(t)$ is obtained once $\varepsilon_c^T(t)$ is determined. $\varepsilon_c^T(t)$ is solved from the dissipated pseudo strain energy (DPSE) balance equation as follows:

$$\text{DPSE}^A = \text{DPSE}^T = \int_0^t \sigma_c^T(t) d\varepsilon_R^T \quad (\text{E1a.6})$$

in which DPSE^A is the apparent DPSE that is measured from the test; and DPSE^T is the true DPSE that is calculated by integrating the product of $\sigma_c^T(t)$ and the true pseudo strain ε_R^T . ε_R^T is calculated following the same procedure as discussed above for ε_R and it is a function of $\varepsilon_c^T(t)$. Since both $\sigma_c^T(t)$ and ε_R^T are functions of $\varepsilon_c^T(t)$ and $\varepsilon_c^T(t)$ is the only unknown variable in equation E1a.6, $\varepsilon_c^T(t)$ can be solved from equation E1a.6, and then $\sigma_c^T(t)$ is calculated by equation E1a.5. A plot of apparent creep stress, apparent creep strain, pseudo strain and true creep stress, true creep strain, true pseudo strain of a damaged asphalt mixture are presented in figure E1a.1. It shows that when the apparent creep stress is controlled as constant, the true creep stress in the intact material actually increases with time. The true creep strain in the intact material is also larger than the apparent creep strain.

The last step in determination of the initial damage density for the healing process is to calculate the damage density with the increase of time in the creep phase and identify the damage density at the end of the creep phase as the initial damage density. The damage density is calculated as follows:

$$\phi = V_b \% \left[1 - \frac{\sigma_c^A}{\sigma_c^T} \right] \quad (\text{E1a.7})$$

where ϕ is the damage density; σ_c^A is the apparent creep stress; σ_c^T is determined as above; and $V_b\%$ is the volumetric percentage of the asphalt mastic because cracks can only grow in the asphalt mastic rather than in the aggregate. A plot of the damage density versus time for the asphalt mixture with the binder AAD and binder AAM is given in figure E1a.2. The initial damage density of the AAD mixture is about 5.25% and that of the AAM mixture is around 5.16%.

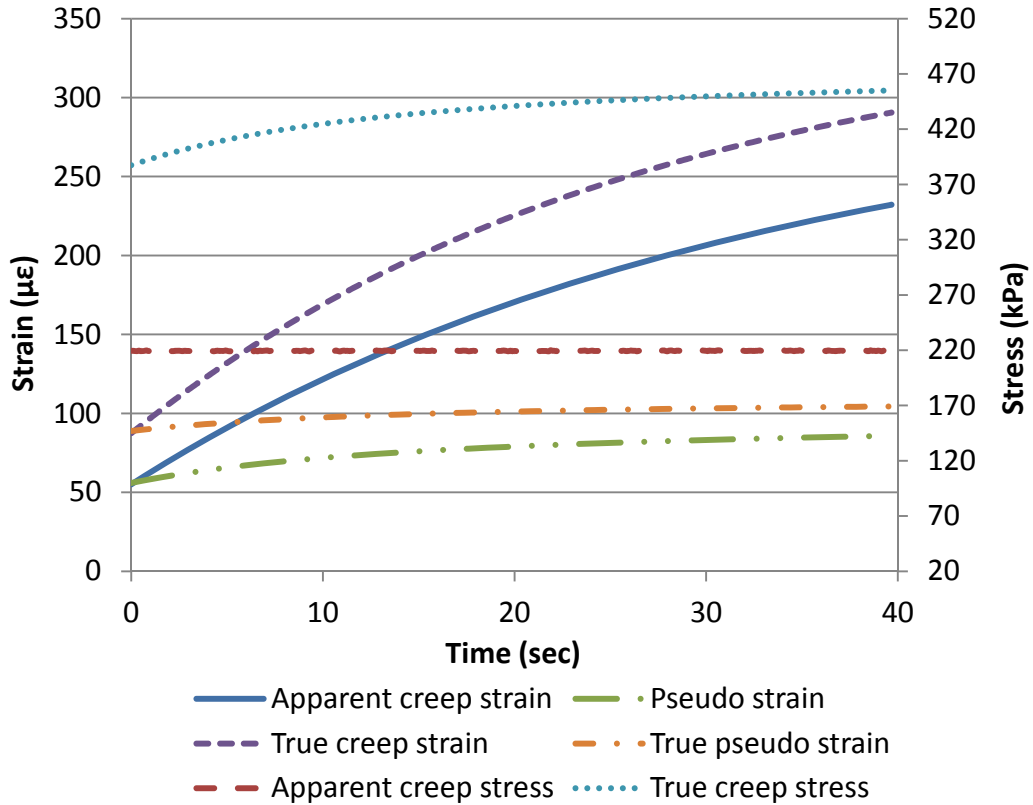


Figure E1a.1. Apparent stress/strain and true stress/strain in the creep phase of a destructive revised creep and recovery test.

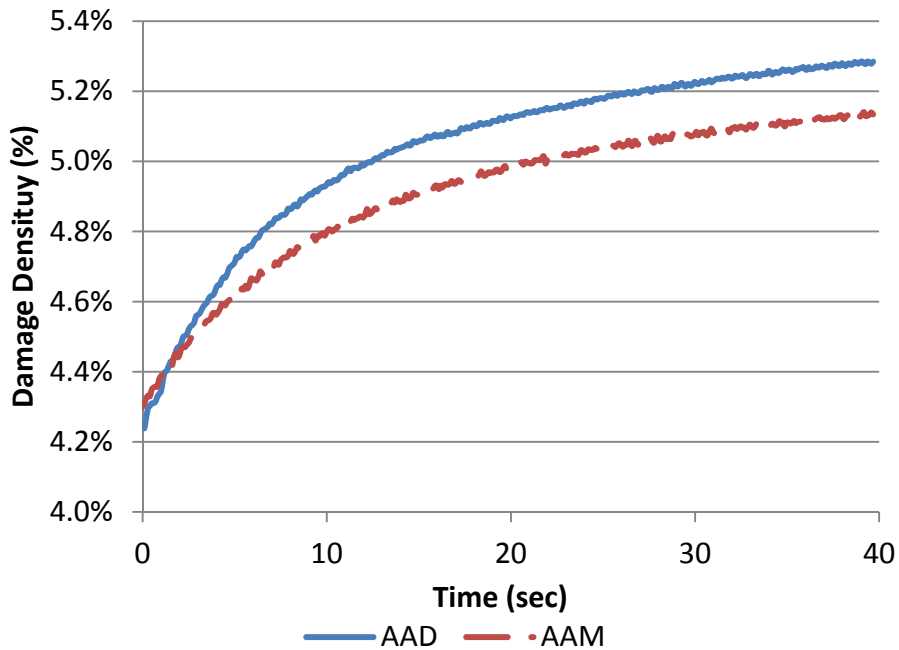


Figure E1a.2. Damage density versus time in the creep phase of destructive revised creep and recovery test.

2. Fracture and Healing Properties of Field Cores

In the previous quarterly report, the analytical procedure to find the actual crack length in any loading cycle was provided. As mentioned before, the Correspondence Principle together with an FE model were used to find the exact crack length in each load cycle. The next step was to find the fracture and healing properties of the tested specimen under repeating loading in the OT test. The traditional tests to measure the fatigue cracking susceptibility of mixes such as the four point bending beam test, are very expensive and time consuming (Zhu et al. 2009, Ramsamooj, 1991, Kallas et al. 1971). Different approaches are used to find the crack initiation and propagation mechanisms, namely, the conventional fatigue relationship based on regression equations, dissipated energy approach and fracture mechanics approach. (T.O.Medani et al. 2000, Pais et al. 2010, Paris et al. 1963).

Since the crack length can be calculated accurately in each cycle, this research utilized the generalized Paris' law in conjunction with Psuedostrain energy release concept to determine healing and fracture properties (Cleveland et al. 2003, Cleveland et al. 2002). The observations of the test results show that a lot of healing occurs during each displacement cycle. By using the pseudo strain energy and correspondence principle concepts the fracture and healing parameters can be obtained for each tested sample. The pseudo displacement is calculated by equation E1a.8.

$$U_r = \frac{P_{LVE}(t)}{k_r} \quad (E1a.8)$$

where P_{LVE} is the linear visco-elastic force and k_r is the reference stiffness with the value of the maximum load in the first load cycle divided by the maximum opening. Figure E1a.3 shows the reference displacement plotted against the measured load in a specific load cycle. As shown in figure E1a.3 the dissipated work area under the tensile part is related to the crack growth and the dissipated work under the compressive area is related to the healing.

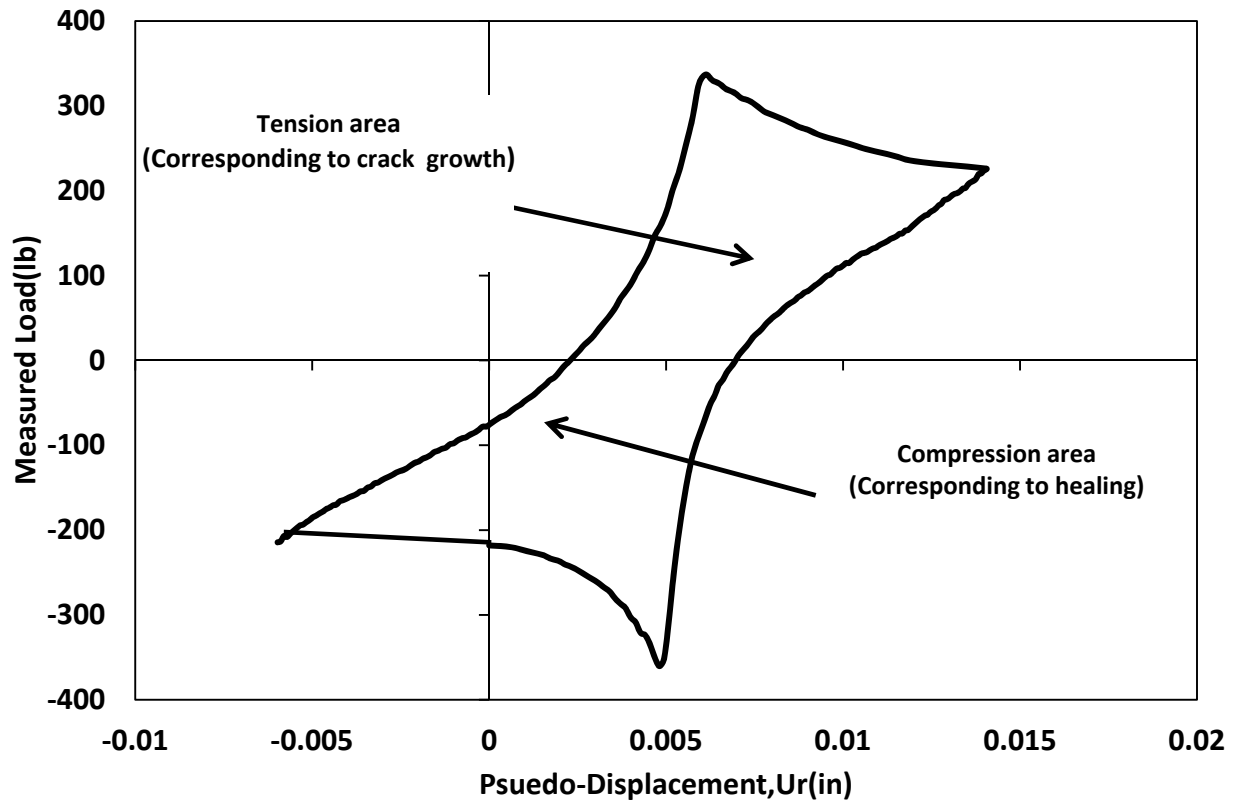


Figure E1a.3. Pseudo-displacement versus measured visco-elastic load.

By obtaining the crack length and dissipated work as functions of the displacement cycles, the J integral can be calculated using E1a.9 for both healing and fracturing modes.

$$J_R = \frac{\frac{\partial W_{R1}(N)}{\partial N}}{\frac{\partial(c.s.a)}{\partial N}} \quad (E1a.9)$$

Where the J_R is the J-integral, $\frac{\partial W_{R1}(N)}{\partial N}$ is the rate of change of dissipated work and $\frac{\partial(c.s.a)}{\partial N}$ is the rate of change of the crack surface area. The common version of Paris's law ($\frac{dC(N)}{d(N)} = A(J_R)^n$) does not give realistic results in this case. As mentioned before, the energy release rate decreases as the crack grows in the OT test. Therefore, the general format of Paris's law does not give reasonable answers. Consequently, the format shown in equation E1a.10 is used to determine the Paris's Law coefficients.

$$\frac{dC(N)}{d(N)} = A \left[\frac{WR1(N)}{c.s.a} \right]^n \quad (E1a.10)$$

where:

$$c.s.a = 2bC(N) \quad (E1a.11)$$

The power function is used to fit to the crack growth and the WRt(tension) versus load cycles. The same equations are used to find the healing properties B and m. As previously discussed, a significant amount of healing occurs during a very short time interval in each cycle.

The plots of WRt and WRc(compression) against load cycles for a lab compacted specimen with 4.1 percent air voids and PG 67-22 binder are shown in figures E1a.4 and E1a.5.

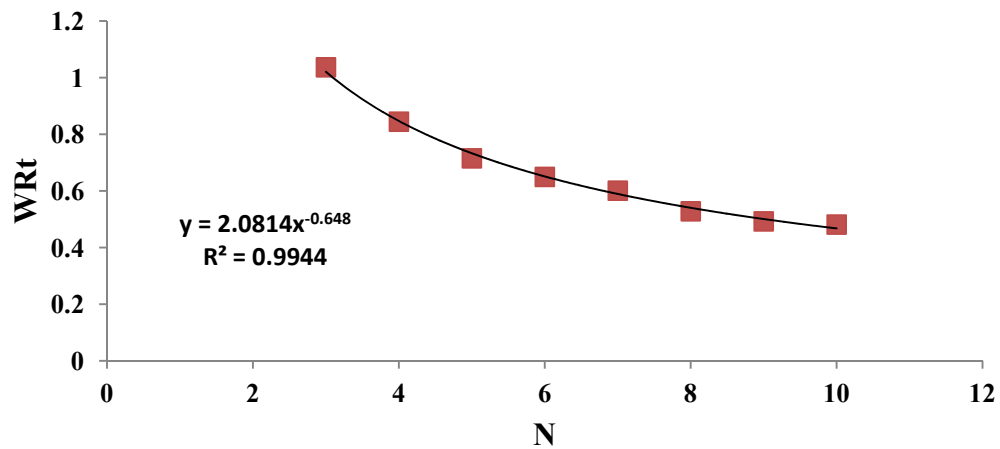


Figure E1a.4. WRt versus load cycles.

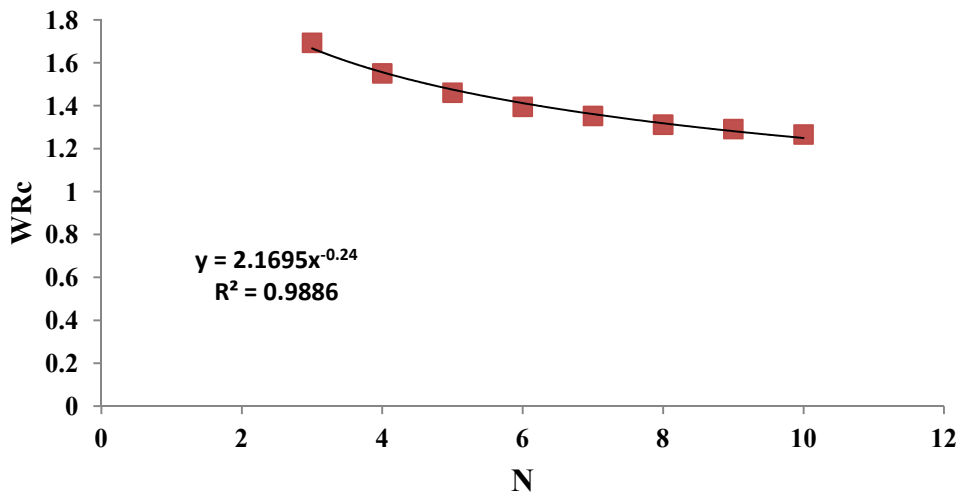


Figure E1a.5. WRC versus load cycles.

Table E1a.1 shows fracture and healing properties of this specimen.

Table E1a.1. Calculated fracture and healing properties.

A	n	B	m
0.07	1.06	0.02	2.86

The results also indicate that the healing occurs at a higher rate compared to the fracture.

3. Fine Aggregate Mixture Testing

In this quarter, the fine aggregate mixture (FAM) specimens for the Dynamic Mechanical Analyzer (DMA) were tested to determine their air void contents. Since the DMA specimens are cored from samples with a 6 in. diameter made by the SuperPave gyratory compactor, the DMA specimens cored from the outer circle of the 6 in diameter specimen have a larger air void content than those cored from the inner circle, which is consistent with what was observed in the pilot testing. This indicates that the closer to the center of the 6 in diameter gyratory specimen, the lower is the air void content. This pattern was found in both samples made with the Nustar PG67-22 binder and samples made with the Valero PG64-16 binder, as shown in figures E1a.6 and E2a.7.

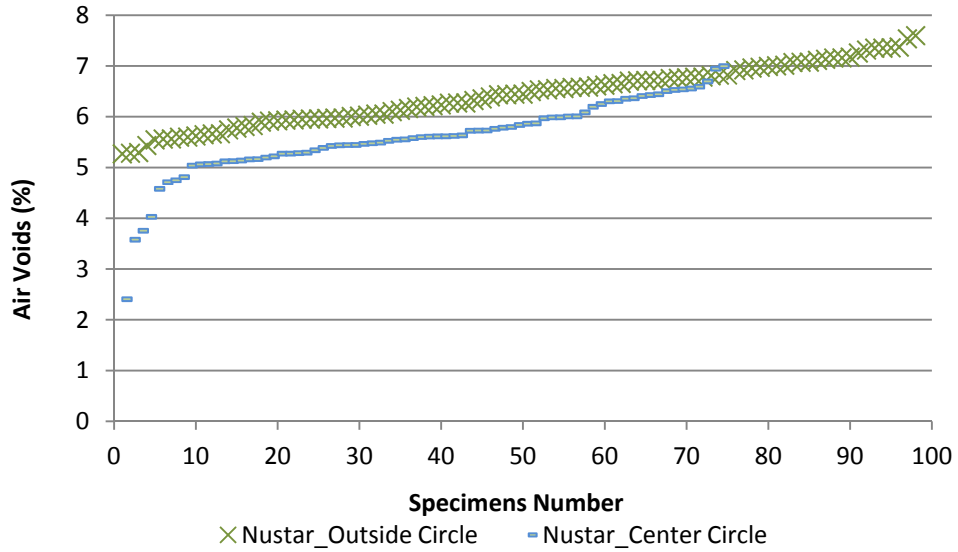


Figure E1a.6. Nustar PG67-22 with Hanson Limestone Specimens air void distribution.

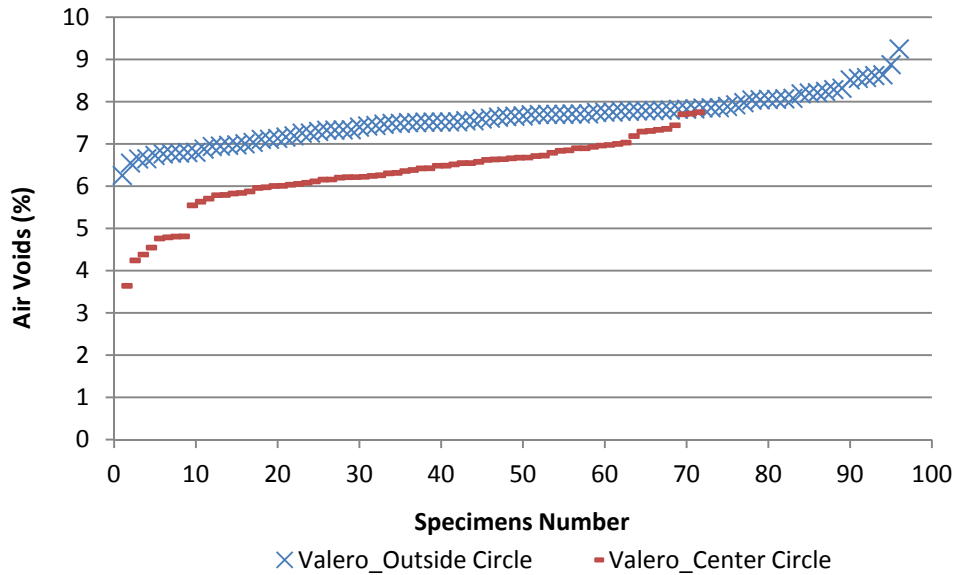


Figure E1a.7. Valero binder PG64-16 with Hanson Limestone Specimens air void distribution.

A test protocol and a data analysis method were adopted in this quarter based on linear viscoelastic theory to characterize the viscoelastic properties of undamaged fine aggregate mixtures. The test method uses a uniaxial tensile creep test to estimate the dynamic modulus and the phase angle of the FAM. The tests are conducted on asphalt mixture specimens at three temperatures (10, 23 and 30°C) to determine the tensile properties at each temperature and then to construct the master curve. The determined properties include the magnitude and phase angle of the tensile complex modulus (Luo and Lytton 2010).

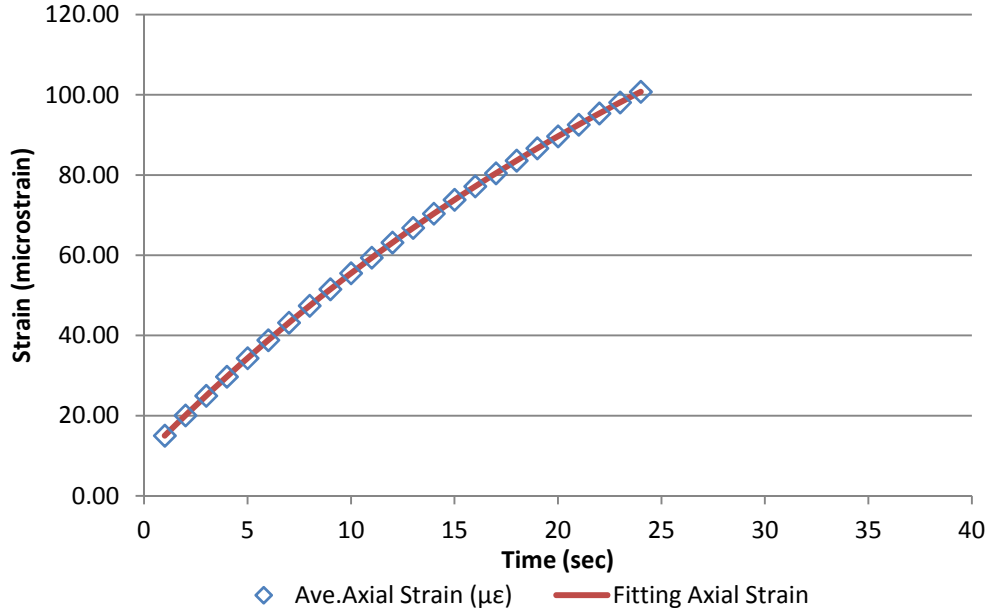


Figure E1a.8. Measured strain vs. fitted strain for Nustar_51_Aged 4 Weeks at 10°C.

Firstly, an undamaged creep test is conducted by controlling the tensile strain level to 100 microstrains and the strain response will be collected and then be fitted using the model shown in equation E1a.12 as follows:

$$\varepsilon = a * (1 - \exp(-b * t)) + c \quad (E1a.12)$$

Where a, b and c are the fitting parameters; t is the time, sec.

The relaxation modulus and the stress and strain have the following relationship:

$$\bar{E}(s) = \frac{\bar{\sigma}(s)}{s\bar{\varepsilon}(s)} \quad (E1a.13)$$

By applying inverse Laplace transforms, the relaxation modulus can be obtained. Then based on the relationship between the complex modulus and the relaxation modulus, the following equation could be established:

$$E^*(\omega) = i\omega L\{E(t)\}_{s=i\omega} = \left[s\bar{E}(s) \right]_{s=i\omega} \quad (E1a.14)$$

Using equation 14, the complex modulus and the phase angle could be calculated respectively. In order to construct the master curve of the FAM, the CAM model was used to achieve this goal.

$$|E^*(\omega)| = \frac{E_g}{\left\{ 1 + \left[\frac{\omega_c}{\omega \cdot 10^{C(T-T_r)}} \right]^{R_E} \right\}^{\frac{R_E}{\log 2}}} \quad (\text{E1a.15})$$

Where E_g = glassy modulus of the asphalt mixture, MPa; ω_c = crossover frequency of the asphalt mixture for modulus, rad/sec; R_E = rheological index of the asphalt mixture for modulus; and C = slope of the time-temperature shift factor for modulus.

As recommended by Luo and Lytton (Luo and Lytton 2010), the Williams-Landel-Ferry (WLF) function is recommended to calculate the time-temperature shift factor for Bahia's model (Luo and Lytton 2010; Zhang et al. 2011).

$$\varphi = \frac{\varphi_m}{\left\{ 1 + \frac{\log \left(\frac{\omega_m}{\omega \cdot 10^{\frac{C_1(T-T_r)}{C_2+(T-T_r)}}} \right)}{R_\varphi} \right\}^{\frac{m}{2}}} \quad (\text{E1a.16})$$

Where φ_m = the maximum phase angle for modulus, degrees; ω_m = the frequency rad/sec; m , R_φ = fitting parameters for modulus phase angle; T_r = reference temperature; and $C1$ and $C2$ = regression constants in the WLF function.

Since the FAM has an asphalt content of 10.3%, it is found that the phase angle of the specimens tested in ranges from 40 to 70 degrees as shown in figures E1a.10 and E1a.12, which is much higher than its corresponding coarse aggregate mixture. And the four weeks aged specimen Nustar_51 has a higher magnitude of complex modulus than the unaged Specimens Nustar_88 as shown in figure E1a.9. If the stress can be well controlled without significant variations, and the strain can be collected to the desired level $1\mu\text{m}$ rather than 0.001mm , this creep test is an efficient and reliable way to construct the master curve of FAM. However, it is found that the built-in LVDT precision of the DMA machine cannot achieve the desired strain precision. Therefore, the current creep testing results will only be used as a reference to back-check the dynamic cyclic loading testing results until the desired strain precision will be achieved.

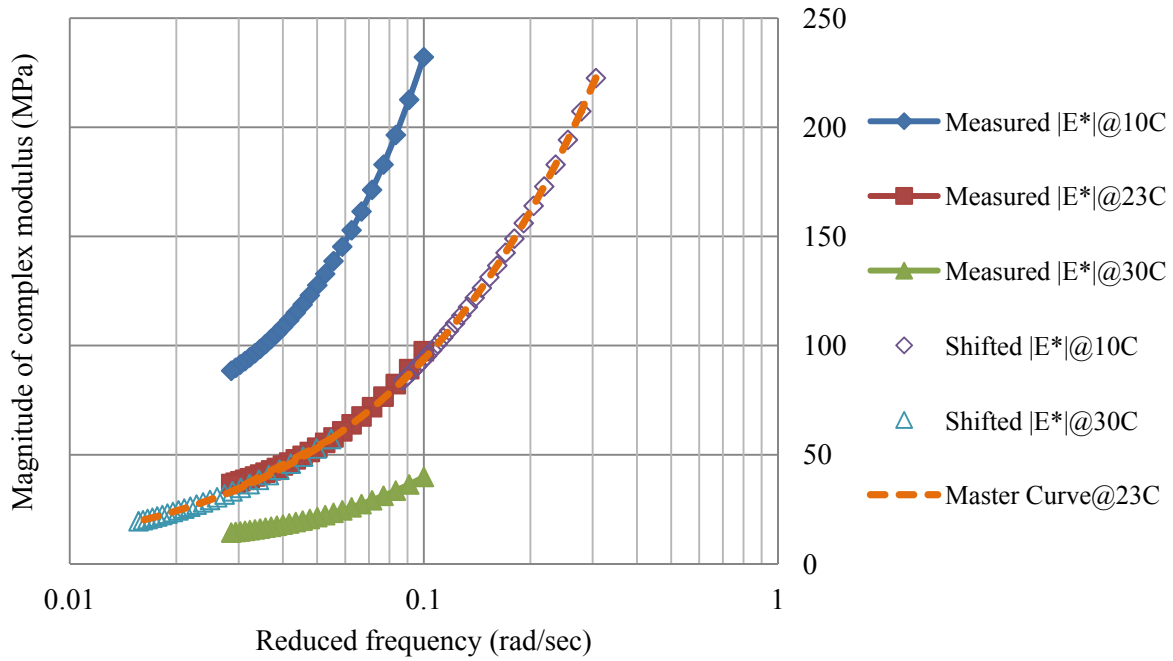


Figure E1a.9. Magnitude of tensile dynamic modulus at different temperatures and master curve at 23°C for specimens Nustar_88_Unaged.

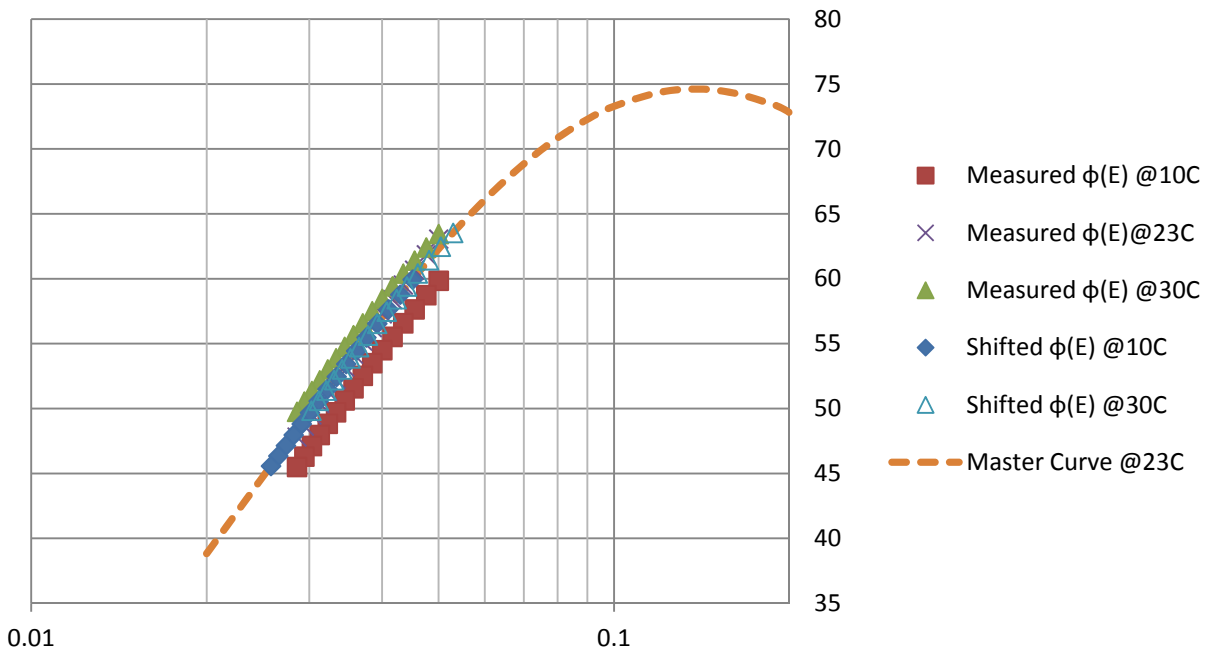


Figure E1a.10. Magnitude of tensile phase angle at different temperatures and master curve at 23°C for specimens Nustar_88_Unaged.

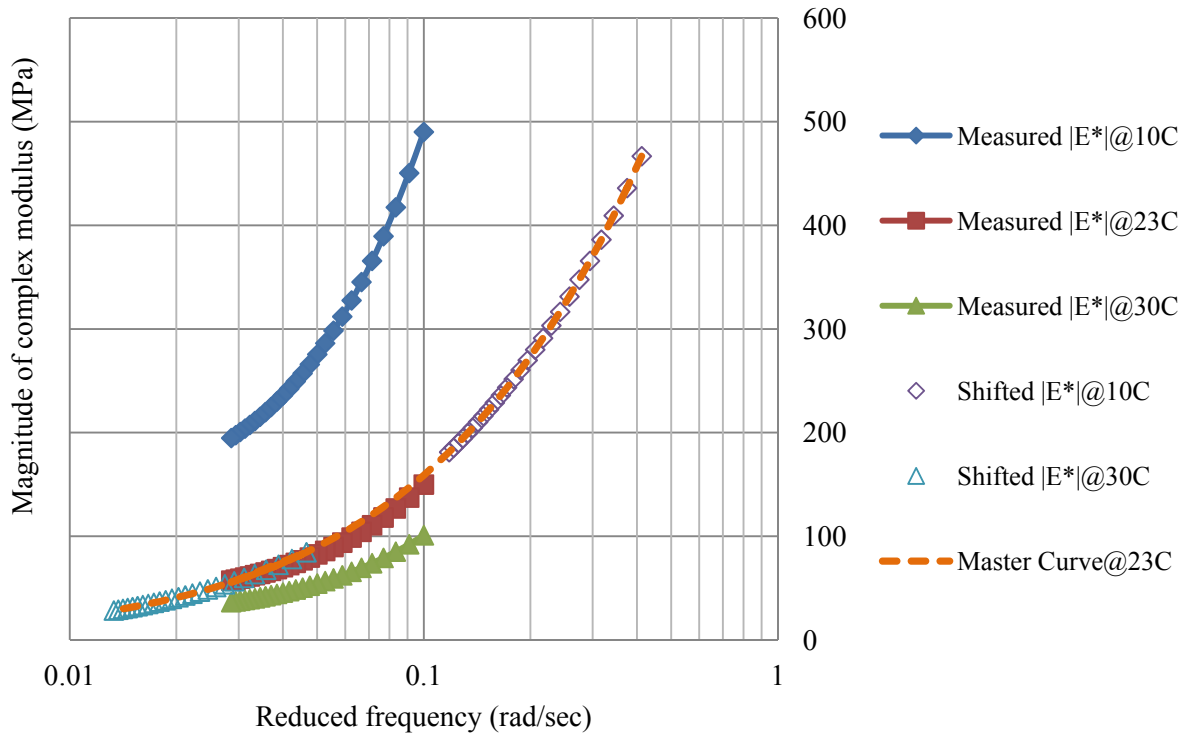


Figure E1a.11. Magnitude of tensile dynamic modulus at different temperatures and master curve at 23°C for specimens Nustar_51_Aged 4 weeks.

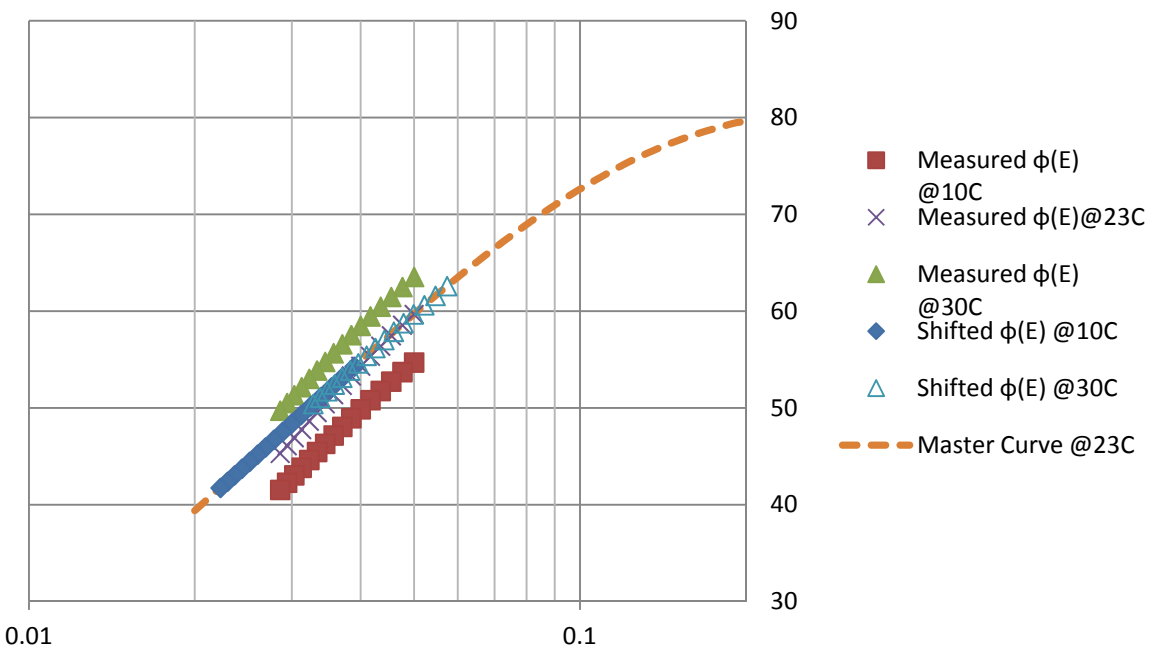


Figure E1a.12. Magnitude of tensile phase angle at different temperatures and master curve at 23°C for specimens Nustar_51_Aged 4 weeks.

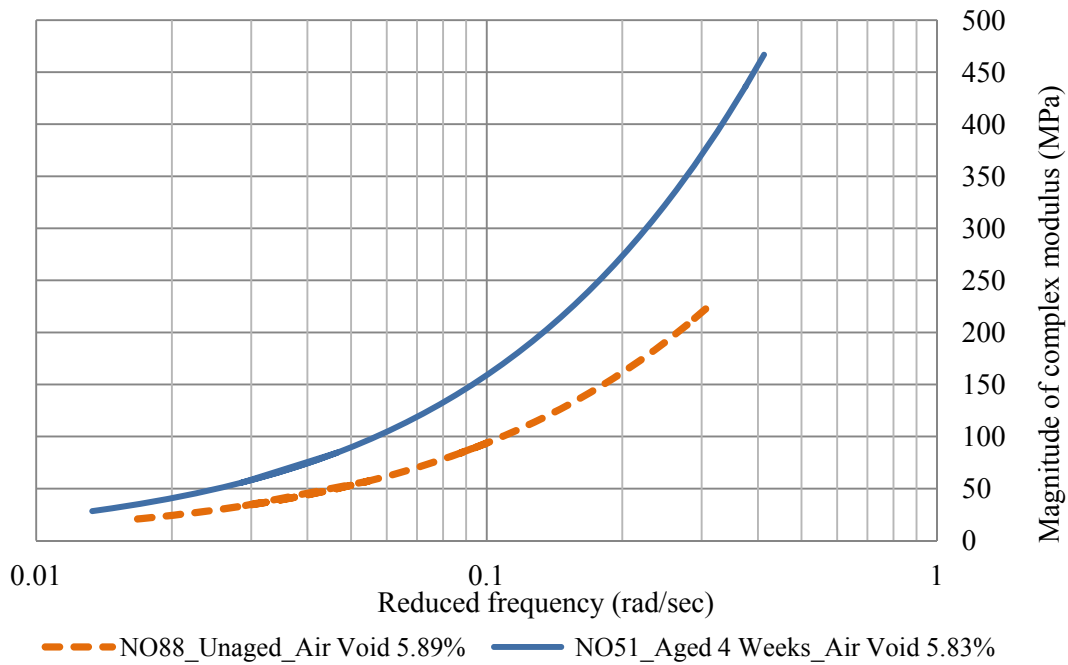


Figure E1a.13. Magnitude of tensile dynamic modulus at different temperatures and master curve at 23°C for specimens Nustar_51_Aged 4 weeks and Nustar_88 Unaged.

Significant Results

The initial damage density for the healing process is prerequisite to quantify healing of a damaged asphalt mixture. It requires determining the change of the damage density with the increase of time in the creep phase. In order to determine the evolution of the damage density, both the apparent creep stress/strain and the true creep stress/strain are needed, which can be solved using the constitutive equations and the DPSE balance equation.

The OT test method was shown to be able to find both the healing and fracture properties of the aged asphalt mixes.

Significant Problems, Issues and Potential Impact on Progress

The procedure for determining the change of the damage density in the creep phase as discussed above involves complex analysis techniques, such as the Laplace Transform, integration of the hereditary integral, curve fitting, etc., and a number of hand-writing derivations. To ensure accurate results, all calculations should be carried out very carefully. It seems that this task is complex and redundant, but it can be conducted automatically using Excel. The expression of each variable is carefully typed in the Excel, and all algorithms are embedded in the Excel as a formula or a macro program that solves the problem automatically. In addition, the curve fitting

is conducted by the software Matlab to enhance the accuracy. Once the Excel template is established, the data analysis is very efficient.

There are some problems to get the time to use the OT machine.

There are two major problems involved in the testing process: 1) the precision of the strain is 0.001mm in the data collection process, which is too high for this testing protocol; 2) the desired stress level is too low compared to the loading capacity of this machine, therefore, the stress oscillations are quite large during the creep test. The testing results vary significantly from specimen to specimen.

Work Planned Next Quarter

After determining the initial damage density of the healing process, the next step is to determine the damage density of a damaged asphalt mixture in the healing process. More specifically, the decrease of the damage density with time in the recovery phase is required from a revised creep and recovery test. In order to solve this problem, the following steps are planned to be studied in the next quarter, including: 1) determine the recovery modulus of undamaged asphalt mixtures from the nondestructive test; 2) calculate the pseudo strain in the recovery phase of the destructive test; 3) determine the true residual strain and the true internal stress of the damaged asphalt mixtures from the destructive test; 4) determine the decrease of the average crack size from the destructive test.

The same approach will be applied to the field cores with the different stiffness gradients. The stiffness gradient can be plugged into FE program to find the strain profiles above the crack in aged mixes. This method will allow us to determine the fracture and healing properties of both lab-compacted samples as well as cores taken from aged asphalt layers in the field.

The tensile fatigue properties of the FAM specimens made with Nustar PG67-22 binder and samples made with the Valero PG64-16 binder will be evaluated in the next quarter.

References

Cleveland, G. S., Button, J. W., and Lytton, R. L. (2002). "Geosynthetics in Flexible and Rigid Pavement Overlay systems to Reduce Reflection Cracking." TTI Report.

Cleveland, G., Lytton, R., and Button, J. (2003). "Using Pseudostrain Damage Theory to Characterize Reinforcing Benefits of Geosynthetic Materials in Asphalt Concrete Overlays." Transportation Research Record: Journal of the Transportation Research Board, 1849(-1), 202-211.

Kallas, B. F., and Puzinauskas, V. P. (1971). "Flexure Fatigue Tests on Asphalt Paving Mixtures." ASTM Special Technical Publication (Compendex), 47-66.

Luo, R., and Lytton, R. L. (2010). "Characterization of the Tensile Viscoelastic Properties of an Undamaged Asphalt Mixture." *Journal of Transportation Engineering*, 136(3), 173-180.

Medani, T. O., and Molenaar, A. A. A. (2000). "A Simplified Practical Procedures for Estimation of Fatigue and Crack Growth Characteristics of Asphaltic Mixes." *International Journal of Road Materials and Pavement Design*, 10.

Pais, J. C., and Minhoto, M. J. (2010). "The prediction of fatigue life of asphalt mixtures using four-point bending tests." 11P.

Paris, P. C., and F., E. (1963). "A Critical Analysis of Crack Propagation Laws." *Transactions of the ASME. Journal of Basic Engineering*, No.3(Series D), 85.

Ramsamooj, D. V. (1991). "Prediction of fatigue life of asphalt concrete beams from fracture tests." *Journal of Testing and Evaluation*, 19(Compendex), 231-239.

Wineman, A. S. and Rajagopal, K. R. (2000). *Mechanical Response of Polymers: an Introduction*. Cambridge University Press, Cambridge.

Zhang, Y.Q., Luo, R., and Lytton, R. L. (2011). "Anisotropic Viscoelastic Properties of Undamaged Asphalt Mixtures." *Journal of Transportation Engineering*, 302, 1943-5436.

Zhu, G., Wu, S., Liu, R., and Zhou, L. (2009). "Study on the fatigue property for aged asphalt mixtures by using four point bending tests." 6th International Forum on Advanced Material Science and Technology, IFAMST 2008, June 12, 2008 - June 14, 2008, Trans Tech Publications Ltd, Hong Kong, China, 289-294.

Work element E1b: Binder Damage Resistance Characterization (DRC) (UWM)

Subtask E1b-1: Rutting of Asphalt Binders

Work Done This Quarter

Work this quarter was dedicated to closer inspection of data collected during the previous two quarters, which included Multiple Stress Creep and Recovery (MSCR) testing of binders and mastics along with Repeated Creep and Recovery (RCR) testing of binders. This additional analysis was deemed necessary to determine the relationship between binder and mastic rut resistance. Also, binder results were correlated to mixture results at the same temperature. Asphalt mixture testing was conducted at 46°C. Mixture testing (Flow Number, FN) was conducted at two stress levels, 50 and 150 psi (345 and 1034 kPa). The average of the Jnr and %R in the secondary zone of mixtures from FN test results were used for correlating with binder results.

Analyses of the variability of MSCR results were also continued and finalized with conducting several analysis methods on data of modified MSCR tests with 30 and 60 cycles of creep and recovery at three stress levels of 100, 3200 and 10000 Pa.

In addition, the research team has applied the iPAS imaging software developed for the ARC on 10 regular asphalt mixtures in order to capture the effect of aggregate structure on mixture

rutting performance. The samples were cut and scanned in three sections and the images were analyzed to obtain the number of aggregate-on-aggregate contacts, total contact length and contact orientations. Thereafter, the results of image analysis are correlated with the performance of mixtures in terms of FN cyclic creep test.

Significant Results

The correlation between binder and mastic Jnr and %R values are shown in figure E1b-1.1. The results show that the binder and mastic results are highly correlated for Jnr values. The correlations are very good at all temperatures and stress levels.

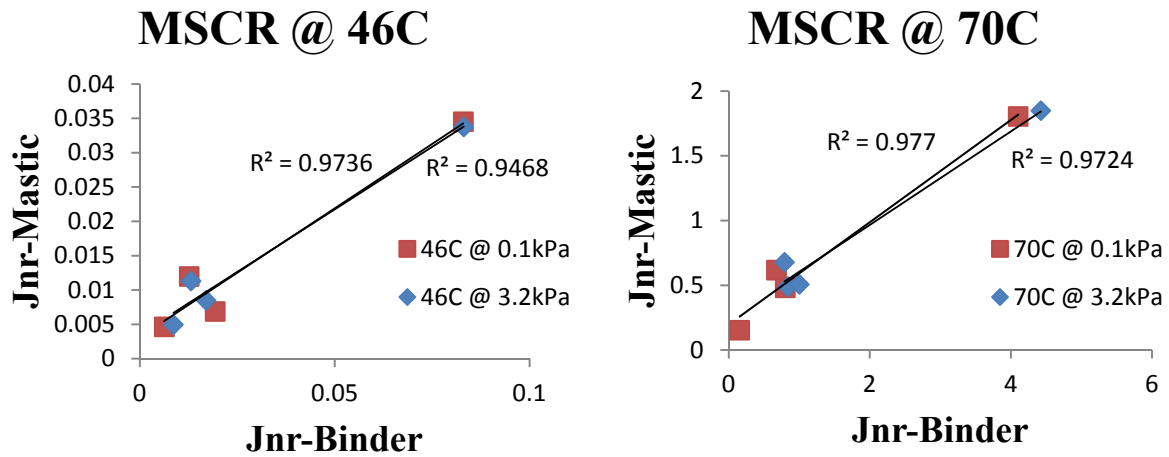


Figure E1b-1.1. Graph. Binder and mastic MSRCR Jnr correlation.

Figure E1b-1.1 shows a linear relationship for the Jnr of binders and mastics. The relationship is not as strong when correlating %R of the binders with mastics, where the relationship appears more scattered, as shown in figure E1b-1.2.

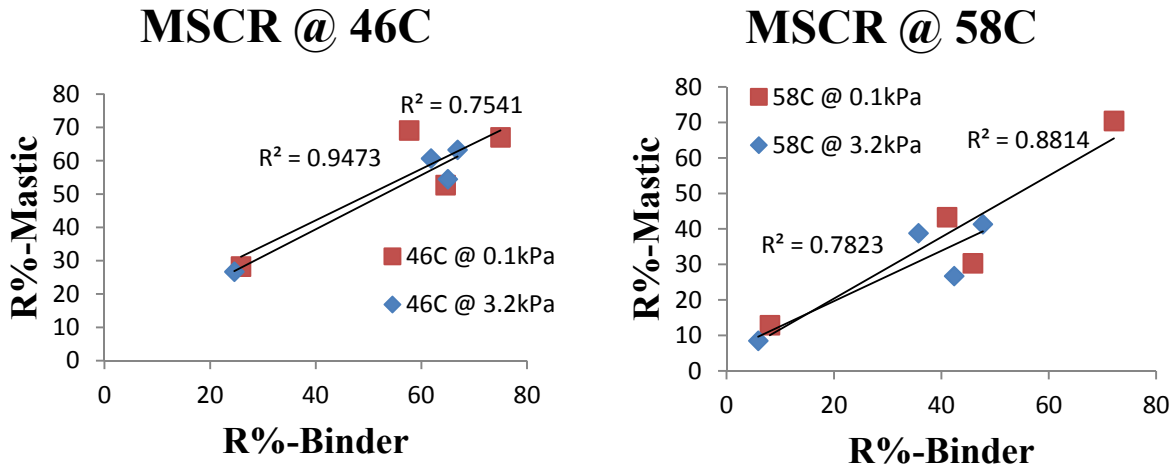


Figure E1b-1.2. Graph. Binder and mastic MSCR R% correlation.

Binders Jnr values were correlated to mixture FN data at the same temperature (46C). Figure E1b-1.3 shows a summary of these results.

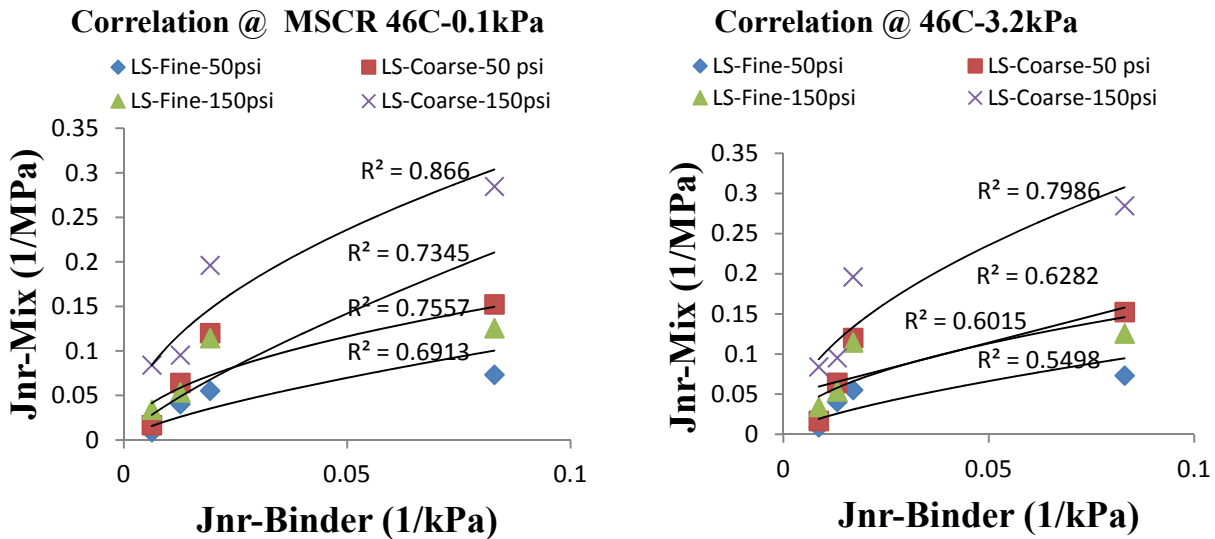


Figure E1b-1.3. Graph. Binder and mixture Jnr correlation at 46C.

These results indicate that the correlation between binder MSCR results and mixture performance is good but not as high as binder or mastic data. This can be an indication of the importance of the effect of aggregate structure on mixture performance, especially in the secondary zone. Also it can be concluded that binder properties are very important with respect to mixture behavior; however, for predicting mixture performance, binder results alone are not sufficient and the effect of aggregate structure needs to be considered. Also, it should be

mentioned that the %R of the binders and mixtures were correlated and the correlation was not as good as Jnr. These observations are similar to those reported above for mastics.

To examine the effect of the number of cycles of creep and recovery under each stress level, the MSCR tests were conducted according to the following methods:

- Method A - MSCR as described in AASHTO TP 70-09 or ASTM D7075-10 standards.
- Method B - Conducting the tests for 30 cycles of creep and recovery under each of the three stress levels of 0.1 kPa, 3.2 kPa, and 10 kPa.
- Method C - Conducting the tests for 60 cycles of creep and recovery under each of the three stress levels of 0.1 kPa, 3.2 kPa, and 10 kPa.

Statistical analysis was performed to quantify the difference between the Standard MSCR and Methods B and C.

The results indicated that adding more cycles has a significant effect on binder behaviour, especially at high temperatures. To understand how adding more cycles affects response, a four-element Burger model was used to fit the data with various cycles. The Burger model has the advantage of separating the binder response into elastic, viscous and delayed elastic responses and it can show binder behavior clearly. These results confirmed that there is significant difference between binder behavior at 10 and 30 cycles but after 30 cycles the change in binder behavior in each cycle reduces and the binder behavior shows more consistency. After 30 cycles, the values for different elements in Burger model are converging and the difference between cycle 30 and 60 is not considerable. These findings indicate that there is no need to go more than 30 cycles because more consistent response is observed and also the delayed elasticity effects are reduced. From these analyses, it can be suggested that 30 cycles for each stress level would be good alternative for current MSCR test.

In order to characterize the internal aggregate structure of mixtures and observe the effect of that on mixture rutting performance, ten mixes are analyzed using the iPAS software. Four of these mixtures were fine graded with the same gradation but three different binder additives, namely CBE (oxidized polyethylene), SBS (linear styrene-butadiene-styrene block copolymer) and GTR (ground tire rubber) in addition to the one with Flint Hills (FH) neat binder. The other four mixtures were produced with the same binders used for fine mixes but with a coarse graded aggregate blend (same aggregate source). The last two mixes are field mixes compacted in the lab. The mixes are cut in the middle and two cuts in one inch from the middle section, giving six faces. The sections are scanned and one image of each section is analyzed. The results show that there is an agreement between the internal aggregate structure in terms of total contact lengths in effective aggregate skeletons, and the rutting performance of mixtures. The results are shown in figure E1b-1.4. This concept of estimating total contact length will be further explored to understand the true role of binders in mixture rutting.

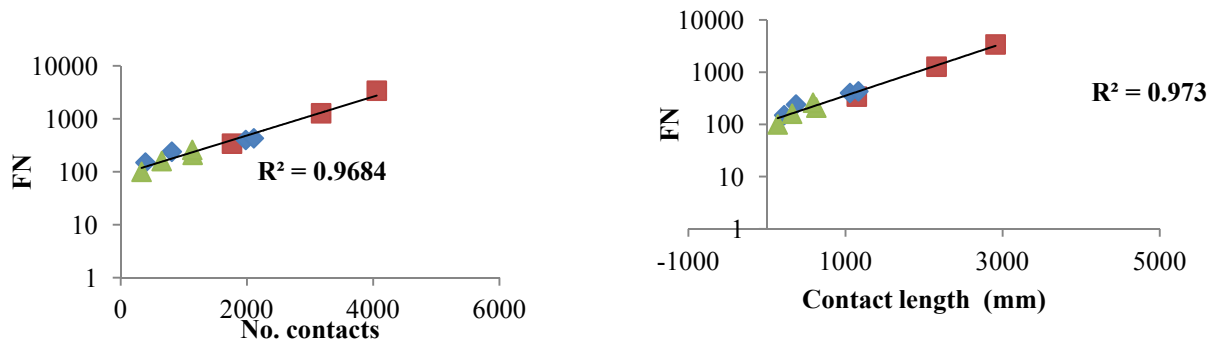


Figure E1b-1.4. Graph. Correlation of aggregate structure indices with Flow Number.

Significant Problems, Issues and Potential Impact on Progress

None.

Work Planned Next Quarter

Work for next quarter will focus on the following tasks:

- Further study on the modified MSCR procedures and finalizing results to give the final recommendations to modify the current procedure.
- Investigate the relationship between binder elasticity and mixture results, in terms of rutting performance.
- Develop new Analogical model to predict binder behavior in MSCR test.
- Comparison of field and lap compacted mixes in terms of internal structure.
- Comparison of effect of aggregate structure and binder properties on rutting performance.

Presentations and Publications

Bahia, H.U., and A. Golalipour, Analysis of MSCR variability workability, Presentation made to Expert Task Group Meeting on Asphalt Binders, Sep 2011.

Bahia, H.U., N. Tabatabaee, C. Clopotel, and A. Golalipour, Evaluation of Using the MSCR Test for Modified Binder Specification, Accepted for presentation at the Annual meeting of the Canadian Technical Asphalt Association, Nov 2011.

Subtask E1b-2: Feasibility of Determining Rheological and Fracture Properties of Asphalt Binders and Mastics using Simple Indentation Tests

Work Done This Quarter

In this quarter a set of experiments was done using the temperature control system developed during last quarter on mastics with different concentrations of mineral fillers to identify any correlation between indentation and DSR test results. The base binder used was Flint Hills PG58-22 which was blended with two types of mineral fillers: AN1 and LH1. AN1 is an andesite filler type with a specific gravity of 2.60 and LH1 is a hard limestone with a specific gravity of 2.65. The mastic samples were prepared with three different concentrations of mineral fillers: 10%, 30% and 40%. The materials used in testing matrix are shown in table E1b-2.1.

Table E1b-2.1. Mastic samples.

Binder	Mineral Filler Type	Concentration of Filler	Replicates
FH 58-28	AN1	10%	2
FH 58-28	AN1	30%	2
FH 58-28	AN1	40%	2
FH 58-28	LH1	10%	2
FH 58-28	LH1	30%	2
FH 58-28	LH1	40%	2

Significant Results

The samples shown in table E1b-2.1 were tested at 24 °C using indentation and in the DSR at 100 Pa and 3200 Pa stress levels (two replicates for each indentation and DSR). The creep and recovery procedure in the DSR was the same as in the indentation test: three minutes of loading and 12 minutes of recovery. As reported in previous quarterly reports, theoretical solutions for creep compliance in indentation boundary value problems assume that the sample size is infinite. Therefore, correction factors to account for boundary effects are needed when using these solutions as discussed and applied in previous report.

A typical example of the correlation is shown in figure E1b-2.1, which shows that there is reasonable agreement between rheological properties obtained from indentation test and DSR for mastics. The corrected creep compliance at 180 seconds (i.e., end of loading step) measured from indentation and DSR tests are compared in figure E1b-2.2. The creep compliance from indentation tests were also corrected for size effects. Correlations between J_{nr} obtained from the DSR and indentation test also improved after accounting for finite size effects as indicated in figure E1b-2.3. Furthermore, it was observed that the ranking of mastics in terms of percent recovery from the DSR and indentation tests is very similar (figure E1b-2.4).

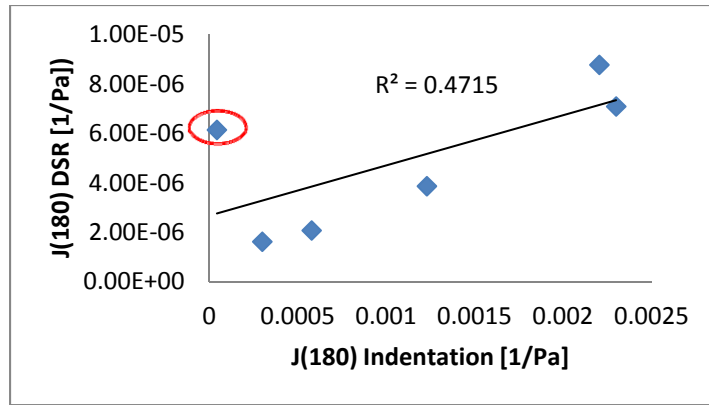


Figure E1b-2.1. Graph. Correlation between J (180) obtained by DSR (3200Pa) and indentation test

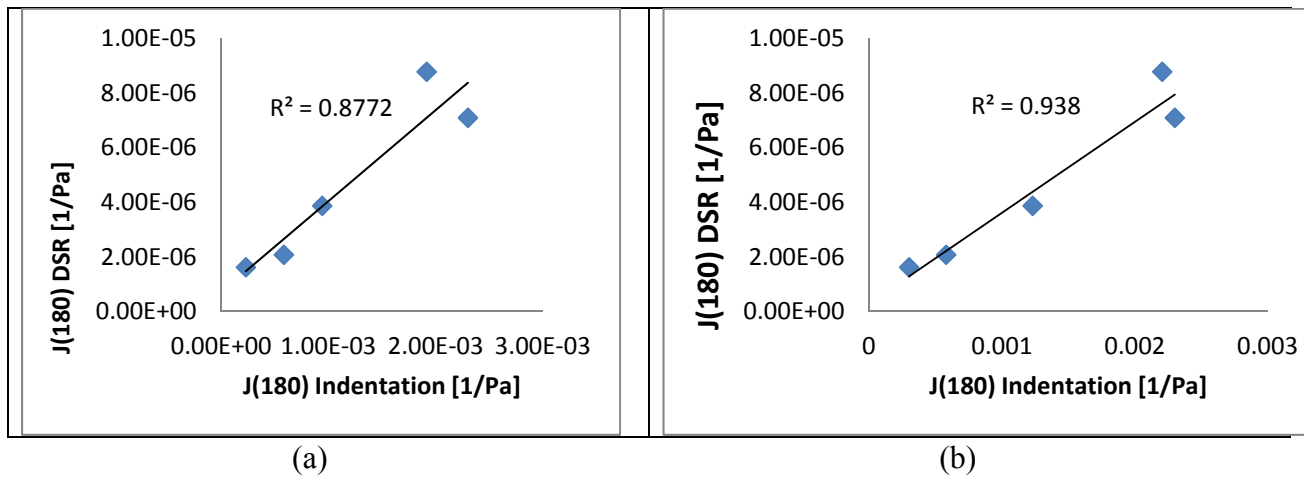


Figure E1b-2.2. Graph. Correlation of J(180) from DSR and indentation test (a) 100 Pa and (b) 3200 Pa.

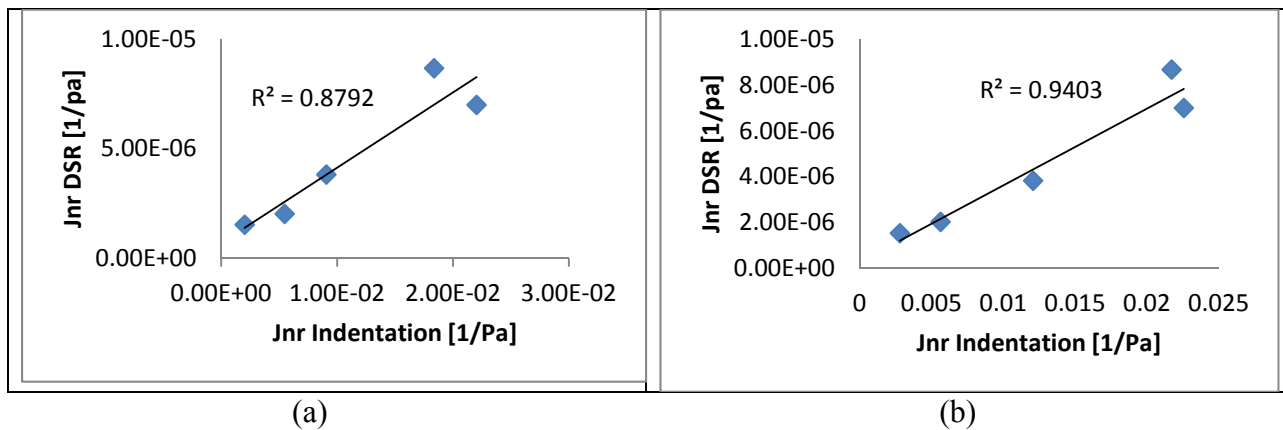


Figure E1b-2.3. Graph. Correlation of Jnr from DSR and indentation test (a) 100 Pa and (b) 3200 Pa.

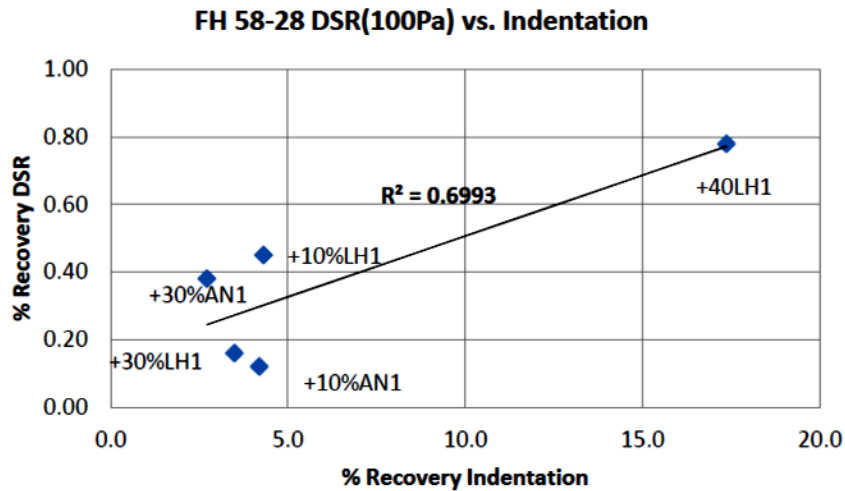


Figure E1b-2.4. Graph. Correlation of % Recovery from DSR and indentation test.

The results show that the rheological properties measured using simple indentation tests are similar to what is obtained from the DSR test.

Significant Problems, Issues and Potential Impact on Progress

None.

Work Planned Next Quarter

Efforts will focus on writing a consolidated report for work element E1b: “Binder Damage Resistance Characterization” following the 508 format. This report includes experimental results and analysis obtained during the development of the indentation system for rheological characterization of asphalt binders.

Work Element E1c: Warm and Cold Mixes

Subtask E1c-1: Warm Mixes (UWM)

Work Done This Quarter

Work continued in investigating the impacts of WMA additives on binder and mixture workability. Previous research identified aggregate gradation as the most influential factor on mixture workability. Furthermore, numerous mixtures evaluated did not demonstrate sensitivity to compaction temperature within the generally accepted temperature ranges for WMA production. To evaluate this effect a coarse graded mix was designed using the Bailey method in an effort to produce a mix design with more sensitivity to compaction temperature. Mixes prepared using a conventional and polymer modified binder from the same source and different

WMA additives. The mix design method proposed in NCHRP 9-43 was applied to define minimum mixing and compaction temperatures based on coating, volumetric, and compactability requirements. Asphalt binder workability was also evaluated through continued development of the Asphalt Lubricity test and use of a binder creep test to define compaction temperature thresholds.

The impacts of WMA additives and reduced aging due to lower production temperatures was further investigated through development of a thin film aging method and evaluation of asphalt binder performance using WMA additives categorized as waxes, mineral foaming additives, and surfactants. The thin film method was developed to isolate the effects of reduced aging temperature on oxidation for evaluation of WMA. Binder performance properties were measured at high and intermediate temperatures using conventional SuperPave test protocols and recently developed tests, specifically the multiple stress creep and recovery (MSCR) test and the Linear Amplitude Sweep (LAS) test. Also, low temperature properties were estimated using a frequency sweep at intermediate temperatures and inter-conversion to estimate creep stiffness from shear properties.

Collaboration with UNR to evaluate the impacts of reduced temperatures and remaining moisture in aggregate on potential for moisture damage. The experiment was completed and summarized in a paper submitted to the Transportation Research Board. The work included the use of the bitumen bond strength test to evaluate the effects of moisture on the bond between the aggregate and asphalt and the mixture dynamic modulus test after three freeze thaw cycles to assess mixture performance.

The research team has been unable to obtain any WMA field projects with WisDOT, however efforts for coordination continue. UNR continues to test the materials collected on PTH14 in Manitoba.

Work began in compiling Chapters 1-3 of the draft final report. These chapters cover the problem statement/introduction, literature review, and experimental design. Work will continue to summarize research results and submit the report next quarter.

Significant Results

The inability of the decrease in viscosity due to the use of WMA to fully explain the reductions in mixing and compaction temperatures realized during production, other methods to evaluate asphalt binder workability have been investigated. Results for the creep test were in agreement with mixture compaction data, indicating that density can be achieved at compaction temperatures considerably below the temperature that corresponds to the conventional viscosity threshold for unmodified binders of 280 cP. Modifications made to the Asphalt Lubricity test significantly improved the repeatability of the test. The revised procedure is currently being used to evaluate the impacts of asphalt binder modification, WMA additive type, and WMA additive concentration on asphalt binder coefficient of friction. In regards to NCHRP 9-43 mix design evaluation, it was found that the minimum mixing and compaction temperatures are controlled by the compactability requirement, not mixture volumetrics or aggregate coating.

Asphalt binder performance evaluation found that aging temperature has more influence on binder performance than the presence of most additives. The most significant effects were observed on high temperature performance properties and when short term aging temperature was reduced from conventional temperatures (163°C) to an aging temperature representative of WMA (130°C). Specifically, it was found that these temperatures correspond to an approximately 3°C decrease in high temperature continuous grade and one grade reduction for the MSCR grading recommended in AASHTO MP19 (i.e. from “E” to “V”). More detailed results are provided in the submission to TRB.

Both the BBS test and E* ratio were able to detect the influences on both temperature and WMA additive type on moisture resistance. Furthermore, both tests produced similar ranking of the materials. More detailed results are provided in the submission to TRB.

Significant Problems, Issues and Potential Impact on Progress

WisDOT has not piloted any WMA on state projects this construction season. The research team continues to work with the WisDOT Bureau Technical Services to obtain field sections.

Work Planned Next Quarter

Development of Mixing and Compaction Guidelines for WMA

The research team will continue to apply the NCHRP 9-43 WMA mix design procedure to fine and coarse aggregate gradations and a variety of WMA additives. A second aggregate source that demonstrates high water absorption (~2.5%) will be included in the study to assess the impacts of using absorptive aggregates on the mix design procedure. Work will continue on the creep and lubricity tests to define the contribution of asphalt binder workability to mixture compaction.

Impacts of Reduced Aging on Binder and Mixture Performance

Efforts will continue to evaluate the effects of reduced aging temperature and WMA additives on both asphalt binder and mixture performance. Specifically, mixture tests used to verify binder testing results will include the Flow Number Test for high temperature performance, the indirect tension test (IDT) for fatigue performance, and the thermal stress restrained specimen (TSRST) test for low temperature cracking. To evaluate the impacts of reduced aging mixes will be aged at different temperatures and aging times. Work will also continue investigating the impacts of WMA technologies on moisture damage and application of the BBS to evaluate the relationship between temperature, aggregate moisture, and the development of bond strength between the asphalt and aggregate.

Final Report

Chapters 1-3 of the final report will be submitted. Work will begin on Chapter 4: Results and Analysis, completion of the mixture testing matrix is required prior to finalizing the chapter.

Papers and Posters **Submitted** in the Last Quarter

Alavi, M., E. Hajj, A. Hanz, and H.U. Bahia. “Evaluating Adhesion Properties and Moisture Damage Susceptibility of Warm Mix Asphalts Using Bitumen Bond Strength (BBS) and

Dynamic Modulus Ratio (ESR) Tests.” Submitted to the 91st Annual Meeting of the Transportation Research Board. *Transportation Research Board of the National Academies*, Washington D.C., 2012.

Hanz, A., G. Andreoni, and H.U. Bahia. “Evaluation of the Effects of Reduced Binder Aging on Performance for WMA Using a Simple Thin Film Aging Method.” Submitted to the 91st Annual Meeting of the Transportation Research Board. *Transportation Research Board of the National Academies*, Washington D.C., 2012.

Teymourpour, P., L. Tashman, and H.U. Bahia. “Critical Considerations in Mixture Design Warm Mix Asphalt.” Submitted to the 91st Annual Meeting of the Transportation Research Board. *Transportation Research Board of the National Academies*, Washington D.C., 2012.

Subtask E1c-2: Improvement of Emulsions’ Characterization and Mixture Design for Cold Bitumen Applications (UWM)

Work Done This Quarter

The research team continued collaboration with Heritage Research Group (HRG), a private sector company with extensive field experience in cold mix applications. Collaboration this quarter was focused on simulating field mixing and compaction procedures in the laboratory in attempt to standardize a coating analysis procedure and laboratory compaction and curing procedure. HRG provided UW with recommended starting aggregate moisture and emulsion contents for analysis. Laboratory compaction procedures were also modified to accommodate reported field experience from HRG.

A coating test procedure based off of ASTM D 7229, Standard Test Method for Preparation and Determination of Bulk Specific Gravity of Dense Graded Cold Mix Asphalt Specimens by Means of the Superpave Gyratory Compactor, was finalized. Key changes made to the coating procedure were the use of a mechanical bucket mixer to remove subjectivity in the mixing process, an increase in mixing time from 90 seconds to 2.5 minutes based on industry recommendation, and mixture agitation for 2.5 minutes, 24 hours after the initial mixing based on industry recommendations. To further reduce subjectivity in the analysis, imaging software was used to provide an indication of coating based on contrast of pixel intensity. The output of the analysis procedure is a percentage of coated particles.

An analysis of the effect of curing time on the volumetric properties of CMA mixtures was also completed. Specimens were compacted in a modified gyratory compactor according to ASTM D 7229 using low volume road ($E < 0.3$ million ESALs) specifications (i.e. $N_{max} = 75$ gyrations at 600 kPa). The bulk and theoretical maximum specific gravities were calculated at 24 hours after compaction and again after full curing (72 hours at 60 C). It was found that the fully cured bulk specific gravities were significantly different than the 24 hour measurements, while the theoretical maximum specific gravity did not demonstrate any significant change with curing. The change in bulk specific gravity due to curing had a significant effect on the volumetric analysis of the samples. This behavior demonstrates the need for curing specifications in CMA mix design procedure.

Significant Findings

Literature suggests that aggregate coating in CMA is a function of the physical and chemical properties of both the aggregate and the emulsion. More specifically, coating is a function of dust content, aggregate reactivity (in terms of pH), aggregate moisture content, gradation, emulsion particle size distribution, viscosity, residual asphalt content, and emulsion reactivity among other factors. In addition, it has been noted that aggregate coating is also dependent on the method and extent of mixing. Research this quarter attempted to identify significant factors in aggregate coating in a sensitivity analysis isolating aggregate gradation, aggregate moisture content, mixing method (in terms of mixture agitation), and emulsion content using a single aggregate and emulsion source (and grade). Table E1c-2.1 is a summary of the testing matrix used for this sensitivity analysis.

Table E1c-2.1: Coating sensitivity analysis test matrix (from Swiertz et al. 2011).

Factors	Possible Levels	Description
Aggregate Source	1	Limestone/Natural Sand Blend
Asphalt Emulsion	1	Anionic E-150
Pre-mix Aggregate Moisture Content ¹	3	SSD -1%, SSD, SSD + 1%
Residual Mixture Asphalt Content	3	4.5%, 5.0%, 5.5%
Aggregate Gradation ²	3	Fine, Base, Coarse
Mix Schedule	2	Non-agitated, 24 hr agitation

¹Percent by total weight of dried aggregate.

²A base gradation was selected by industry recommendation. Subsequent “fine” and “coarse” gradations were produced by adjusting the stockpile blends of limestone and natural sand proportions.

As mentioned earlier, coating was quantified using the Image Processing & Analysis System (iPAS) software, which uses pixel contrast intensities to provide a percentage of coated particles. Attempts were made to photograph the samples in the same ambient conditions and at the same angle; however, any deviation in photograph angle or ambient conditions between photographs could cause bias in the results. As a result, an office scanner with a fixed-area sample frame has been employed to standardize the sample area for analysis and picture quality. The setup is shown in figure E1c-2.1.



Figure E1c-2.1. Photograph. Coating analysis frame with CMA sample (left); scanned CMA image for CMA sample (right).

As a result of the sensitivity study completed during this quarter, there appears to be an optimum aggregate coating (highest percent coated) that is a function of residual asphalt content, aggregate moisture content, and aggregate gradation. Mixtures that were agitated up to 24 hours after the initial mixing generally exhibited better coating when compared to non-agitated mixes, independent of aggregate moisture content. However, it was observed that an excess of moisture (high emulsion content paired with high aggregate moisture content) may reduce the coating achieved in the mixture. It was noted that exposing dry aggregates to moisture for up to 24 hours prior to mixing, as opposed to immediate mixing after exposure to moisture, did not appear to influence the coating. This is an important observation as it simplifies the laboratory coating procedure by allowing mixing shortly after aggregate exposure to moisture.

It was noted that significant mass loss occurs over time as a result of water loss for compacted CMA samples during last quarter's work. To quantify the effect of this mass loss on the volumetric properties of CMA mixtures, compacted samples were tested for bulk specific gravity (G_{mb}) and theoretical maximum specific gravity (G_{mm}) at 24 hours after compaction and after accelerated curing, 72 hours at 60 °C. The differences in specific gravities between curing times were compared using a simple t-test at the $\alpha=0.05$ level, as shown in table E1c-2.2. The differences in G_{mb} between the 24 and 72 hour cured samples were confirmed to be significant for all three trial gradations, demonstrating the dependence of measured G_{mb} on curing time, while the G_{mm} did not demonstrate a significant change due to prolonged curing.

Table E1c-2.2: Effect of curing time on the volumetric properties of CMA mixtures (from Swiertz et al. 2011).

	Gradation		
	Base	Coarse	Fine
24 hr Cured G_{mb}	2.382	2.397	2.333
72 hr Cured G_{mb}	2.446	2.473	2.381
p-value ($\alpha = 0.05$)	0.002	0.00009	0.001
24 hr Cured G_{mm}	2.499	2.504	2.480
72 hr Cured G_{mm}	2.511		
p-value ($\alpha = 0.05$)	0.632		

The results indicate that the effect of curing needs only to be taken into account for G_{mb} determination and subsequent volumetric analysis. As such, accurate accounting of the total moisture in the mixture can be used to predict fully cured G_{mb} values, and hence, fully cured volumetric properties which would be useful if acceptance criteria for CMA are based on volumetrics.

Significant Problems, Issues and Potential Impact on Progress

None

Work Planned Next Quarter

The following work is planned for next quarter:

- *Revising Coating Procedure:* The coating analysis presented in this report was completed using photographs of the coating samples processed through the iPAS software. More work is needed to finalize the procedure detailed steps and examine its repeatability.
- *Mechanical Testing:* Mechanical testing of compacted and/or cored specimens will be completed to provide insight into CMA strength gain as it relates to curing time, and strength relative to volumetric analyses. This will be critical in developing a mix design procedure for CMA. Field coring of constructed CMA pavements is expected to take place before winter of this year.

Presentations and Publications

Swiertz, D., P. Johannes, L. Tashman, and H. Bahia. Evaluation of Laboratory Coating and Compaction Procedures for Cold Mix Asphalt. Submitted for publication in the *Journal of the Association of Asphalt Paving Technologists (AAPT)*, 2011.

Cited References

ASTM D 7229 Standard Test Method for Preparation and Determination of Bulk Specific Gravity of Dense Graded Cold Mix Asphalt Specimens by Means of the Superpave Gyratory Compactor. American Society for Testing and Materials, 2008.

Swiertz, D., P. Johannes, L. Tashman, and H. Bahia. Evaluation of Laboratory Coating and Compaction Procedures for Cold Mix Asphalt. Submitted for publication in the *Journal of the Association of Asphalt Paving Technologists (AAPT)*, 2011.

CATEGORY E2: DESIGN GUIDANCE

Work element E2a: Comparison of Modification Techniques (UWM)

Work Done This Quarter

The research team focused on preparation of the final report. Following the proposed outline for the report, the research team began gathering financial data and started working on the determination of the costs associated with modification techniques.

Significant Results

Factors affecting relative cost include type of additive and procedures for incorporating into asphalts. Due to their chemical composition, different polymers have different mechanisms of interacting with the asphalt binder. These different mechanisms of reaction translate in different time of reaction and as a consequence, different times for batching. The time required to complete a batch is closely related to the asphalt plant productivity; so by increasing the time for one batch, the productivity is reduced. Also, the fuel consumption and labor costs per batch are increased when the batching time increases. It was found that some polymers require lower temperature for mixing. This fact translates into a reduction of the fuel costs. The labor costs, fuel costs and the cost associated with the decrease in productivity have to be also taken into consideration in calculating the final costs. It was also found that some polymers cause a reduction in the viscosity. The reduction in viscosity is quantified by a reduction in the number of passes a roller has to perform in order to achieve the desired densification in the field.

Examples of the savings that can be achieved by using one polymer in place of another were determined by discussions with one of the polymer producers. Some of the key factors that could be included are as follows.

- Batch size
- Percent asphalt in the mix(PMA)
- % polymer A in PMA
- Time for mixing polymer
- Temperature of mixing and storage
- Temperature of compaction

- Number of roller passes during compaction.

Significant Problems, Issues and Potential Impact on Progress

None.

Work Planned Next Quarter

Work for next quarter will focus correlating the costs with performance and preparing the draft final report.

Work element E2b: Design System for HMA Containing a High Percentage of RAP Materials (UNR)

Work Done This Quarter

This work element is a joint project between University of Nevada, Reno and University of Wisconsin–Madison. The research team continued development on a ‘RAP Workability’ procedure which allows for the estimation of the change in mixing and compaction requirements for high percentage RAP and RAS mixtures. A simple verification procedure utilizing ‘artificial RAP’ materials was completed and it was determined that the procedure is capable of estimating RAP binder viscosity within an average of six percent for three test temperatures and two binder replacement levels. A simple test matrix was also completed to demonstrate the sensitivity of the procedure to RAP source and fresh binder grade in terms of estimated blended binder viscosity. Two commonly used warm mix additives were also tested to demonstrate their effect on the mixing and compaction temperatures of high RAP mixes.

The proposed procedure was extended to mixtures containing both RAP and RAS at high percentages. Blends containing both RAP and RAS materials were hypothesized to behave (in terms of blended binder viscosity) as a linear combination (weighted average) of the RAP material tested alone and RAS material testing alone, for a given fresh binder grade and source. This is a direct extension of the RAP/RAS blend testing completed at low temperature in the BBR presented in previous reports and publications. Results indicated that the procedure fails to consistently estimate the blended binder viscosity, prompting a possible need for revising the proposed procedure.

Concerns over changes in sample geometry (flow at high temperature) in the DSR at the highest proposed test temperature (110 °C) prompted a comparison between results obtained using the previously proposed high temperature range (76-115 °C) against the same material tested at more conventional test temperature range (58-96 °C). It was demonstrated that testing within the lower temperature range produced more reasonable results when compared to results obtained using the previously recommended range of temperatures (76-115°C). Additional testing is being completed to confirm these initial results.

The effective binder properties of the Manitoba field-produced RAP mixtures were determined by various methodologies including, grading of the recovered binders, blending chart process, mortar procedure, and backcalculation of binder properties from measured dynamic modulus of mixtures using the Hirsch model and the modified Huet-Sayegh model. A paper was submitted to the 91st Annual Transportation Research Board Meeting, January 22-26, 2012, Washington DC.

The subtask E2d-3, “Develop a Mix Design Procedure,” was completed. The data analysis was conducted for the mixing temperature records, grades of the recovered binders, volumetric properties and mechanical properties using the dynamic modulus. The work is currently being finalized to provide recommendations for the most appropriate laboratory mixing procedure for HMA mixtures with RAP.

Significant Results

The proposed RAP binder workability characterization procedure presented last quarter was further applied to a test matrix containing three RAP sources each tested with two fresh binders, PG 58-28 and PG 64-22, for a total of six unique RAP source – fresh binder combinations. All six combinations were tested at the same binder replacement levels (0, 10, and 20 % binder replacement by weight). Table E2b.1 displays the ‘temperature change profile’ for all six cases tested. The temperature change profile is defined as the change in degrees Celsius of the estimated mixing (or compaction) temperature per unit (percent) increase in RAP binder replacement. The estimated mixing or compaction temperature is found using the guidelines set in ASTM 2493 – Viscosity Temperature Charts for Asphalts to create the viscosity – temperature profile, while the viscosity ranges identified for the mixing and compaction temperatures are defined as 0.17 ± 0.02 Pa-sec and 0.28 ± 0.03 Pa-sec, respectively. Note that each RAP – fresh binder combination produces a unique temperature change profile, indicating that all RAP and fresh binder grades should be tested individually for characterization; similar to what was demonstrated using the continuous grading procedure.

Table E2b.1. Temperature change profile sensitivity to RAP source.

RAP/RAS Source	Fresh Binder Grade	Temperature Change Profile [$^{\circ}\text{C}/\%\text{RAP}$]	
		Mixing Temperature Range	Compaction Temperature Range
WISCONSIN A (RAP)	58-28	0.35	0.35
	64-22	0.09	0.12
WISCONSIN B (RAP)	58-28	0.22	0.24
	64-22	0.03	0.04
CANADIAN (RAP)	58-28	0.21	0.21
	64-22	0.15	0.16

Blending a more heavily aged RAP binder with a fresh binder produces a blended binder with a higher viscosity at a given test temperature when compared to the fresh binder alone. However, the slopes of the viscosity – temperature profiles for the fresh binder and blended binder do not

have to be the same. The blended binder viscosity – temperature profile should exhibit a slope less than that of the fresh binder profile as a result of the more heavily aged (less temperature susceptible) RAP binder. That is, the viscosity – temperature profiles should not intercept in the applicable range of viscosities. However, it was determined that the viscosity – temperature profiles for some RAP – fresh binder combinations did in fact intersect within or immediate after the designated range in viscosities for determining the mixing temperatures. Researchers discovered that testing at 115 °C would often cause the sample to deform and ‘bleed out’ of the DSR geometry, producing viscosity values lower than expected (less material to resist the torque). This, in turn, resulted in an estimated viscosity – temperature profile that exhibited a higher slope than expected.

In light of the above-mentioned concern, samples were retested in a temperature range more suitable for DSR testing with 25 mm geometry. Mortar and fresh binder samples were tested within a temperature range of 58 – 94 °C in six degree increments. It was found that the slope of the estimated blended binder profile was reduced when testing in the lower temperature range, and diverged from the fresh binder viscosity – temperature profile. It was also noted that the fresh binder viscosity – temperature profile exhibited a significantly different slope when tested in the lower temperature range as compared to the high temperature range profile slope. It was generally noted that the estimates of mixing and compaction temperatures obtained by testing in the lower temperature range were more reasonable and intuitive than the estimates obtained using the high temperature range. More testing will be needed to confirm these results, and a comparison of the fresh binder estimates using the DSR should be compared against RV measurements for completeness.

In this quarter, several methods of estimating the effective PG grade of the binder in field-produced mixtures designed with RAP were evaluated in this study. Good correlations were observed between the estimated critical temperatures from the blending chart process and the measured ones from the recovered asphalt binders. In some cases, the blending chart process underestimated or overestimated the critical temperatures of recovered binders by 2°C. Both methods showed significant increase in the binder critical temperatures (i.e. warmer temperatures) with the increase in RAP content, particularly when 50% RAP was used. Specifically, the low critical temperatures of the binders recovered from the 50% RAP mixtures were 7 to 8°C warmer than those recovered from the virgin mixture (i.e. 0% RAP). This observation is mainly related to the assumption that full blending is occurring between the virgin and the RAP binders.

The mortar approach showed promising results in determining the effective PG grade of the mixture. Though the method was sensitive to the percent of RAP and the type of virgin binder used in the mixture, it did not result in drastically different mixtures binder properties for the 0% and 50% RAP mixtures. Overall, the mortar procedure resulted in high, intermediate and low critical temperatures than are lower (i.e. softer) than those determined for recovered asphalt binders. The mortar results for low critical temperatures were further confirmed with measured fracture temperatures on the various mixtures. The low critical temperatures from the mortar procedure were comparable and consistent with the performance of the mixtures to thermal cracking. Consequently, this procedure may be well indicating that a certain level of blending is occurring between the virgin and RAP binders in a mixture. Hence, further evaluation of the

proposed mortar procedure is prompted necessary using a larger set of mixtures that cover different binder types and sources at multiple levels of RAP content.

The Hirsch model provided reasonable estimates to backcalculate binder shear modulus at high temperature from the measured mixture dynamic modulus. However, some difficulties exist in estimating the high temperature PG grade, particularly when dealing with soft binders like the ones used in this study. The difficulties arise from, first the difference in temperatures between the dynamic modulus testing and PG grading temperatures and second, the limitation in the formulation of the Hirsch model at high temperatures and low frequencies. Subsequently, in order to get reasonable estimates, the binder modulus at high temperature was estimated from the backcalculated moduli (using Hirsch model) at lower temperatures from the mixture dynamic modulus.

The modified Huet-Sayegh model was used to estimate the high PG of the asphalt binders from the measured dynamic modulus of the corresponding mixtures. This approach resulted in high critical temperatures that are, respectively, similar and higher than those determined for the recovered binders and using the Hirsch model. The data showed good correlation between the characteristic times of the binders and mixtures, hence, allowing for the determination of the binder properties from the measured dynamic modulus of the mixture. However, this relationship was highly dependent on temperature and need to be verified with other types of mixtures.

In summary, this study was specific to the use of RAP in typical mixtures in Manitoba, Canada, and further research is required on different types of RAP mixtures and different virgin PG grades to verify and validate the methods evaluated as part of this study. Particularly, the mortar procedure provided promising results and need to be further examined.

Significant Problems, Issues and Potential Impact on Progress

None

Work Planned Next Quarter

The following work is planned for next quarter:

- As noted, verification of the proposed ‘low temperature’ range will be completed. The verification process will include verification of the fresh binder in a comparison between the DSR and RV as well as an artificial RAP verification procedure (identical to the procedure used for the ‘high temperature’ range testing that was presented last quarter.
- The workability procedure will be extended and modified to include modified fresh binders.
- The effect of blending time on the blended binder continuous grade/viscosity estimates will be explored, especially for the DSR measurements. It is hypothesized that allowing the mortar samples to condition at elevated temperature will allow for greater blending. The time allowed to blend should be similar to the time used in the mixing/handling process in the field.

Cited References

ASTM D 2493 – Viscosity Temperature Charts for Asphalts. American Society for Testing and Materials, 2009.

Subtask E2b-2: Compatibility of RAP and Virgin Binders

Work Done this Quarter

Rheology and Automated Flocculation Titrimetry (AFT) was completed on extracted binders from RAP and blended binders (RAP extracts and virgin binders) to determine the compatibility of the samples. RAP binders from sources in Iowa, South Carolina, and California were extracted using both cyclohexane and toluene:ethanol (85:15). The extracted samples were blended at several concentrations with two different RTFO-aged ARC binders, BI-0001 and BI-0002. The results of the AFT (ASTM D6703-01) compatibility study, thus far, have been mixed. In most cases the results indicate an increase in asphaltene content, as expected, and indicate an increase in the polarity of the overall asphalt chemical composition. Initially, it was believed that the increase in asphaltene content was accompanied by an improvement in the solvent power of the maltenes. However, as the rheological data was obtained, the stiffening that is observed indicates that the AFT parameters usually attributed to the maltenes and whole asphalt are a better indication of the total polarity of the system and not necessarily the compatibility of the blended binders. AFT was also performed on samples obtained from the NCHRP 9-12 project, in which extracted RAP binders actually softened the virgin binders. The data suggest that there is a good indication that a multi-dimensional compatibility test would be better suited for determining aged and virgin binder blend compatibility used to predict performance.

The AFT performed thus far in this study has been a one-dimensional compatibility measurement that was focused primarily on the precipitation of asphaltenes using iso-octane and only provided an indication of the polar character of the blended binders. While this works well for unmodified, virgin binders, it has shown to be deficient when determining the compatibility of the blended aged and virgin binders. This is due to the highly polar nature of aged binders which overwhelms the determination of the character of the solvent fraction.

Significant Results

None.

Significant Problems, Issues and Potential Impact on Progress

None.

Work Planned Next Quarter

As a means to develop a better understanding of the properties of blends between RAP and virgin binders the Bitumen Solubility Model, or BISOM test, was developed at Nynas Bitumen and is a modified approach to determining the internal stability, or compatibility, of a material

(Redelius 2004; Hansen 2007). The AFT is still used for determining a multi-dimensional material compatibility.

The BISOM test is a suite of Heithaus (AFT) titrations of asphalt dissolved in toluene with different solvents of known Hansen solubility parameters. Each solvent that is utilized is selected to help determine particular chemical characteristics relating to the stability of the system: a measurement of polar, dispersive, and hydrogen-bonding characteristics.

In the next quarter, the materials and blends used up to this point will be tested using the BISOM method. Three dimensional analyses of their compatibility profiles will be used to help demonstrate the effects of blending aged and virgin binders and relate them to the physical properties of the materials. Additionally, the results will be used to help predict which aged and virgin binders are most likely to perform well when blended.

Work element E2c: Critically Designed HMA Mixtures (UNR)

Work Done This Quarter

Work continued to evaluate the applicability of the recommended deviator and confining stresses for the flow number test. In this quarter, the two mix designs for Wisconsin materials have been verified. For each of the nine aggregate sources, the Aggregate Imaging System (AIMS) results are being analyzed in order to characterize the aggregates and determine their influence on the asphalt mixture permanent deformation performance. Flow number testing continued and is being conducted at three different temperatures: 1) 50% reliability high pavement temperature from LTPPBind, 2) at the effective pavement temperature (T_{eff}) from NCHRP 9-33A, and 3) T_{eff} plus 6°C. Flow number testing have been completed for FLDOT under braking and non-braking conditions for 7, 4 and 2% air void content at the different testing temperatures. In addition, testing for NCDOT has been completed for all temperatures but only under non-braking conditions. The asphalt binders from the various sources were evaluated using the of multiple stress creep recovery (MSCR) test.

The work on converting the pulse duration in time domain for a given pavement response into frequency domain using the Fast Fourier Transformation (FFT) has been completed. The concept of predominant frequency(ies), f_p , to predict all components of the pavement responses was verified for different pavement structures and conditions including those with Cement Treated Base (CTB). A paper entitled: “Establishing Equivalent Loading Frequencies in Static Multilayer Analyses to Simulate Dynamic Responses in Asphalt Layer” was submitted to the 91st Annual Transportation Research Board Meeting, January 22-26, 2012, Washington DC.

Significant Results

An investigation of the existence of predominant frequency, f_p (or frequencies) and the ability to predict critical pavement responses in asphalt layers using those predominant frequencies has been completed. The study used an extensive database of computed pavement response histories of four different asphalt pavement structures (thin and thick) at two temperatures (70 and 104°F)

subjected to a tandem axle load at three speeds (10, 40 and 60 mph) using the pavement response analysis program 3D-Move.

The conversion of load duration to frequency and the validity of using one response component (σ_{zz}) alone in the estimation of t_p were explored. Instead of focusing on only σ_{zz} as in the previous studies, in this investigation attention is given to all pavement response components (stresses and strains). In addition, verification of whether the use of a consistent set of f_p value(s) can in fact adequately capture all components of pavement response has also been undertaken. The viscoelastic properties that are representative for the predominant (or equivalent) frequencies from frequency sweep data were used.

A major contribution of the study is that the critical responses and performance in a flexible pavement system can be successfully simulated with a static multilayer elastic analysis (within $\pm 10\%$) by assigning elastic modulus to HMA based on appropriately selecting the corresponding predominant or equivalent frequency, f_p , (or frequencies). Generalized equations for estimating those f_p values for all pavement structures, temperatures and vehicle speeds under consideration have been developed. Good fitting parameters (R^2) were observed for all evaluated cases. Furthermore, the impact of loading frequency on predicted asphalt distresses was assessed for rutting and bottom-up fatigue cracking following the MEPDG approach. The main findings of the study are summarized as follows:

- The pulse width in HMA layer strongly dependent on the pavement response under consideration. Some pavement responses (e.g., vertical stress, σ_{zz} and transverse strain, ε_{yy}) represent purely compressive or tensile state of load-induced response, while other pavement responses (e.g., longitudinal strain, ε_{xx} and vertical strain, ε_{zz}) consists of tension and compression components.
- For the evaluated cases, single predominant frequencies (f_p) for the ε_{yy} and σ_{zz} response histories were observed for the HMA layer and they were generally unaffected by the depth of the response point, pavement structure and HMA temperature.
- In certain cases multiple f_p values within an HMA layer are recommended when using simplified static elastic analyses to match with dynamic viscoelastic responses. Since the analysis with f_p values give very reasonable response estimation for the entire HMA layer, it may be concluded that the use of predominant frequencies is a valid simplification.
- The f_p value(s) are proportional to the vehicle velocity, irrespective of HMA thickness and pavement temperature.
- Generalized equations for estimating the f_p value(s) for all pavement structures, temperatures and vehicle speeds under consideration have been developed. The f_p value(s) are proportional to the vehicle velocity, irrespective of HMA thickness and pavement temperature. It should be noted that the computed regression equations are based on data that were determined under temperatures of 70 and 104°F and vehicle speeds between 10 and 60 mph. It is recommended that these equations not be used outside the specified ranges for temperature and speed without further checks.

- Overall, good correlations were observed between the viscoelastic dynamic responses and the static multilayer elastic responses using appropriate predominant frequencies. Additionally, the MEPDG approach was used to estimate the pavement responses. The data show that the $1/t_p$ and $1/(2\pi t_p)$ conversions, respectively, underestimate and overestimate the normal strains when compared with the viscoelastic dynamic responses. In the case of vertical stress (σ_{zz}) all approaches considered resulted in very similar values (within $\pm 10\%$).
- The impact of loading frequency on predicted asphalt distresses was assessed for rutting and bottom-up fatigue cracking. The results show that the use of proposed f_p value(s) along with static multilayer elastic resulted in rut depths that are within $\pm 10\%$ of those determined using the viscoelastic dynamic responses. The rut depth in the HMA layer was either underestimated or overestimated when respectively, the $1/t_p$ or $1/(2\pi t_p)$ loading frequency conversions were used. In the case of bottom-up fatigue cracking, the use of the proposed f_p value(s) and the $1/t_p$ conversion resulted in fatigue predictions that are within $\pm 10\%$ of those determined using the viscoelastic dynamic responses. The $1/(2\pi t_p)$ conversion resulted in a significant overestimation of bottom-up fatigue cracking.

Significant Problems, Issues and Potential Impact on Progress

None

Work Planned for Next Quarter

Continue the evaluation of the various mixtures according to the Flow Number Task Force experimental plan.

Work element E2d: Thermal Cracking Resistant Mixes for Intermountain States (UNR & UWM)

Work Done This Quarter

This work element is a joint project between University of Nevada Reno and University of Wisconsin–Madison. In this quarter, all of the E*-compression testing and extraction and recovery testing has been completed. Following that process, nearly 60% of the Carbonyl Area (CA) measurements have been completed, with the remaining 40% having been sent to Texas A&M for testing. Further samples are in the process of being tested. Progress continues on the low shear viscosity (LSV) and binder master curve measurements, with nearly 45% of that testing has been completed. Further refinement of the Thermal Stressed Restrained Specimen Test (TSRST) testing procedure is being finalized. A set up to measure the thermal strain of an unrestrained specimen was developed and implemented (figure E2d.1). In addition to the stress buildup curve, the test now allows for the measurement of the thermal strain as a function of temperature change. The stress and strain measurements are used to calculate the relaxation modulus of the mix.

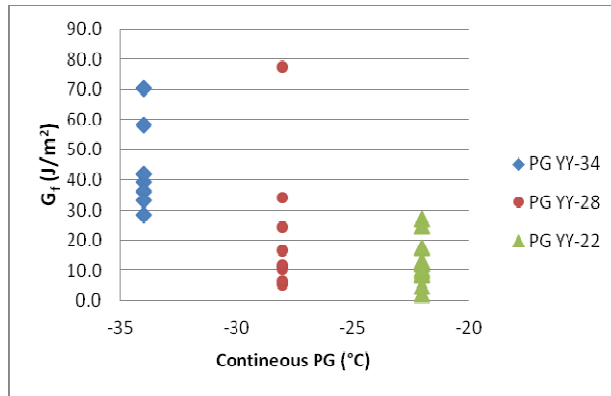


Figure E2d.1. Photo. TSRST set-up for measuring fracture properties and thermal strain.

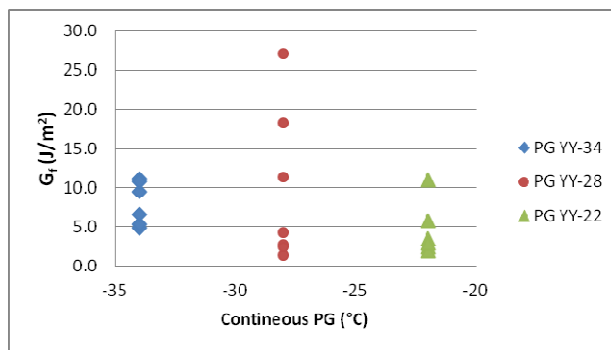
Effort this quarter also focused on solving the partial differential equation (PDE) of oxygen pressure for the transport and reaction of oxygen in asphalt-aggregate matrix. The model is described extensively in the ARC Quarterly report dated January 2008. By knowing the pavement temperature profile and kinetic parameters of asphalt binder used in asphalt mixture the value of oxygen pressure at each radius in asphalt mastic can be determined over time. Afterward, the values of partial oxygen pressure are used to calculate the amount of Carbonyl (CA) over time at each radius as a measure of aging of asphalt binder in mixture. A program was written in Matlab to solve for the partial oxygen pressure numerically based on Finite difference method.

Efforts have begun to identify potential field validation sites for the developing thermal cracking modeling efforts. One location has been selected with nearly 50% of the required binder extraction and recovery testing being complete to date. Other potential locations are being sought with further materials testing to follow.

The BBR-SENB test was evaluated as a possible alternative to the DTT test, and its ability to capture the ductile-brittle transition of binders at low temperature and differentiate between binders of the same BBR low temperature performance grade. To this end, the large database of materials tested using the SENB were categorized based on their respective performance grades and compared to evaluate the capability of the BBR-SENB to capture differences within the same grade. Figure E2d.2 shows comparisons made between a range of modified and unmodified binders from the pooled fund phase II WRI verification sections and LTPP sections, tested at -12°C and -24°C using the SENB.



(a)



(b)

Figure E2d.2. Graph. Difference in performance as measured by the SENB G_f for binders of the same PG, tested at (a) -12°C , and (b) -24°C .

Figure E2d.2 clearly shows a significant difference in fracture energy for binders classified as the same performance grade using the Superpave BBR specification. It can be seen that binders of same PG grade can show up to a 10 times difference in fracture energy. These plots clearly demonstrate the need to use the SENB to measure fracture energy (G_f) and differentiate between different modified and unmodified binder systems in terms of low temperature performance.

Significant Results

The E^* -tension testing protocol has been established, validation testing is taking place, as well as initial experimental matrix samples are currently being tested. From the same test data, dynamic modulus in tension, E^* -tension, as well as creep compliance, $C_t(t)$, can be determined. Considerations for both measures are underway until the most appropriate testing parameter can be identified.

Further information regarding the influences of mixture properties into the oxidative aging of binders has included in a paper submitted for publication and presentation at the 2012 TRB Annual Meeting. This paper entitled “Differentiating Oxidative Aging of Asphalt Binders and Mixtures” investigated the differences between the hardening susceptibility (HS) and rate of

carbonyl growth with time between binders aged in pressure aging vessel (PAV) pans and binders aged in mixtures in the laboratory.

The general findings of this portion of the investigation indicate that there is an appreciable difference in the HS, which is the increase in the low shear viscosity (LSV) as a function of carbonyl area (CA), between the unmodified PG64-22 and the SBS modified PG64-28 binders. This is indicated by figure E2d.3. The mixture identification nomenclature is organized as follows: for example, NV22_4.5 would indicate Nevada aggregates mixed with PG64-22 binder at 4.5% binder content and aged in a 60°C forced draft oven for the prescribed time period (0, 3, 6, or 9 months).

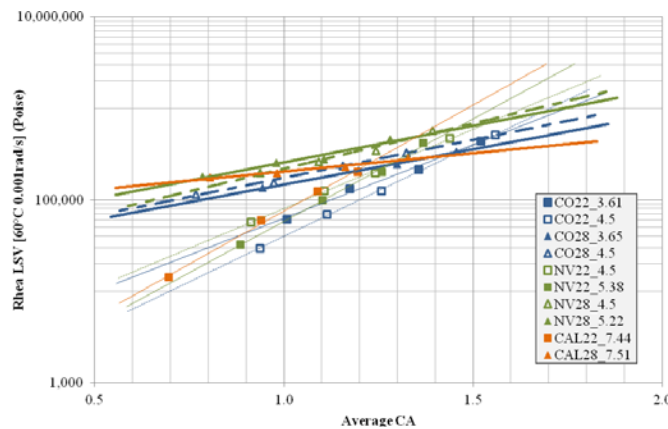
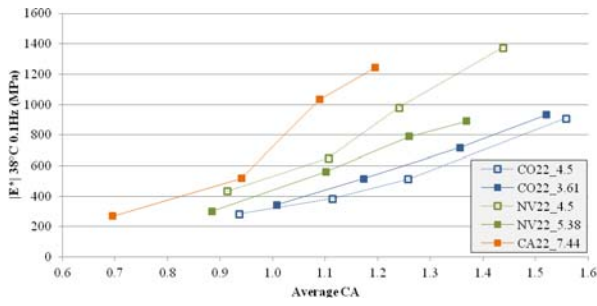


Figure E2d.3. Graph. Hardening susceptibilities of binders in mixtures.

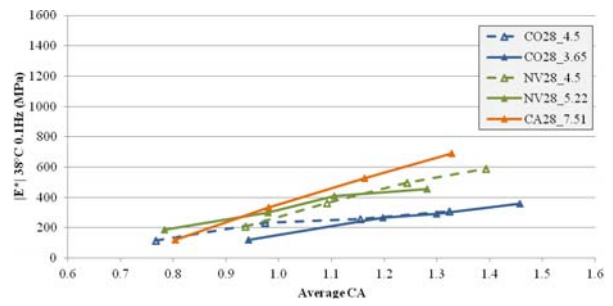
Further considerations included the comparison of E^* in compression with respect to the CA measurements. Figure E2d.4 presents both the E^* values for both binders and the percent increase of the E^* values with respect to the original E^* value at 0 months as a function of CA. While many noted differences in figure E2d.3 may be considered, the most significant is the difference in HS between the mixtures themselves. This difference in mixture HS values nearly necessitates deviation from the binders aged in PAV pans, unless a significant amount of unwanted variability is introduced to mask the differences.

Further consideration of figure E2d.4, indicates that for the PG64-22 binder, there is a lateral shifting of the CA values corresponding to the aggregate absorption. Colorado has the lowest absorption and the highest CA for a given aged state. California shows the lowest CA measures, again with Nevada in between. A similar result is noted with the PG64-28 mixtures. However, the trend is not as clear as with the PG64-22 mixtures.

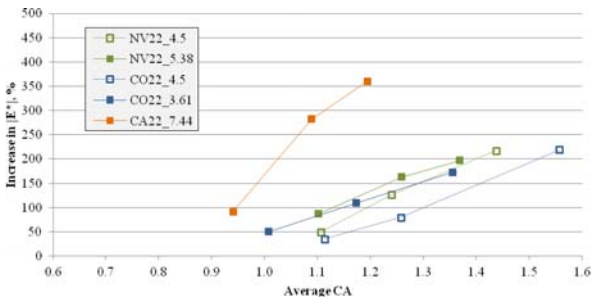
As could be expected from figure E2d.4, the HS values are different between the PAV pan aged and the mixture aged binders as indicated by figure E2d.5 for both binders.



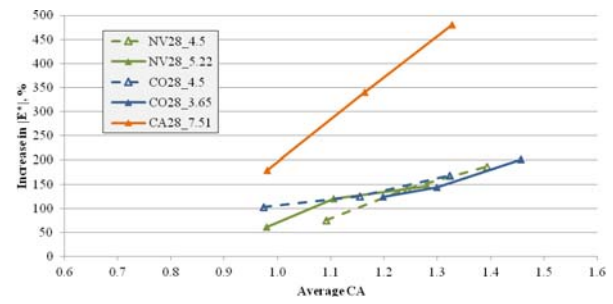
(a) PG 64-22 Dynamic Modulus



(b) PG 64-28 Dynamic Modulus

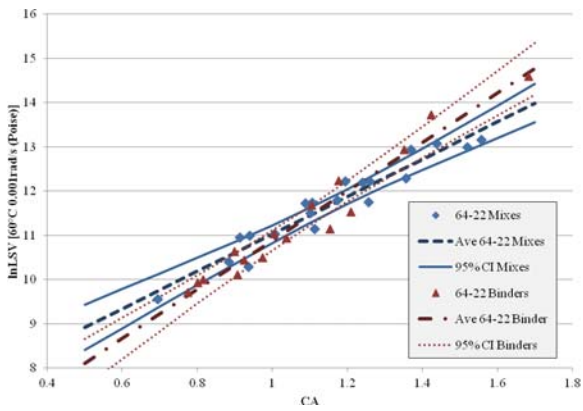


(c) PG64-22 Percent Increase in $|E^*|$

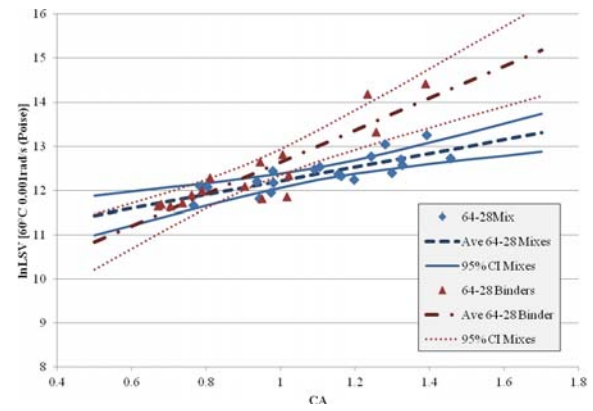


(d) PG64-28 Percent Increase in $|E^*|$

Figure E2d.4. Graph. Dynamic modulus and percent increase vs. carbonyl.



(a)



(b)

Figure E2d.5. Graph. 95% Confidence interval of hardening susceptibility for (a) PG64-22 and (b) PG64-28 binders.

Another important factor investigated in the BBR-SENB was the ability to capture the brittle-ductile transition behavior of binders at low temperatures. To this end, the glass transition temperature was measured using the dynamometric system for the pooled fund phase II and WRI verification sections binders. SENB results in terms of fracture energy (G_f), fracture toughness (K_{IC}) and fracture deflection were plotted based on the relative distance of the test temperature to the respective binder's glass transition temperature. Figure E2d.6 shows the aforementioned plots.

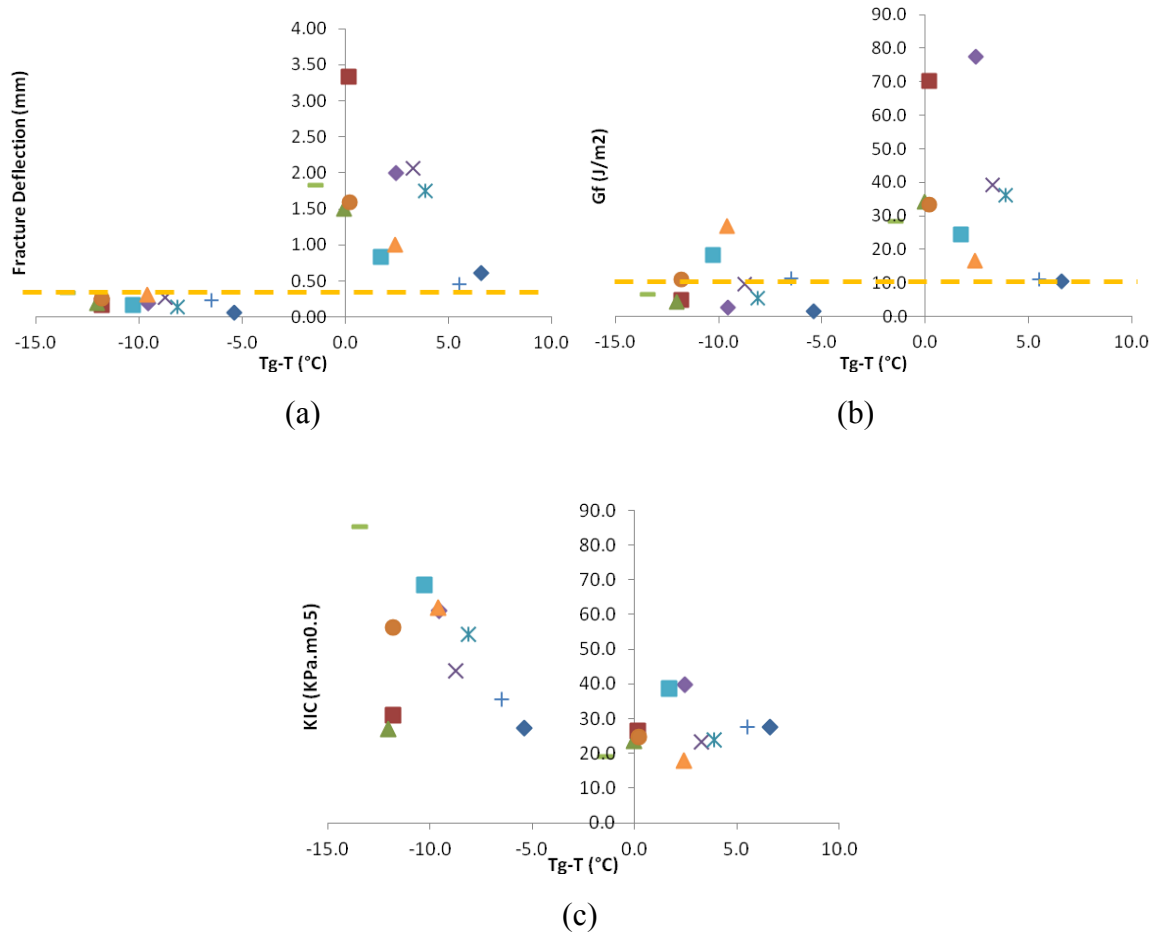


Figure E2d.6. Graph. Demonstration of the brittle-ductile transition behavior using SENB parameters (a) fracture deflection, (b) fracture energy, and (c) fracture toughness.

The data points in figure E2d.6 (a) show that a clear differentiation between the brittle (below T_g) and ductile/ductile-brittle regime above the T_g can be observed using the fracture deflection. The ductile to brittle cut-off value is harder to discern when using fracture energy, in which the fracture load as well as the fracture deflection influence the results. Although 90% of the binders tested in the brittle temperatures fractured at energies at or below 10.0 J/m², a few binders in the ductile zone also fractured at energies below this value due to negligible or decreasing change of the energy in these binders when moving from ductile to brittle temperatures. The cause of this

unexpected behavior can be seen in figure E2d.6 (c), in which an overall increasing of the fracture toughness (analogous to an increase of fracture load) is observed as the binder enters the brittle temperature zone. This behavior complicates the use of both G_f and K_{IC} as indicators of the ductile-brittle transition in the binder, while the use of fracture deflection is very promising. Considering the relative ease of using the SENB compared to other binder fracture test procedures, the above discussion and results show that the SENB fracture energy and fracture deformation can be used to effectively differentiate binder low temperature performance and establish the binder brittle-ductile transition region. The test is a suitable alternative for the DTT, to be used as a compliment to the current BBR specification.

Significant Problems, Issues and Potential Impact on Progress

Major maintenance activities required on the TSRST equipment has slowed the progress on the development and production testing of those samples.

Delays in the purchase of the additional DSR have slowed the LSV and master curve determination of the binders. However, the new rheometer has been approved is in the process of being ordered.

Work Planned Next Quarter

Significant progress in the measurements of carbonyl, low shear viscosity, and binder master curves are to be completed in this quarter. With the E^* -tension testing underway, investigation onto the E^* -tension and $C_t(t)$ measures will continue. Testing on the TSRST samples are also expected to get underway as the exact testing conditions are determined. Efforts will continue to identify and perform the necessary measures for additional field validation sections.

In the next quarter the research team will complete the AASHTO draft standards on the measurement of the binder Glass Transition Temperature, as well as the use of the Asphalt Thermal Cracking Analyzer (ATCA) to measure mixture glass transition. The team is finalizing results of FE modeling of asphalt mixture glass transition and the development of binder to mixture glass transition prediction models, which will be reported on in detail in the next quarter. In the coming quarter the focus will be on finalizing data analysis and interpretation, in preparation of the final task report on thermal cracking.

Work element E2e: Design Guidance for Fatigue and Rut Resistance Mixtures (AAT)

Work Done This Quarter

Hirsch Model Refinements

Laboratory work continued this quarter on the experiments to refine the Hirsch model. Three experiments were planned to improve the Hirsch model: (1) curing time experiment, (2) limiting modulus experiment, (3) stress dependency experiment. Each of these experiments addresses a specific aspect of the Hirsch model and dynamic modulus testing. The curing time experiment

addresses whether specimen aging significantly affects measured dynamic modulus values. The limiting modulus experiment address whether the limiting minimum modulus is a HMA is significantly affected by the modulus of the aggregate used in the mixture. Finally, the stress dependency experiment address the effect of stress level on the limiting minimum modulus of HMA. Specimen fabrication and testing continued based on the approved work plan. Specimen fabrication and testing is approximately 75 percent complete.

Resistivity Model Refinements

The objective of this work is to refine the rutting model developed in NCHRP Projects 9-25 and 9-31 to better address modified binders by using data from the multiple stress creep recovery tests to characterize the binders. A final experimental design for the resistivity model refinements was developed based on the aggregates selected for the Hirsch model refinement. It includes nine binders with high temperature grade ranging from PG 58 to PG 82. Five of the binders are polymer modified, one is air blown, and three are neat. Eighteen mixtures will be tested. A total of 34 binder/mixture/temperature combinations will be used in the testing. Specimen fabrication for this experiment was initiated this quarter.

Fatigue Model Refinements

Two papers detailing the fatigue analysis were completed and submitted to the Association of Asphalt Paving Technologists.

1. "Modeling Fatigue Damage Functions for Hot Mix Asphalt," by Donald W. Christensen, Jr. and Ramon F. Bonaquist
2. "Analysis of FHWA ALF Fatigue Data Using a Continuum Damage Approach," by Donald W. Christensen, Jr. and Ramon Bonaquist.

A presentation was made to the Models Expert Task Group describing Work Element E2e.

Work Planned Next Quarter

Laboratory work will continue for the Hirsch model, resistivity model, and continuum damage fatigue model refinements. Analysis of the data from these experiments will proceed concurrently with the laboratory testing.

Significant Problems, Issues and Potential Impact on Progress

The laboratory experiments in this Work Element are behind schedule. Materials have been procured and laboratory work proceeding. These experiments will be completed during 2011.

TABLE OF DECISION POINTS AND DELIVERABLES FOR ENGINEERED MATERIALS

Name of Deliverable	Type of Deliverable	Description of Deliverable	Original Delivery Date	Revised Delivery Date	Reason for changes in delivery date
E1a- Model and Algorithm (TAMU)	Model and Algorithm	The model and algorithm for testing and analysis of damaged asphalt mixtures in tension	9/1/11	08/31/12	Late arrival of aggregates for fabrication specimens.
E1a- Continuum Damage Permanent Deformation Analysis for Asphalt Mixtures (TAMU)	Final Report	Ph.D. dissertation at TAMU that describes the viscoplastic mechanism for permanent deformation of the asphalt mixtures and provides the testing protocols and analysis methods to acquire the input parameters of the PANDA program.	12/31/2010	8/31/12	Late arrival of aggregates
E1a- Develop a RDT DMA Testing Protocol (TAMU)	Technology Transfer	This new testing protocol is stress controlled repeated tension testing method and will be used to replace the previous torsional DMA testing method	08/15/2010	Complete	Presented as Technology Development #14
E1a- Standardize Testing Procedure for Specifications (TAMU)	AASHTO Specification	Develop a Standard Specification to use as a comparative test to evaluate fracture properties, healing and moisture damage of FAM	4/30/11	Submitted	Expanded scope
E1a- Develop a New DMA Testing Protocol for Compression (TAMU)	AASHTO Specification	Develop a Standardized testing method to use as a comparative test to evaluate compressive properties of FAM	9/15/11	3/15/12	More time need due to the machine data acquisition deficiency (machine built-in LVDT cannot meet needed strain precision) will fabricate special grip to incorporate the external magnetic sensor
E1b1-5: Standard Testing Procedure and Recommendation for Specifications (UWM)	Draft Report	Report on final conclusions and proposed procedures and specifications	7/11	3/13	Additional work planned in project extension. The reports for E1b-2 and E1b1-5 are combined. (report "O")
	Final Report		1/12	10/13	

Name of Deliverable	Type of Deliverable	Description of Deliverable	Original Delivery Date	Revised Delivery Date	Reason for changes in delivery date
E1b-2i. Literature review (UWM)	Draft Report	Review of previous work on indentation and closed formed solution to the indentation problem.	7/09	3/13	Additional work planned in project extension.
E1b-2iii. Preliminary testing and correlation of results (UWM)	Draft Report	The use of indentation test for characterization of asphalt binders.	1/10	10/13	The reports for E1b-2 and E1b1-5 are combined.
E1b-2iv. Feasibility of using indentation tests for fracture and rheological properties (UWM)	Draft Report	Report on Finite element simulations of the indentation test and correlations with DSR results.	1/11	3/13	(report "O")
	Final Report		4/11	10/13	
E1c-1ii. Effects of Warm Mix Additives on Mixture Workability and Stability (UWM)	Draft Report	Report of reviewed relevant literature and studies (to be combined with final report)	10/08	Complete	Additional work planned in the project extension. (Integrated with report "P")
	Final Report		1/09		
	Draft Report	Impacts of WMA Additives on Asphalt Binder Performance and Mixture Workability	4/11	3/13	
	Final Report		1/12	10/13	
E1c-1v. Field Evaluation of Mix Design Procedures and Performance Recommendations (UWM)	Draft Report	Report on WMA Field Evaluation of Mix Design Procedures and Performance	10/11	3/13	
	Final Report		1/12	10/13	
E1c-2: Improvement of Emulsions' Characterization and Mixture Design for Cold Bitumen Applications (UWM)	Practice	Mix design method for cold-in-place recycling (CIR) that is consistent with the Superpave technology and that can be used to define the optimum combination of moisture content and emulsion content.	12/11	3/13	Additional work planned in project extension. (Integrated with report "Q")
	Practice	Mix design method for cold mix asphalt (CMA) that is consistent with the Superpave technology and that can be used to define the optimum combination of moisture content and emulsion content.	03/12	10/13	
E1c-2i: Review of Literature and Standards (UWM)	Draft Report	Review of Literature and Standards that will be combined with the final draft reports (to be combined with E1c-2vii and E1c-2ix final reports)	7/08	Complete	Additional work planned in project extension. (Integrated with report "Q")
	Final Report		10/08		
	Draft Report		4/09		
	Draft Report		7/09		
	Draft Report		1/10		
E1c-2iii: Identify Tests and Develop Experimental Plan (UWM)	Draft Report	Reports outlining the required tests and experimental plan for the study (to be combined with E1c-2vii and E1c-2ix final reports)	4/09	Complete	
	Draft Report		10/09		
E1c-2v. Conduct Testing Plan (UWM)	Draft Report	Report on the results and analysis of tests run in accordance to test plan (to be combined with E1c-2vii and E1c-2ix final reports)	10/09	Complete	

Name of Deliverable	Type of Deliverable	Description of Deliverable	Original Delivery Date	Revised Delivery Date	Reason for changes in delivery date
E1c-2vii. Validate Guidelines (UWM)	Draft Report	Draft report of the performance and Rheological and Bond Properties of Emulsions (to be combined with E1c-2vii final report)	7/09	3/13	Additional work planned in the project extension. (Integrated with report "Q")
	Final Report	Final report of the performance and Rheological and Bond Properties of Emulsions	4/11	10/13	
E1c-2ix. Develop CMA Performance Guidelines (UWM)	Draft Report	Draft and final report of the performance guidelines of Cold Mix asphalt pavements	10/11	3/13	
	Final Report		1/12	10/13	
E2a-4: Write asphalt modification guideline/report on modifier impact over binder properties (UWM)	Draft Report	Report summarizing effect of modification on low, intermediate, and high temperature performance of asphalt binders. It includes guidelines for modification and cost index for different modification types	10/11	3/13	Delay caused by difficulty in obtaining economic information for use of different modifiers.
	Final Report	Report in 508 format that addresses comments/concerns from Draft Report	1/12	10/13	Additional work planned in the project extension. (Report "N")
E2b-1: Develop a System to Evaluate the Properties of RAP Materials (UNR with UWM input)	Draft Report	Report on Test Method to Quantify the Effect of RAP and RAS on Blended Binder Properties without Binder Extraction (To be combined with E2b1-b draft and final reports) (UWM input)	4/09	6/30/2013	Additional work planned in the project extension. (All reports integrated into report "G")
	Final Report		4/09	12/31/2013	
	Practice	Recommend the most effective methods for extracting RAP aggregates based on their impact on the various properties of the RAP aggregates and the volumetric calculations for the Superpave mix design.	12/10	6/30/2013	
E2b-1.b: Develop a System to Evaluate the Properties of the RAP Binder (UWM)	Draft Report	Report on the developed testing and analysis procedure system to estimate the RAP binder properties from binder and mortar testing including fracture results.	10/11	6/30/2013	Additional work planned in project extension. (All reports integrated into report "G")
	Final Report		1/12	12/30/2013	

Name of Deliverable	Type of Deliverable	Description of Deliverable	Original Delivery Date	Revised Delivery Date	Reason for changes in delivery date
E2b-3: Develop a Mix Design Procedure (UNR)	Draft report	Report summarizing the laboratory mixing experiment.	02/12	6/30/2013	Additional work planned in project extension. (All reports integrated into report "G")
	Final report		08/12	12/31/2013	
E2b-4: Impact of RAP Materials on Performance of Mixtures And E2b-5: Field Trials (UNR)	Draft report	Report summarizing the laboratory and field performance of field mixtures.	02/12	6/30/2013	
	Final report		08/12	12/31/2013	
E2c-2: Conduct Mixtures Evaluations (UNR)	Draft report	Approach to identify critical conditions of HMA mixtures	09/11	Complete	N/A
	Final report		03/12	N/A	N/A
E2c-3: Develop a Simple Test (UNR)	Draft report	Report summarizing the evaluation of mixtures from the Flow Number Task Force group.	11/11	N/A	N/A
	Final report		05/12	N/A	N/A
E2c-4: Develop Standard Test Procedure (UNR)	Practice	Recommended practice to identify the critical condition of an HMA mix at the mix design stage to avoid accelerated rutting failures of HMA pavements.	12/11	N/A	N/A
E2c-5: Evaluate the Impact of Mix Characteristics (UNR)	Draft report	Report summarizing the impact of mixture characteristics on the critical condition of the HMA mixes	02/12	N/A	N/A
	Final report		08/12	N/A	N/A
E2d-2: Identify the Causes of the Thermal Cracking (UNR)	Draft report	Report summarizes the testing and findings for materials from LTPP sections.	12/11	4/30/2013	Additional work planned in the project extension. (All reports integrated into report "I")
	Final report		06/12	10/31/2013	
E2d-3: Identify an Evaluation and Testing System (UNR with UWM input)	Draft report	Low Temperature Cracking Characterization of Asphalt Binders by Means of the Single-Edge Notch Bending (SENB) Test (UWM input)	04/11	4/30/2013	Additional work planned in the project extension. (All reports integrated into report "I")
	Final report		10/11	10/31/2013	
E2d-4: Modeling and validation of the Developed System (UNR with UWM input)	Draft report	Thermal cracking characterization of mixtures by means of the unified Tg-TSRST device. (UWM input) Model that can effectively simulate the long-term properties of HMA mixtures in the intermountain region and assess the impact of such properties on the resistance of HMA mixtures to thermal cracking.	10/11	4/30/2013	Additional work planned in the project extension. (All reports integrated into report "I")
	Final report		04/12	10/31/2013	
	Model		03/12	4/30/2013	

Name of Deliverable	Type of Deliverable	Description of Deliverable	Original Delivery Date	Revised Delivery Date	Reason for changes in delivery date
E2d-5: Develop a Standard (UNR with UWM input)	Draft standard	Draft standards for the use of the SENB, binder Tg and the ATCA device (Mixture Tg). (UWM input)	10/11	4/30/2013	Additional work planned in the project extension. (All reports integrated into report "I")
E2d-5: Develop a Standard (UNR with UWM input)	Final standard		01/12	10/31/2013	
E2d-5: Develop a Standard (UNR with UWM input)	Draft standard	Draft standard for the use of the TSRST with cylindrical specimens compacted using the SGC.	03/11	4/30/2013	Delayed due to issues with specimens breaking at the edge. Working on refining sample preparation. Added the capability of measuring the strain change during testing. (Report "I")
	Final standard		01/12	10/31/2013	
E2e: Improved Models	Models	Improved composition to engineering property models. <ul style="list-style-type: none"> Hirsch Model for dynamic modulus Resistivity Model for rutting resistance Continuum Damage Fatigue Model Permeability 	1/1/2012	6/30/12	Testing delays
E2e: New Model	Model	Damage tolerance as a function of mix fracture properties	12/31/2012	N/A	New work
E2e: Report documenting Work Element E2e	Draft Report	Draft Report for Design Guidance for Fatigue and Rut Resistance Mixtures	1/1/2012	3/31/2012	Testing delays and addition of damage tolerance as a function of mix fracture properties.
	Final Report		3/31/2012	12/31/2012	

Engineered Materials Year 5	Year 5 (4/2011-3/2012)												Team	
	4	5	6	7	8	9	10	11	12	1	2	3		
(1) High Performance Asphalt Materials														
E1a: Analytical and Micro-mechanics Models for Mechanical behavior of mixtures														TAMU
E1a-1: Analytical Micromechanical Models of Binder Properties									D,JP				F	
E1a-2: Analytical Micromechanical Models of Modified Mastic Systems									D		SW, M&A		F	
E1a-3: Analytical Models of Mechanical Properties of Asphalt Mixtures			P(2)						D,JP		SW, M&A		F	
E1a-4: Analytical Model of Asphalt Mixture Response and Damage						P(2)			D		SW, M&A		F	
E1b: Binder Damage Resistance Characterization														UWM
E1b-1: Rutting of Asphalt Binders														
E1b-1-i: Literature review														
E1b1-2: Select Materials & Develop Work Plan														
E1b1-3: Conduct Testing														
E1b1-4: Analysis & Interpretation			JP											
E1b1-5: Standard Testing Procedure and Recommendation for Specifications	P				D		JP						F	
E1b-2: Feasibility of determining rheological and fracture properties of asphalt binders and mastics using simple indentation tests (modified title)														UWM
E1b-2i: Literature Review														
E1b-2ii: Proposed SuperPave testing modifications														
E1b-2iii: Preliminary testing and correlation of results	JP													
E1b-2iv: Feasibility of using indentation tests for fracture and rheological properties								D					F	
E2a: Comparison of Modification Techniques														UWM
E2a-1: Identify modification targets and material suppliers														
E2a-2: Test material properties														
E2a-3: Develop model to estimate level of modification needed and cost index														
E2a-4: Write asphalt modification guideline/report on modifier impact over binder properties								D					F	
E2c: Critically Designed HMA Mixtures														UNR
E2c-1: Identify the Critical Conditions														
E2c-2: Conduct Mixtures Evaluations							D,F							
E2c-3: Develop a Simple Test					JP				D		F			
E2c-4: Develop Standard Test Procedure											D,F			
E2c-5: Evaluate the Impact of Mix Characteristics													D	F
E2d: Thermal Cracking Resistant Mixes for Intermountain States														UNR/UWM
E2d-1: Identify Field Sections														
E2d-2: Identify the Causes of the Thermal Cracking										D	P		F	
E2d-3: Identify an Evaluation and Testing System	D			JP				F			P			
E2d-4: Modeling and Validation of the Developed System				JP				D			F,P			
E2d-5: Develop a Standard				JP				D			F,P			
E2e: Design Guidance for Fatigue and Rut Resistance Mixtures														AAT
E2e-1: Identify Model Improvements														
E2e-2: Design and Execute Laboratory Testing Program														
E2e-3: Perform Engineering and Statistical Analysis to Refine Models														
E2e-4: Validate Refined Models														
E2e-5: Prepare Design Guidance									D				F	
(2) Green Asphalt Materials														
E2b: Design System for HMA Containing a High Percentage of RAP Material														UNR
E2b-1: Develop a System to Evaluate the Properties of RAP Materials				JP				D,P					F	
E2b-2: Compatibility of RAP and Virgin Binders	P													WRI
E2b-3: Develop a Mix Design Procedure								JP,P					D	F
E2b-4: Impact of RAP Materials on Performance of Mixtures													D	F
E2b-5: Field Trials													D	F
E1c: Warm and Cold Mixes														UWM
E1c-1: Warm Mixes														
E1c-1i: Effects of Warm Mix Additives on Rheological Properties of Binders														
E1c-1ii: Effects of Warm Mix Additives on Mixture Workability and Stability									D				F	
E1c-1iii: Mixture Performance Testing														
E1c-1iv: Develop Revised Mix Design Procedures														
E1c-1v: Field Evaluation of Mix Design Procedures and Performance Recommendations									D					
E1c-2: Improvement of Emulsions' Characterization and Mixture Design for Cold Bitumen Applications														UWM/UNR
E1c-2i: Review of Literature and Standards														
E1c-2ii: Creation of Advisory Group														
E1c-2iii: Identify Tests and Develop Experimental Plan														
E1c-2iv: Develop Material Library and Collect Materials														
E1c-2v: Conduct Testing Plan						JP								
E1c-2vi: Develop Performance Selection Guidelines						JP								
E1c-2vii: Validate Performance Guidelines														
E1c-2viii: Develop CMA Mix Design Guidelines									P					
E1c-2ix: Develop CMA Performance Guidelines									P					

Deliverable codes
D: Draft Report
F: Final Report
M&A: Model and algorithm
SW: Software
JP: Journal paper
P: Presentation
DP: Decision Point

Deliverable Description
Report delivered to FHWA for 3 week review period.
Final report delivered in compliance with FHWA publication standards
Mathematical model and sample code
Executable software, code and user manual
Paper submitted to conference or journal
Presentation for symposium, conference or other
Time to make a decision on two parallel paths as to which is most promising to follow through

Work planned
Work completed
Parallel topic

Engineered Materials Year 2 - 5	Year 2 (4/08-3/09)				Year 3 (4/09-3/10)				Year 4 (04/10-03/11)				Year 5 (04/11-03/12)				Team
	Q1	Q2	Q3	Q4	Q1	Q2	Q3	Q4	Q1	Q2	Q3	Q4	Q1	Q2	Q3	Q4	
(1) High Performance Asphalt Materials																	
E1a: Analytical and Micro-mechanics Models for Mechanical behavior of mixtures																	TAMU
E1a-1: Analytical Micromechanical Models of Binder Properties				P, JP	JP	P	P	JP		P		P			D, JP	F	
E1a-2: Analytical Micromechanical Models of Modified Mastic Systems				P, JP	JP	P	P				P				D	F, SW, M&A	
E1a-3: Analytical Models of Mechanical Properties of Asphalt Mixtures	P	P, JP		P, JP	JP	P	P	M&A		P, JP(3)	JP (2)	P, M&A	JP(2)	P(2)	D, JP	F, SW, M&A	
E1a-4: Analytical Model of Asphalt Mixture Response and Damage				P, JP	JP	P	P					P		P(2)	D	F, SW, M&A	
E1b: Binder Damage Resistance Characterization																	UWM
E1b-1: Rutting of Asphalt Binders																	
E1b-1-1: Literature review																	
E1b1-2: Select Materials & Develop Work Plan	DP, P		P														
E1b1-3: Conduct Testing						JP		P	DP								
E1b1-4: Analysis & Interpretation		JP	P	JP		JP		P					JP				
E1b1-6: Standard Testing Procedure and Recommendation for Specifications										P		DP	P	D, JP		F	
E1b-2: Feasibility of Determining rheological and fracture properties of asphalt binders and mastics using simple indentation tests (modified title)																	
E1b-2i: Literature Review							D										
E1b-2ii: Proposed SuperPave testing modifications or new testing devices							P										
E1b-2iii: Preliminary testing and correlation of results								D		JP			JP				
E1b-2iv: Feasibility of using indentation tests for fracture and rheological properties						JP		P				P, D			D	F	
E2a: Comparison of Modification Techniques																	UWM
E2a-1: Identify modification targets and material suppliers				DP		DP											
E2a-2: Test material properties								P		P							
E2a-3: Develop model to estimate level of modification needed and cost index																	
E2a-4: Write asphalt modification guideline/report on modifier impact over binder properties												JP			D	F	
E2c: Critically Designed HMA Mixtures																	UNR
E2c-1: Identify the Critical Conditions		JP		D, F		JP	D	F									
E2c-2: Conduct Mixtures Evaluations								D				JP		D, F			
E2c-3: Develop a Simple Test														JP	D, F		
E2c-4: Develop Standard Test Procedure															D, F		
E2c-5: Evaluate the Impact of Mix Characteristics																D, F	
E2d: Thermal Cracking Resistant Mixes for Intermountain States																	UWM/UNR
E2d-1: Identify Field Sections			D, F	D, F	D	F											
E2d-2: Identify the Causes of the Thermal Cracking															D	F, P	
E2d-3: Identify an Evaluation and Testing System					DP	JP	DP, D			JP		JP, P	D	JP	F	P	
E2d-4: Modeling and Validation of the Developed System										JP		P		JP	D	F, P	
E2d-5: Develop a Standard														JP	D	F, P	
E2e: Design Guidance for Fatigue and Rut Resistance Mixtures																	AAT
E2e-1: Identify Model Improvements																	
E2e-2: Design and Execute Laboratory Testing Program																	
E2e-3: Perform Engineering and Statistical Analysis to Refine Models																	
E2e-4: Validate Refined Models																	
E2e-5: Prepare Design Guidance															D	F	
(2) Green Asphalt Materials																	
E2b: Design System for HMA Containing a High Percentage of RAP Material																	UNR
E2b-1: Develop a System to Evaluate the Properties of RAP Materials		JP		P	D	D, F	D		P, JP	JP	P			P	JP	D, P	F
E2b-2: Compatibility of RAP and Virgin Binders																	
E2b-3: Develop a Mix Design Procedure								D			D				JP, P	D, F	
E2b-4: Impact of RAP Materials on Performance of Mixtures																D, F	
E2b-5: Field Trials										JP						D, F	
E1c: Warm and Cold Mixes																	UWM
E1c-1: Warm Mixes																	
E1c-1i: Effects of Warm Mix Additives on Rheological Properties of Binders																	
E1c-1ii: Effects of Warm Mix Additives on Mixture Workability and Stability										JP					D	F	
E1c-1iii: Mixture Performance Testing		P	D	F, DP													
E1c-1iv: Develop Revised Mix Design Procedures						JP		P, DP	DP, P								
E1c-1v: Field Evaluation of Mix Design Procedures and Performance Recommendations															D		
E1c-2: Improvement of Emulsions' Characterization and Mixture Design for Cold Bitumen Applications																	UW/UNR
E1c-2i: Review of Literature and Standards		JP, P, D	F		D1	D3		D6									
E1c-2ii: Creation of Advisory Group																	
E1c-2iii: Identify Tests and Develop Experimental Plan				P, DP	D1		D4										
E1c-2iv: Develop Material Library and Collect Materials																	
E1c-2v: Conduct Testing Plan						JP	D5	P		JP	P				JP		
E1c-2vi: Develop Performance Selection Guidelines										JP	P				JP		
E1c-2vii: Validate Guidelines																	
E1c-2viii: Develop CMA Mix Design Procedure						D2										P	
E1c-2ix: Develop CMA Performance Guidelines																P	

Deliverable codes
D: Draft Report
F: Final Report
M&A: Model and algorithm
SW: Software
JP: Journal paper
P: Presentation
DP: Decision Point

Deliverable Description
Report delivered to FHWA for 3 week review period.
Final report delivered in compliance with FHWA publication standards
Mathematical model and sample code
Executable software, code and user manual
Paper submitted to conference or journal
Presentation for symposium, conference or other
Time to make a decision on two parallel paths as to which is most promising to follow through

Work planned
Work completed
Parallel topic
Delayed

PROGRAM AREA: VEHICLE-PAVEMENT INTERACTION

CATEGORY VP1: WORKSHOP

Work element VP1a: Workshop on Super-Single Tires (UNR)

This work element is complete.

CATEGORY VP2: DESIGN GUIDANCE

Work element VP2a: Mixture Design to Enhance Safety and Reduce Noise of HMA (UWM)

Work Done This Quarter

Researchers this quarter concluded field studies that utilized the Dynamic Friction Tester (DFT) and Circular Track Meter (CTM) devices to measure friction and texture in the field. These devices were on loan from FHWA through Applied Asphalt Technologies (AAT), the company responsible for administering the Equipment Loan Program (ELP). Researchers provided several recommendations to AAT based on their experiences using the DFT and CTM equipment. The data collected were used to compare to laboratory equipment under development to measure texture and friction on lab prepared samples.

The research team made progress in acquiring loose mix samples from area contractors. Loose mix samples were compacted in the laboratory using a Superpave gyratory compactor (SGC). Once compacted, these mixes were tested using the Stationary Laser Profiler (SLP) and the British Pendulum Tester (BPT). Results were compared to field collected data. The comparison demonstrates that field texture can be effectively simulated in a laboratory environment using standard compaction equipment. More mixes were collected this quarter and will continue collecting more before the construction season ends in a few weeks.

The research team also worked diligently to summarize work to date and submitted a manuscript for publication and presentation at the upcoming Transportation Research Board 91st Annual Meeting in 2012. Citation information for this document is given in the “Presentations and Publications” portion of this report. The research team also began working on the final report for this work element, which will be the focal point of the research in the coming quarter.

Significant Results

Researchers used the data collected for this work element to derive models to estimate critical texture spectrum parameters from mixture volumetrics and aggregate properties. The SLP is identified as a potential method to characterize pavement surface texture properties that are critical for estimating friction and skid resistance. Using texture spectral analysis methods, the

SLP system can capture macro-texture properties and limited micro-texture properties that are related to frictional characteristics of in-service field sections. Laboratory test methods are able to estimate friction values obtained using the DFT at low speeds and high speeds. If mixture design properties are known, field texture and friction can be estimated using these laboratory test methods. Because the models developed in this study utilized a limited data set, more mixes are needed to verify the models and validate the model coefficients. With this method, it is believed that mix designers have an improved tool by which to estimate pavement performance in terms of friction.

Significant Problems, Issues and Potential Impact on Progress

Researchers encountered no significant problems or issues this quarter.

Work Planned Next Quarter

Work in the next quarter will focus on the following activities:

- Drafting a final summary report for the VP2 work element.
- Constructing International Friction Index (IFI) values of SLP-BPT measurements for comparison to CTM-DFT measurements.
- Analyzing additional field sections and loose mix samples to confirm that laboratory preparation procedures can simulate field conditions.

Presentations and Publications

Miller, T., D. Swiertz, L. Tashman, N. Tabatabaee, and H. Bahia, "Characterization of Asphalt Pavement Surface Texture." Publication submitted to the Transportation Research Board Annual Meeting 2012. 01 August 2011.

Miller, T. "FHWA Equipment Loan Program Summary." Internal report submitted to Applied Asphalt Technologies for incorporation into annual report for FHWA. 01 September 2011.

CATEGORY VP3: MODELING

Work element VP3a: Pavement Response Model to Dynamic Loads (UNR)

Work Done This Quarter

Continued the work on the *3D-Move Analysis* software. The Pavement Performance Module (PPM) has been integrated into the 3D-Move version 2.0 software and has been under internal evaluation for bugs and errors.

Assisted user's with issues ranging from usage questions, concepts clarifications, and bugs. The 3D-Move Analysis software developing team worked on fixing the reported bugs.

Another concurrent activity during the last quarter was the development of the 3D-Move Analysis: User Guide. This guide is an important document that can be used as a reference by the 3D-Move users as it gives 3D-Move formulation, its capabilities, relevant references, along with three worked examples etc. The User Guide has been divided into the following chapters: 1. Introduction and Features of 3D-Move Analysis; 2. Formulation of 3D-Move Analysis; 3. Menus of 3D-Move Analysis; 4. Project Information; 5. Axle Configuration and Contact Pressure Distribution; 6. Vehicle Suspension and Road Roughness; 7. Traffic Information and Pavement Structure; 8. Material Characterization; 9. Performance Analysis; 10. Response Points; 11. Post Processing; 12. Appendices: Examples; 13. References. This activity is 75% complete.

The effect of tire-pavement contact stress distribution and braking on flexible pavement responses were evaluated while considering moving loads and viscoelastic properties of the asphalt layer. Additionally, the computed pavement responses were used to predict rut depth and bottom-up fatigue cracking in the asphalt layer following MEPDG approach for pavement distresses computations.

Significant Results

The PPM that is available in version 2.0 includes pavement condition prediction relative to asphalt distress modes (top-down cracking, bottom-up cracking and rutting) and rutting in unbound layers. This undertaking had become unexpectedly involved because of the need to consider traffic loading from non-uniform contact stress distributions. When non-uniform contact stress conditions are considered, the location of maximum response is not readily predictable. The maximum response locations need to be evaluated internally by the software.

The new version of 3D-Move (version 2) has been alpha-tested and the beta-testing is underway. There have been many issues, which were mainly brought upon due to the difference in US vs. SI units as many of the Pavement Performance Models are unit sensitive. This version is expected to be released by in November 2011.

A comprehensive study was conducted to assess the impact of non-uniform contact stress distribution on pavement responses and performance. The study utilized three different pavement sections and laboratory-measured mixture properties for the HMA layer. The measured non-uniform contact stresses data showed a much larger contact area and substantial variation in contact stress distribution than the conventional uniform conditions often assumed in pavement analyses. Regardless of the asphalt layer thickness, mixture type and braking condition, all three uniform contact stress distributions (circular, square and elliptical) overestimated the maximum vertical strains and thus HMA rut depth by as much as 71% when compared to those from non-uniform contact stress distribution. For non-braking condition, an increase of 34 to 71% in HMA rut depth was observed for the uniform stress distributions when compared to the non-uniform stress distribution. The HMA rut depth was 3 to 4 times larger for the pavements subjected to braking condition regardless of the type and shape of the tire-pavement contact stress distribution. Numbers of cycles to fatigue failure under non-braking condition for the uniform contact stress distributions were within 15% of those determined for the non-uniform stress

distributions. Braking further increased this limit to as much as 27%, indicating the importance of the consideration of braking in pavement performance analyses.

Significant Problems, Issues and Potential Impact on Progress

The release of version 2.0 of the software was delayed because of extensive verification of the Pavement Performance Module (PPM).

The 3D-Move Analysis verification plan was postponed until the release of the version 2.0 of the software that will have the various new features and address the various bugs.

Work Planned Next Quarter

Continue working on the 3D-Move model to make it a menu-driven software. Complete the beta-testing of version 2.0 of the software. Continue to solve any issues and bugs that users may encounter. Continue to maintain the 3D-Move Forum.

TABLE OF DECISION POINTS AND DELIVERABLES FOR VEHICLE-PAVEMENT INTERACTION

Name of Deliverable	Type of Deliverable	Description of Deliverable	Original Delivery Date	Revised Delivery Date	Reason for Changes in Delivery Date
VP2a-4: Run parametric studies on tire-pavement noise and skid response (UWM)	Draft Report	Draft report on proposed design guideline for noise reduction, durability, safety and costs	1/10	12/11	Final analysis being performed and completing draft report.
VP2a-7: Proposed optimal guideline for design to include noise reduction, durability, safety and costs (UWM)	Final Report	Final report on proposed design guideline for noise reduction, durability, safety and costs	1/12	9/12	Reports integrated into report "R".
VP3a-4: Overall Model (UNR)	Software	Release of version 2.0 of the 3D-Move pavement response model	06/11	12/11	Extensive verification of the Pavement Performance Module (PPM) delayed the release of version 2.0 of the software.
	Draft report	Summarizing <i>3D-Move Analysis</i> software	12/11	N/A	N/A
	Final report		06/12	N/A	N/A
	Software	Release of final version of the 3D-Move pavement response model	03/12	N/A	N/A

Vehicle-Pavement Interaction Year 5

	Year 5 (4/2011-3/2012)												Team	
	4	5	6	7	8	9	10	11	12	1	2	3		
(1) Workshop														
VP1a: Workshop on Super-Single Tires														UNR
(2) Design Guidance														
VP2a: Mixture Design to Enhance Safety and Reduce Noise of HMA														UWM
VP2a-1: Evaluate common physical and mechanical properties of asphalt mixtures with enhanced frictional skid characteristics														
VP2a-2: Evaluate pavement macro- and micro-textures and their relation to tire and pavement noise-generation mechanisms														
VP2a-3: Develop a laboratory testing protocol for the rapid evaluation of the macro and micro-texture of pavements				P										
VP2a-4: Run parametric studies on tire-pavement noise and skid response														
VP2a-5: Establish collaboration with established national laboratories specialized in transportation noise measurements. Gather expertise on measurements and analysis														
VP2a-6: Model and correlate acoustic response of tested tire-pavement systems					JP	P								
VP2a-7: Proposed optimal guideline for design to include noise reduction, durability, safety and costs						P	D				F			
(3) Pavement Response Model Based on Dynamic Analyses														
VP3a: Pavement Response Model to Dynamic Loads														UNR
VP3a-1: Dynamic Loads														
VP3a-2: Stress Distribution at the Tire-Pavement Interface														
VP3a-3: Pavement Response Model														
VP3a-4: Overall Model			SW							D			F, SW	

Deliverable codes

- D: Draft Report
- F: Final Report
- M&A: Model and algorithm
- SW: Software
- JP: Journal paper
- P: Presentation
- DP: Decision Point

Deliverable Description

- Report delivered to FHWA for 3 week review period.
- Final report delivered in compliance with FHWA publication standards
- Mathematical model and sample code
- Executable software, code and user manual
- Paper submitted to conference or journal
- Presentation for symposium, conference or other
- Time to make a decision on two parallel paths as to which is most promising to follow through

	Work planned
	Work completed
	Parallel topic

Vehicle-Pavement Interaction Years 2 - 5

	Year 2 (4/08-3/09)				Year 3 (4/09-3/10)				Year 4 (04/10-03/11)				Year 5 (04/11-03/12)				Team
	Q1	Q2	Q3	Q4	Q1	Q2	Q3	Q4	Q1	Q2	Q3	Q4	Q1	Q2	Q3	Q4	
(1) Workshop																	
VP1a: Workshop on Super-Single Tires																	UNR
(2) Design Guidance																	
VP2a: Mixture Design to Enhance Safety and Reduce Noise of HMA																	UWM
VP2a-1: Evaluate common physical and mechanical properties of asphalt mixtures with enhanced frictional skid characteristics				DP													
VP2a-2: Evaluate pavement macro- and micro-textures and their relation to tire and pavement noise-generation mechanisms				DP													
VP2a-3: Develop a laboratory testing protocol for the rapid evaluation of the macro and micro-texture of pavements		M&A												P			
VP2a-4: Run parametric studies on tire-pavement noise and skid response						JP		D	JP								
VP2a-5: Establish collaboration with established national laboratories specialized in transportation noise measurements. Gather expertise on measurements and analysis																	
VP2a-6: Model and correlate acoustic response of tested tire-pavement systems									JP, P					JP, P			
VP2a-7: Proposed optimal guideline for design to include noise reduction, durability, safety and costs											P		P		D	F	
(3) Pavement Response Model Based on Dynamic Analyses																	
VP3a: Pavement Response Model to Dynamic Loads																	UNR
VP3a-1: Dynamic Loads			JP														
VP3a-2: Stress Distribution at the Tire-Pavement Interface																	
VP3a-3: Pavement Response Model						SW, v. β					JP						
VP3a-4: Overall Model										SW		SW			D	F, SW	

Deliverable codes

- D: Draft Report
- F: Final Report
- M&A: Model and algorithm
- SW: Software
- JP: Journal paper
- P: Presentation
- DP: Decision Point

Deliverable Description

- Report delivered to FHWA for 3 week review period.
- Final report delivered in compliance with FHWA publication standards
- Mathematical model and sample code
- Executable software, code and user manual
- Paper submitted to conference or journal
- Presentation for symposium, conference or other
- Time to make a decision on two parallel paths as to which is most promising to follow through

- Work planned
- Work completed
- Parallel topic

PROGRAM AREA: VALIDATION

CATEGORY V1: FIELD VALIDATION

Work element V1a: Use and Monitoring of Warm Mix Asphalt Sections (WRI)

Work Done This Quarter

The second annual monitoring of the Manitoba WMA sections was conducted in August. Construction of the WMA sections was completed in July 2010. The main distress noted was transverse cracking. The transverse cracks noted were determined to be reflective transverse cracks from the old pavement. Note that WRI performed a pre-construction distress survey and used GPS coordinates provided by Manitoba Infrastructure and Transportation (MIT) to establish the new monitoring sections in essentially the same locations. Although there is generally about 2 meters difference between the old transverse cracks and the new transverse cracks, the new crack pattern is identical to the old crack pattern; therefore the difference is attributed to inaccuracies in GPS equipment. Core samples were obtained to assess aging differences.

The annual monitoring of the Yellowstone WMA sections, constructed by FHWA Western Federal Lands in 2007, was performed in early September. The Yellowstone sections are still performing excellent with no distress noted. The Yellowstone Park Service maintenance personnel obtained core samples for WRI during the monitoring visit. The core samples were the first samples obtained since the sections have been in service. TAMU is conducting mechanical property testing of the cores and WRI is analyzing the aging properties of the cores with depth.

Significant Results

None.

Significant Problems, Issues and Potential Impact on Progress

None.

Work Planned Next Quarter

No WMA monitoring is planned for the next quarter. Work will continue on the Manitoba and Yellowstone core samples.

Work element V1b: Construction and Monitoring of Additional Comparative Pavement Validation Sites (WRI)

Work Done This Quarter

The second annual monitoring of the Manitoba RAP sections was conducted in August 2011. Manitoba Infrastructure and Transportation (MIT) personnel provided the traffic control, coring equipment, and personnel. MIT personnel are planning to conduct longitudinal profiling of the both the WMA and RAP sections. Only minor distress has occurred at the Manitoba RAP site after two years of service, mainly a couple of transverse cracks. It was noted however that the 50% RAP, 200/300 (softer grade), did not have any transverse cracks.

During the last quarter discussions were held with Arizona DOT personnel about ADOT interest in constructing high-RAP comparative performance sections using two different asphalt sources (same grade) with comparable no-RAP sections. Discussions are continuing with ADOT to possibly find a construction project for the 2012 construction season.

Significant Results

None.

Significant Problems, Issues and Potential Impact on Progress

None.

Work Planned Next Quarter

It is planned to monitor the Minnesota site in October and the Arizona site in November.

CATEGORY V2: ACCELERATED PAVEMENT TESTING

Work element V2a: Accelerated Pavement Testing including Scale Model Load Simulation on Small Test Track

Work Done This Quarter

No activity this quarter. This work element was included in order to accommodate any accelerated testing that may occur during the project.

Significant Results

None.

Significant Problems, Issues and Potential Impact on Progress

None.

Work Planned Next Quarter

No accelerated (field) testing is planned.

Work element V2b: Construction of Validation Sections at the Pecos Research & Testing Center

This work element is included to indicate that this may be a possibility for accelerated pavement testing for ARC research because it is a facility in the TAMU system.

CATEGORY V3: R&D VALIDATION

Work element V3a: Continual Assessment of Specifications (UWM)

Work Done This Quarter

Work this quarter entailed finalizing data analysis for the 2010-2011 Western Cooperative Test Group (WCTG) round-robin binder testing program. Researchers continued to coordinate mixture and binder testing efforts for the 2011-2012 WCTG test program and coordinated post-Asphalt Research Consortium (ARC) activities with the Rocky Mountain Asphalt User Producer Group (RMAUPG) steering committee leaders. A proposal for evaluating the PG+ protocols were submitted to this group and is currently being discussed amongst RMAUPG leaders, and optimism remains high for carrying on the test protocols outlined in this work element beyond ARC Year 5. Researchers also began drafting a final report for the V3a work element.

Analysis efforts focused on evaluating the Multiple Stress Creep and Recovery (MSCR) test method to evaluate modified binders and their role in pavement performance. After analyzing WCTG round-robin binder test results, researchers identified significant differences in the results, particularly in the first cycles at each stress level and the need for more cycles to reach the steady state. Analysis results were shared with Binger ETG members. Discussion about the need to change the MSCR test to include several conditioning cycles is undergoing. Also cycles to achieve steady-state behavior before calculating the response is under consideration. An extensive analysis of Jnr and PG grading was conducted and presented to the ETG. Changes to TP 70 and MP19 were formulated and discussed with ETG members.

Significant Results

Analysis of MSCR test results indicated that increasing the number of cycles can yield more consistent results. Researchers observed more fluctuation in the initial five test cycles, which may be attributed to material conditioning. Findings indicate that a consistent response can be

achieved for 30 loading cycles, and results also show that delayed elasticity effects are reduced following several conditioning cycles. As such, the test method should be updated to include a certain number of conditioning cycles at each stress level. Further research on the proposed method and comparison with mixture data needs to be performed.

Problems and Implications for Work

None.

Work Planned Next Quarter

Work in the next quarter will focus on the following tasks:

- Participating in WCTG binder and mixture testing.
- Compiling WCTG binder data for all participating laboratories.
- Facilitating RMAUPG leadership in preparing a presentation that outlines forthcoming collaborative efforts at the RMAUPG annual meeting.
- Drafting a final report for this work element.

References

“Superpave Protocols for Modified Asphalt Binders.” National Strategic Highway Research Program, Project 9-10, February 2001.

Work element V3b: Validation of the MEPDG Asphalt Materials Models Using New MEPDG Sites and Selected LTPP Sites (UNR, UWM)

Subtask V3b-1: Design and Build Sections (Start Year 1, Year 2, and Year 3)

Subtask V3b-2: Additional Testing (Start Year 2, Year 3, and Year 4)

Work Done This Quarter

None

Significant Results

None

Significant Problems, Issues and Potential Impact on Progress

Only two agencies have committed to the construction of MEPDG sites: the Washoe RTC in northern Nevada in 2008, The South Dakota DOT in 2009/2010. The researchers are facing significant hesitation from the DOTs to use the MEPDG to design and construct HMA pavements. The level of this work element has been reduced.

Work Planned Next Quarter

None

Subtask V3b-3: Select LTPP Sections (Start Year 1 thru Year 5)

Work Done This Quarter

In this quarter, the research team continued to evaluate the BBR-SENB (Single Edge Notched Beam) test and the LAS (Linear Amplitude Sweep) test on selected LTPP binders in order to evaluate the correlations of these binder properties with low temperature and fatigue cracking performance in the field.

The Single Edged Notched Beam Test for Low Temperature Resistance:

The LTPP materials tested include binders with SHRP ID numbers designated in table V3b-3.1. All binders were subject to RTFO aging. Table V3b-3.1 shows fracture energy (G_f) and fracture toughness (K_{IC}) of the LTPP binders measured at -12°C . Due to the different climatic conditions in the LTPP sections, it was decided to normalize the amount of cracking in each section to its corresponding Freeze Index (degree days below 0°C). Also, the ranking of the binders based on normalized field performance, PG grade, fracture energy, and fracture toughness is presented in table V3b-3.1. Generally, similar ranking for binders is observed for field performance and G_f . This is further demonstrated in the table by comparing the sum of differences in ranking, for which G_f gives the lowest sum of differences indicating that it is the best indicator to field cracks count as compared to PG grade or K_{IC} .

Table V3b-3.1. SENB results at -12°C for LTPP binders.

SHRP ID	PG Grade	RANK Based on PG grade	No. of Transverse cracks per section/ Freeze Index ($\times 10^{-3}$)	RANK Based on Cracks count	G_f (J/m^2)	RANK Based on G_f	K_{IC} ($\text{kPa}\cdot\text{m}^{0.5}$)	RANK Based on K_{IC}
370901	64-22	4	702.58	7	5.45	7	26.83	6
370903	70-22	4	343.25	6	6.24	6	55.03	1
90961	58-34	2	9.26	4	44.2	2	31.98	5
90962	58-28	3	6.18	2	11.87	4	37.57	4
90903	64-22	4	24.71	5	10.98	5	38.54	3
89a902	52-40	1	7.01	3	103.82	1	23.12	7
350903	58-22	4	1	1	21.31	3	40.93	2
Sum of ranking difference = Sum of (Field Cracks – Other Rank)		14	-	0	-	8	-	16

The ability of the SENB load-deflection curve to clearly estimate the low temperature performance of the binders can be seen in figure V3b-3.1. The section ID and respective LTPP performance index for each curve are presented on the plots. It can be seen that a very wide

range of change in fracture deflection and consequently in G_f exists between binders. Furthermore, binders with the higher fracture energy also show the best field performance. The SENB test clearly discriminates among the various binder types in terms of low temperature performance. These results also indicate the potential of using G_f as thermal cracking performance index for asphalt binders.

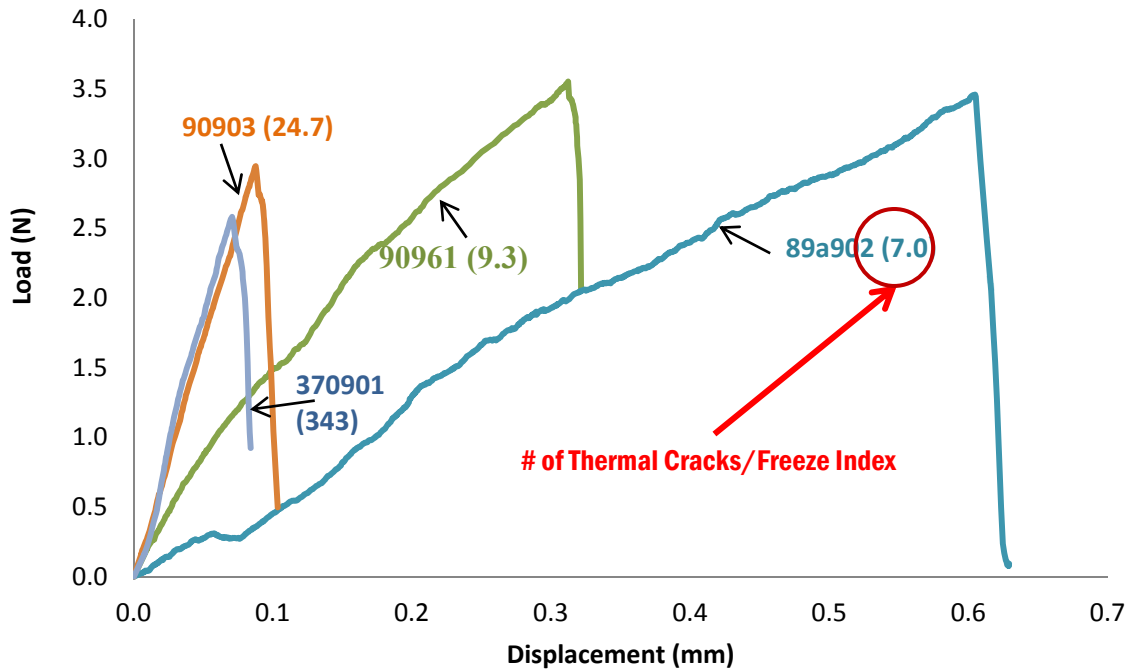


Figure V3b-3.1. Graph. Comparison of SENB load-deflection curves for LTPP binders. Lower performance index shows better performance [Labels: LTPP code (Performance Index)]

The Linear Amplitude Sweep Test for Fatigue Resistance:

Additional testing was done to investigate the role of asphalt binder in fatigue resistance of pavements. Characterization of 24 asphalt binders obtained from the material library of the Long-Term Pavement Performance (LTPP) program was completed using the Linear Amplitude Sweep test. Asphalt binder is known to be critical in determining the fatigue cracking resistance of asphalt pavements. However, there are other factors that also affect asphalt pavement fatigue. Thus, layer thicknesses, subgrade type, and climate were considered in addition to binder fatigue performance. Binder fatigue life at 1% strain was used as the indicator of binder fatigue performance. Table V3b-3.2 provides a summary of the LTPP sections evaluated, including binder fatigue results.

An initial analysis of variance (ANOVA) revealed all factors except for binder fatigue life significantly impact fatigue cracking. However, further investigation revealed relationships between LAS results and field cracking exist for “weak” pavement structures which include:

- Asphalt layer thickness less than 6”

- And/or base thickness less than 6''
- And/or fine grained subgrade (modulus less than 20,000 psi)

Existence of a relationship between binder fatigue life and pavement performance for weaker structures only could imply these structures experience strain-controlled fatigue whereas stronger structures experience stress controlled fatigue. Also, the results for “weak” sections validate the LAS test are capable of predicting asphalt binder contribution to pavement fatigue when strain control testing prevails.

Table V3b-3.2. Summary of LTPP sections.

SHRP ID	Binder PG	Binder Test Temperature (°C)	Climate Type*	Subgrade USGS Classification	Asphalt Concrete Thickness (in)	Base Thickness (in)	Base Type	Total Cracking**	Binder Nf(1%)
04-B901	76-10	39.1	DN	SC	7.9	10.8	Untreated	328.0	4.05E+06
04-B903	70-10	39.1	DN	SC	7.4	10.8	Treated	337.9	3.29E+06
09-0902	64-28	23.0	WF	SP	4.6	18.5	Untreated	3.6	1.13E+06
09-0903	64-22	23.0	WF	SP	6.8	6.3	Treated	5.1	1.71E+06
09-0960	58-28	23.0	WF	SP	6.5	6.4	Treated	4.2	2.37E+06
09-0962	58-28	23.0	WF	SP	6.1	6.2	Treated	6.9	5.76E+06
12-0902	64-16	35.4	WN	SP	7.5	11.0	Untreated	0.0	1.27E+06
30-0903	64-22	23.1	DF	SW	5.0	1.0	Untreated	1.6	2.36E+06
31-0902	58-22	25.4	DF	CL-ML	7.1	12.0	Untreated	65.5	6.41E+06
31-0903	64-28	25.4	DF	CL-ML	6.2	12.5	Untreated	175.5	1.88E+06
34-0901	64-22	25.2	WF	SM	4.9	6.5	Treated	13.7	1.28E+07
34-0902	58-22	25.2	WF	SM	5.7	6.7	Treated	0.0	5.55E+05
34-0961	76-28	25.2	WF	SM	6.4	5.6	Treated	274.3	5.03E+06
35-0903	58-22	33.1	DN	ML	10.9	10.5	Untreated	1.2	4.31E+06
37-0901	64-22	30.7	WN	ML	5.4	3.4	Treated	37.7	3.81E+06
37-0902	64-22	30.7	WN	CL-ML	5.3	3.2	Treated	47.2	5.93E+06
37-0903	70-22	30.7	WN	CL-ML	5.3	3.4	Treated	83.0	4.96E+07
37-0960	76-22	30.7	WN	CL-ML	7.5	5.5	Treated	73.1	5.54E+06
37-0962	76-22	30.7	WN	CL-ML	8.5	4.5	Treated	0.0	4.49E+08
37-0963	64-22	30.7	WN	CL-ML	7.5	6.0	Treated	12.7	5.11E+06
37-0964	76-22	30.7	WN	CL-ML	7.5	6.0	Treated	51.1	2.25E+06
37-0965	70-22	30.7	WN	CL-ML	8.0	5.5	Treated	17.7	8.15E+05
89-A901	52-34	14.4	WN	CL-ML	8.2	14.7	Untreated	0.0	4.93E+06
89-A903	52-40	14.4	WN	CL-ML	7.4	16.1	Untreated	0.7	5.99E+06

* WN=wet no-freeze, WF=wet freeze, DN= dry no-freeze, DF= dry freeze

** Fatigue cracking is measured as cracked area per 500 m of pavement length.

Figures V3b-3.2, V3b-3.3, and V3b-3.4 show the correlation between fatigue cracking and binder fatigue life for sections with weak subgrades, thin asphalt pavements, and thin bases, respectively. Note there are outliers, but these can be explained as:

- Section 35-0903 is the only section in a dry-no freeze climate with a weak subgrade.
- Section 31-0902 is the only section with spot patching and a weak subgrade.
- Section 34-0902 is the thickest pavement section within the thin classification.
- Section 09-0902 has a very thick base compared to the other thin pavement sections.
- 34-0961 is the only section in a wet climate with freezing with a thin base.
- 37-0960 is the only section to have experienced seal coating recently and have a thin base.

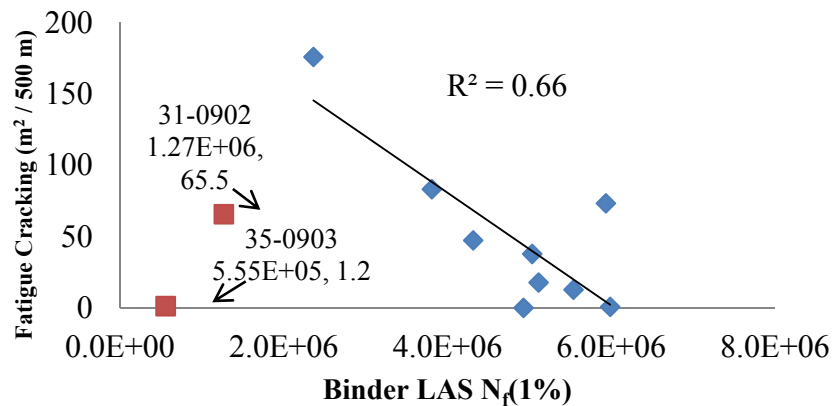


Figure V3b-3.2. Graph. Comparison between field fatigue cracking and binder fatigue life at 1% strain for sections with low sub grade moduli.

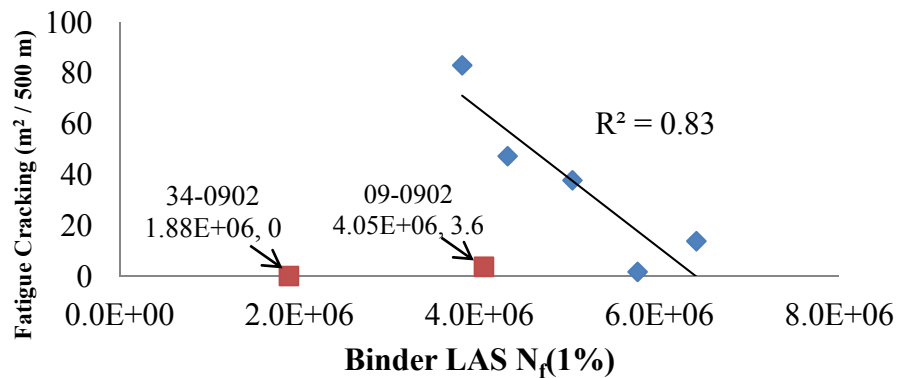


Figure V3b-3.3. Graph. Comparison between field fatigue cracking and binder fatigue life at 1% strain for sections with thin asphalt layers.

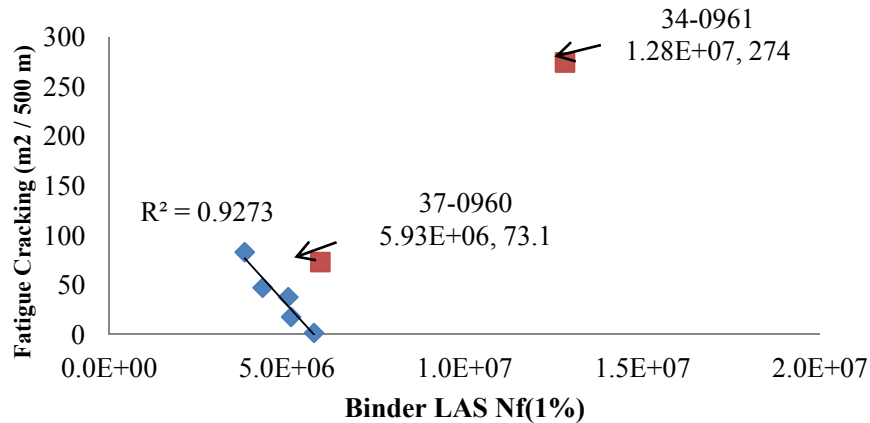


Figure V3b-3.4. Graph. Comparison between field fatigue cracking and binder fatigue life at 1% strain for sections with thin bases.

Work Planned Next Quarter

In the next quarter the research team will focus on further analysis of the LTPP experimental data available and integrating results into the final reports. Efforts will also be made to set preliminary performance thresholds and criteria for low temperature binder performance based on the BBR-SENB.

Work Element V3c: Validation of PANDA (TAMU)

Work Done this Quarter

Please refer to the details presented in work elements M4c, F1d-8, and F3c. These work elements outline what has already been accomplished in validating the constitutive models that are implemented in PANDA as well as the validation work that will be carried out in the coming quarter.

In summary, in this quarter, PANDA is calibrated and validated against the ALF data. Table V3c.1 lists the tests used to calibrate PANDA. Table V3c.2 lists the tests which have been used to validate the PANDA model. These tests have not been used in the calibration process.

Also, in this quarter, we have started to carry out the ARC testing plan. The aging data based on the dynamic modulus test are available and currently used for calibration and validation of the oxidation aging model.

Table V3c.1. Summary of the test used for identification of the PANDA.

Test	Temperature (° C)	Stress level (kPa)	Confinement (kPa)	Loading time (Sec)	Rest period (Sec)
Complex Modulus test	-10, 10, 35, 55	-	140	-	-
Repeated creep-recovery test with variable loading (VL)	55	Varies	140	0.4	200
Test	Temperature (° C)		Strain rate (sec ⁻¹)		
Uniaxial constant strain rate test	5		7 × 10 ⁻⁶ ; 2.1 × 10 ⁻⁵ ; 3 × 10 ⁻⁵ ; 5.5 × 10 ⁻⁵		

Table V3c.2. Summary of the test used for validation of the PANDA.

Test	Stress level (kPa)	Loading time (Sec)	Rest period (Sec)	
Repeated creep-recovery test with constant loading level and time (CLT)	827	0.1, 0.4, 1.6, 6.4	0.9	
Repeated creep-recovery test with variable loading time (VT)	827	Sequence of (0.05, 0.1, 0.4, 1.6, 6.4)	0.05, 1, 200	
Repeated creep-recovery test with reversed variable loading time (RVT)	827	Sequence of (6.4, 1.6, 0.4, 0.1, 0.05)	200	
Test	Temperature (° C)	Stress level (kPa)	Strain level (μ ε)	Strain rate (sec ⁻¹)
Complex Modulus test	-10, 10, 35, 55			
	12			2.7 × 10 ⁻⁴ ; 4.6 × 10 ⁻⁴
Uniaxial constant strain arte test	25			5 × 10 ⁻⁴ ; 1.5 × 10 ⁻³ ; 4.5 × 10 ⁻³ ; 1.35 × 10 ⁻²
	40			3 × 10 ⁻⁴ ; 10 ⁻³ ; 3 × 10 ⁻³
Cyclic stress control	5	1525		
	19	250, 750		
Cyclic strain control	5		1750	
	19		1200, 1500	

Significant Results

See the significant results sections in work elements M4c, F1d-8, and F3c.

Significant Problems, Issues and Potential Impact on Progress

See the significant results sections in work elements M4c, F1d-8, and F3c.

Work Planned Next Quarter

Focus will be placed on validation of PANDA using the ARC testing plan. Tables V3c.3 to V3c.8 list the modified testing matrices for the ARC testing in tension and compression for dry, moisture conditioned, and aged specimens.

Table V3c.3. Summary of the ARC tests in tension for no aging no moisture conditioned specimens.

Group	Test Procedure	Temperature	Level	Air Void	Purpose	
No Aging No Moisture	AASHTO TP-62	Various	50-75 microstrains	7% AV	VE Calibration	
	Uniaxial Constant Strain Rate test	5	Rate:5E-6/sec		7% AV	Damage Calibration
			Rate:1E-5/sec			
			Rate:5E-5/sec			
		19	Rate:5E-4/sec			Damage Validation
			Rate:5E-3/sec			
			Rate:5E-2/sec			
	CX	5	Nf = 1000		7% AV	Validation
			Nf = 10000			
		19	Nf = 1000			
Nf = 10000						
RCRT-VRT	19	Unknown	Healing Calibration			

Table V3c.4. Summary of the ARC tests in tension for moisture conditioned specimens.

Group	Test Procedure	Temperature	Level	Moisture Condition	Air Void	Purpose	
No Aging Moisture Conditioning	AASHTO TP-62	Various	50-75 microstrains	80%-12Hr	7% AV	Moisture Calibration	
		Various		80%-24Hr			
		Various		60%-24Hr			
	CX	5	5	Nf = 1000		80%-12Hr	Validation
				Nf = 10000		80%-24Hr	
				Nf = 1000			
				Nf = 10000			
		19	19	Nf = 1000		80%-12Hr	Validation
				Nf = 10000		80%-24Hr	
				Nf = 1000			
				Nf = 10000			
	RCRT-VRT	19	Unknown	80%-12Hr		80%-24Hr	Healing Calibration/Validation

Table V3c.5. Summary of the ARC tests in tension for aged specimens.

Group	Test Procedure	Temperature	Level	Aging Condition	Air Void	Purpose
Aging No Moisture	CX	5	Nf = 1000	3 month	7% AV	Validation
			Nf = 10000			
			Nf = 1000	6 month		
			Nf = 10000			
			Nf = 1000	3 month		
			Nf = 10000			
			Nf = 1000	6 month		
			Nf = 10000			
		19	Nf = 1000	3 month	7% AV	
			Nf = 10000			
			Nf = 1000	6 month		
			Nf = 10000			
			Nf = 1000	3 month		
			Nf = 10000			
	Nf = 1000	6 month				
	Nf = 10000					
	RCRT-VRT	19	Unknown	3 month	7% AV	
				6 month		
3 month				4% AV		
6 month						
Uniaxial Constant Strain Rate Tests	19	Rate:5E-3/sec	3 month	7% AV		
			6 month			
			3 month	4% AV		
			6 month			

Table V3c.6. Summary of the ARC tests in compression for no aging no moisture conditioned specimens.

Group	Test Procedure	Temperature	Stress level	LT/RT	Confinement	Air Void	Purpose
No Aging No Moisture	AASHTO TP-62	Various	50-75 microstrains		0	7% AV	VE Calibration
		Various					VP-Validation
	RCRT-VS	19, 40, 55	Varies	LT=0.4sec, RT=30sec	0, 70, 140, 500		VP-Validation
			Varies	LT=0.4sec, RT=5sec	0, 70, 140, 500		VP- Calibration
			Varies	LT=0.4sec, RT=5sec	0, 70, 140, 500		VPS- Validation
	RCRT-CLR	19, 40, 55	840	LT=0.4 sec, RT=1,10, 20, 40sec	140		VPS- Validation
			840	LT=0.4 sec, RT=0.1,0.4, 2, 5sec	140		VPS- Calibration
			840	LT=0.4 sec, RT=0.1,0.4, 1, 5sec	140		Validation
	RCRT-VRT	19, 40, 55	840	LT=0.4 sec, RT=Varies	0, 70, 140, 500		
			840	LT=0.4 sec, RT=Varies	0, 70, 140, 500		
			840	LT=0.4 sec, RT=Varies	0, 70, 140, 500		
	RCRT-VLT	19, 40, 55	840	LT=Varies, RT=30sec	0, 70, 140, 500		Validation
			840	LT=Varies, RT=5sec	0, 70, 140, 500		
			840	LT=Varies, RT=5sec	0, 70, 140, 500		
	RCRT-VST	19, 40, 55	To be determined	LT/RT=Varies	0, 70, 140, 500		Validation
			To be determined	LT/RT=Varies	0, 70, 140, 500		
			To be determined	LT/RT=Varies	0, 70, 140, 500		
	Uniaxial constant strain rate tests	19, 40, 55	Rate:5E-3/sec		0, 70, 140		Calibration of d parameter and identification of alpha parameter.
			Rate:1E-3/sec		0, 70, 140		
			Rate:1E-3/sec		0, 70, 140		

Table V3c.7. Summary of the ARC tests in compression for moisture conditioned specimens.

Group	Test Procedure	Temperature	Stress level	LT/RT	Moisture Condition	Air Void	Purpose
No Aging Moisture Conditioning	AASHTO TP-62	Various	50-75 microstrains			7% AV	Moisture damage calibration
		Various					
		Various					
		Various					
	RCRT-VS	40	Varies	LT=0.4sec, RT=5sec	Level 1	Moisture damage validation	
		55	Varies	LT=0.4sec, RT=5sec	Level 2		

Table V3c.8. Summary of the ARC tests in compression for aged specimens.

Group	Test Procedure	Temperature	Stress level	LT/RT	Aging Condition	Air Void	Purpose
Aging No Moisture	AASHTO TP-62	Various	50-75 microstrains		3 and 6 month	4, 7, 10% AV	Aging model calibration
	RCRT-VS	40	Varies	LT=0.4sec, RT=5sec	3 and 6 month	4, 7, 10% AV	Aging model validation
		55	Varies	LT=0.4sec, RT=5sec	3 and 6 month	4, 7, 10% AV	Aging model validation

PANDA Software

Work Done This Quarter

In this quarter, work has been continued on the development of the main engine and solver of the standalone finite element code PANDA. Figure V3c.1 shows the list of two-dimensional (2D) and three-dimensional (3D) finite elements that are currently implemented in PANDA. The 2D elements can be used to solve plane stress, plane strain, or axisymmetric problems. Moreover, work is in progress of writing the installation and user manual of PANDA. Work is in progress in writing two chapters; the first on “Using PANDA” and the second on “Keywords” for writing the input file for PANDA.

Finally, a Fortran subroutine is coded that includes an extensive library of tensor operations that are useful in the implementation of complex material constitutive models. This tensor library is essential for the numerical implementation of the ARC developed constitutive models into the developed stand-alone software.

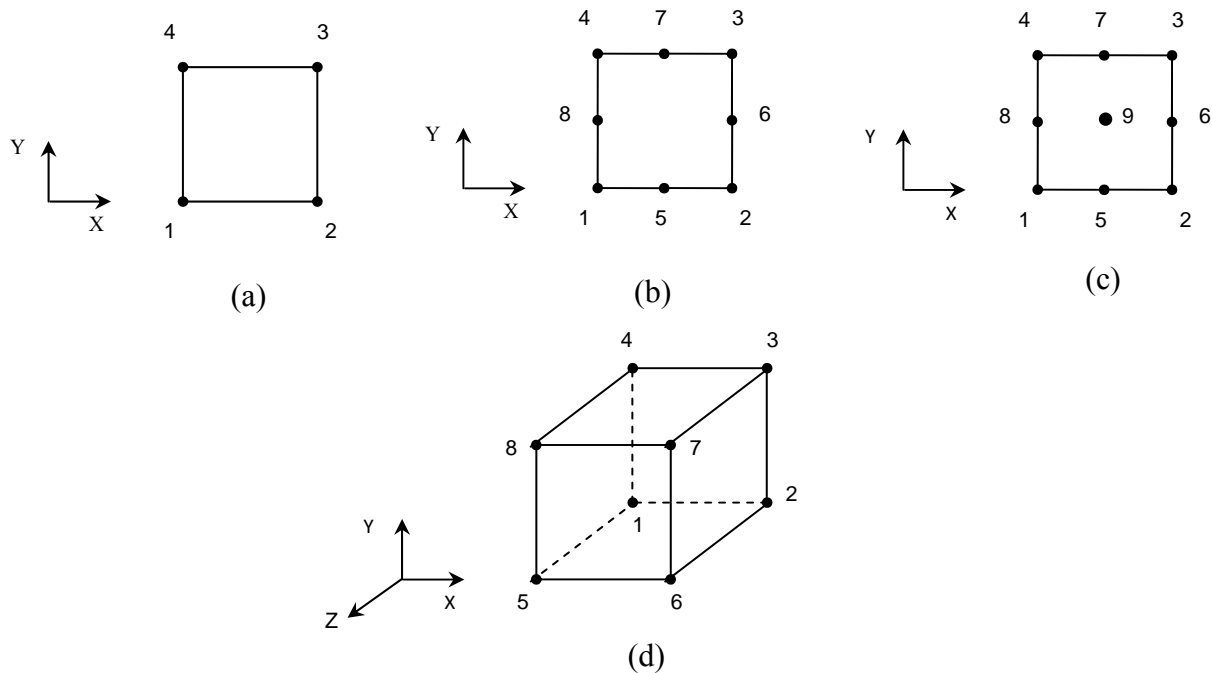


Figure V3c.1. The implemented 2D and 3D finite elements: (a) 2D four-node finite element, (b) 2D eight-node finite element, (c) 2D nine-node finite element, and (d) 3D eight-node brick finite element.

Currently, the steps in running PANDA are:

1. Create an input file

PANDA works by reading and responding to a set of commands (called KEYWORDS) in an input file. The keywords contain the information to define the mesh, the properties of material, the boundary conditions, and to control output from the program.

2. Run PANDA program:

By double click on the execution file of PANDA.exe, the user will be asked to enter the name of the input file.

3. Post-processing:

There is one way for now to look at the results of a PANDA simulation. The results are printed to a text file, which one can be viewed with any text editor. The results include the stresses and strains at each integration point and the reactions and displacements at each node.

Significant Results

None

Significant Problems, Issues and Potential Impact on Progress

None

Work Planned Next Quarter

Work will be continued on creating three-dimensional (3D) finite elements. The work will start in implementing a twenty-node brick 3D finite element that can be used for modeling the 3D pavement structure under realistic wheel loading conditions. The predictions from this element will be validated by comparing the results with the corresponding one from the commercial finite element software Abaqus.

Work Element V3d: Engineered Properties Testing Plan (TAMU)

Work Done this Quarter

The work completed this quarter relates to work described in Work Elements F2c and E1a.

Work Planned Next Quarter

Please refer to Work Elements F2c and E1a.

TABLE OF DECISION POINTS AND DELIVERABLES FOR VALIDATION

Name of Deliverable	Type of Deliverable	Description of Deliverable	Original Delivery Date	Revised Delivery Date	Reason for changes in delivery date
V3a-1: Evaluation of the PG-Plus practices and the motivations for selecting the “plus” tests. (UWM)	Draft Report	Detailed analysis of PG and PG+ tests	10/08	6/12	Additional work planned in project extension. V3a and V3b will not have independent reports. Results will be included as chapters in reports G, I, L, M, O, P and Q.
	Final Report	Report on 508 format on benefits of PG+ and new ARC tests in comparison to PG tests. Repeatability of PG+ and newly developed ARC procedures	12/08	3/13	
V3a-2: Detailed analysis of all PG-Plus tests being proposed or in use today, documentation of benefits and costs of these tests, and comparison with new tests (UWM)	Draft Report	Refer to Draft Report for V3a-1	4/09	6/12	
V3a-4: Development of specification criteria for new tests based on field evaluation of construction and performance (UWM)	Draft Report	Refer to Draft Report for V3a-1	7/09	6/12	Refer to Draft Report for V3a-1
V3a-5: Interviews and surveys for soliciting feedback on binder tests and specifications (UWM)	Draft Report	Report summarizing collaboration between Western Cooperative Test Group (WCTG), the Rocky Mountain Asphalt User-Produce Group (RMAUPG) and UW-Madison	12/11	6/12	Refer to Draft Report for V3a-1
	Final Report	Report in 508 format on Development and maintenance of database for evaluation of PG, PG+, and new ARC tests.	1/12	3/13	

Name of Deliverable	Type of Deliverable	Description of Deliverable	Original Delivery Date	Revised Delivery Date	Reason for changes in delivery date
V3b-3: Select LTPP Sites to Validate New Binder Testing Procedures (UWM)	Draft Report	Report summarizing characterization of LTPP binders by means of the Linear Amplitude Sweep (LAS), Single Edge-Notch Beam (SENB) and Bitumen Bond Strength (BBS) tests.	12/11	6/12	Additional work planned in project extension. V3a and V3b will not have independent reports. Results will be included as chapters in reports G, I, L, M, O, P and Q.
	Final Report	Final report in 508 format on validation/verification of fatigue, thermal cracking, and moisture damage procedures using LTPP binders.	1/12	3/13	
V3c: Validation of PANDA (TAMU)	PANDA Workshop	Workshop on PANDA Models and Validation Results	8/11	4/13	Waiting for full calibration and validation of PANDA
	Draft Report	Documentation of PANDA Models and Validation	11/11	12/31/12	Validation against ARC testing
	Final Report (M5, M4c, F1b-1, F1c, F1d-8, F3c, and V3c)	Documentation of PANDA Models and Validation	3/12	3/31/13	N/A
	UMAT Material	PANDA Implemented in Abaqus	3/12	3/31/13	N/A
	Software	Standalone Software to support the use of and future utility and flexibility of PANDA	3/12	3/13	Creating user friendly interface for PANDA

Validation Year 5	Year 5 (4/2011-3/2012)												Team	
	4	5	6	7	8	9	10	11	12	1	2	3		
(1) Field Validation														
V1a: Use and Monitoring of Warm Mix Asphalt Sections														WRI
V1b: Construction and Monitoring of additional Comparative Pavement Validation sites														WRI
(2) Accelerated Pavement Testing														
V2a: Accelerated Pavement Testing including Scale Model Load Simulation on small test track (This work element will include all accelerated pavement testing)														WRI
V2b: Construction of validation sections at the Pecos Research & Testing Center														WRI
(3) R&D Validation														
V3a: Continual Assessment of Specification														UWM
V3a-1: Evaluation of the PG-Plus practices and the motivations for selecting the "plus" tests.							D			F				
V3a-2: Detailed analysis of all PG-Plus tests being proposed or in use today, documentation of benefits and costs of these tests, and comparison with new tests														
V3a-3: Development of protocols for new binder tests and database for properties measured														
V3a-4: Development of specification criteria for new tests based on field evaluation of construction and performance			P							JP				
V3a-5: Interviews and surveys for soliciting feedback on binder tests and specifications		P								D	F			
V3b: Validation of the MEPDG Asphalt Materials Models and Early Verification of Technologies Developed by ARC using new MEPDG Sites and Selected LTPP sites														UNR/UWM/ WRI
V3b-1: Design and Build Sections											D		F	UNR
V3b-2: Additional Testing (if needed)														
V3b-3: Select LTPP Sites to Validate New Binder Testing Procedures							JP				D	F		UWM
V3b-4: Testing of Extracted Binders from LTPP Sections														
V3b-5: Review and Revisions of Materials Models														
V3b-6: Evaluate the Impact of Moisture and Aging														
V3c: Validation of PANDA														TAMU
V3d: Engineered Properties Testing Plan	JP		JP	P(4)										

Deliverable codes
D: Draft Report
F: Final Report
M&A: Model and algorithm
SW: Software
JP: Journal paper
P: Presentation
DP: Decision Point

Deliverable Description
Report delivered to FHWA for 3 week review period.
Final report delivered in compliance with FHWA publication standards
Mathematical model and sample code
Executable software, code and user manual
Paper submitted to conference or journal
Presentation for symposium, conference or other
Time to make a decision on two parallel paths as to which is most promising to follow through

 Work planned
 Work completed
 Parallel topic

Validation Years 2 - 5	Year 2 (4/08-3/09)				Year 3 (4/09-3/10)				Year 4 (04/10-03/11)				Year 5 (04/11-03/12)				Team
	Q1	Q2	Q3	Q4	Q1	Q2	Q3	Q4	Q1	Q2	Q3	Q4	Q1	Q2	Q3	Q4	
(1) Field Validation																	
V1a: Use and Monitoring of Warm Mix Asphalt Sections																	WRI
V1b: Construction and Monitoring of additional Comparative Pavement Validation sites																	WRI
(2) Accelerated Pavement Testing																	
V2a: Accelerated Pavement Testing including Scale Model Load Simulation on small test track																	WRI
V2b: Construction of validation sections at the Pecos Research & Testing Center																	WRI
(3) R&D Validation																	
V3a: Continual Assessment of Specification																	UWM
V3a-1: Evaluation of the PG-Plus practices and the motivations for selecting the "plus" tests.		P	D,F											D	F		
V3a-2: Detailed analysis of all PG-Plus tests being proposed or in use today, documentation of benefits and costs of these tests, and comparison with new tests				P	D												
V3a-3: Development of protocols for new binder tests and database for properties measured						JP		P		P							
V3a-4: Development of specification criteria for new tests based on field evaluation of construction and performance					D		P	P			JP	P			JP	F	
V3a-5: Interviews and surveys for soliciting feedback on binder tests and specifications								P		JP		P			D	F	
V3b: Validation of the MEPDG Asphalt Materials Models and Early Verification of Technologies Developed by ARC using new MEPDG Sites and Selected LTPP sites																	UNR/UWM
V3b-1: Design and Build Sections																	D, F
V3b-2: Additional Testing (if needed)																	
V3b-3: Select LTPP Sites to Validate New Binder Testing Procedures					DP		P		JP, DP		P		JP		D	F	
V3b-4: Testing of Extracted Binders from LTPP Sections																	
V3b-5: Review and Revisions of Materials Models																	
V3b-6: Evaluate the Impact of Moisture and Aging																	
V3c: Validation of PANDA																	TAMU
V3d: Engineered Properties Testing Plan										P(2)	JP	P(3), JP					

Deliverable codes
D: Draft Report
F: Final Report
M&A: Model and algorithm
SW: Software
JP: Journal paper
P: Presentation
DP: Decision Point

Deliverable Description
Report delivered to FHWA for 3 week review period.
Final report delivered in compliance with FHWA publication standards
Mathematical model and sample code
Executable software, code and user manual
Paper submitted to conference or journal
Presentation for symposium, conference or other
Time to make a decision on two parallel paths as to which is most promising to follow through

 Work planned
 Work completed
 Parallel topic

PROGRAM AREA: TECHNOLOGY DEVELOPMENT

Work element TD1: Prioritize and Select Products for Early Development (Year 1) (AAT, WRI)

This work element has been completed. Six early development products were identified.

Work element TD2: Develop Early Products (Year 3) (AAT, WRI)

Work Done This Quarter

Table TD2.1 summarizes the progress on the Products for Early Development. The test method for Automated Flocculation Titrimetric Analysis has been published as an ASTM standard method of test, ASTM D6703 – 07. Draft AASHTO Standards have been completed for other 5 products; however, the Draft AASHTO Standard for simplified continuum damage fatigue analysis for the Asphalt Mixture Performance Tester, is being revised significantly based on the findings of the analyses being conducted in the continuum damage fatigue model refinement in Work Element E2e. The Draft AASHTO Standard for Determination of Polymer in Modified Asphalt is available on the outreach portion of the ARC website at:

<http://www.arc.unr.edu/Outreach.html#TechDevelopmentProducts>.

Table TD2.1. Summary of progress on early development products.

No.	Product	ARC Research Program	Format	Estimated Completion Data	ARC Partner	Draft AASHTO Standard?
1	Simplified Continuum Damage Fatigue Analysis for the Asphalt Mixture Performance Tester	Prior	Test Method	3/31/2012	AAT	Yes
2	Wilhelmy Plate Test	Prior	Test Method	Completed	TTI	Yes
3	Universal Sorption Device	Prior	Test Method	Completed	TTI	Yes
4	Dynamic Mechanical Analysis	Prior	Test Method	Completed	TTI	Yes
5	Automated Flocculation Titrimetric Analysis	Prior	Test Method	Completed	WRI	No (ASTM)
6	Determination of Polymer in Asphalt	Prior	Test Method	Completed	WRI	Yes

Work Planned Next Quarter

AAT will continue revising the Draft AASHTO Standard for simplified continuum damage fatigue analysis for the Asphalt Mixture Performance Tester based on the findings from the continuum damage fatigue model refinement in Work Element E2e. Based on the ratings from the ETGs, support will be provided for advancing the selected products through AASHTO for publication as Provisional AASHTO Standards.

Significant Problems, Issues and Potential Impact on Progress

None.

Work element TD3: Identify Products for Mid-Term and Long-Term Development (Years 2, 3, and 4) (AAT, TTI, UNR, UW-M, WRI)

This work element has been completed. A total of 38 mid- and long-term products were identified. Table TD3.1 summarizes these products.

Table TD3.1. Summary of mid- and long-term technology development products.

No.	Product	ARC Work Element	Format	Estimated Completion Date	ARC Partner
7	A Method for the Preparation of Specimens of Fine Aggregate Matrix of Asphalt Mixtures	M1c	Test Method	12/31/2010	TTI
8	Measuring intrinsic healing characteristics of asphalt binders	F1d	Test Method	12/31/2012	TTI / UT Austin
9	Lattice Micromechanical Model for Virtual Testing of Asphalt Concrete in Tension	F3b	Analysis Program	2/28/2012	NCSU
10	Cohesive Zone Modeling as an Efficient and Powerful Tool to Predict and Characterize Fracture Damage of Asphalt Mixtures Considering Mixture Microstructure, Material Inelasticity, and Moisture Damage	F3b	Performance Predicting Model	12/31/2010	University of Nebraska
11	Pavement Analysis Using Nonlinear Damage Approach (PANDA)	F3c	Test Method	12/31/2012	TTI

Table TD3.1 continued. Summary of mid- and long-term technology development products.

12	Test Methods for Determining the Parameters of Material Models in PANDA (Pavement Analysis Using Nonlinear Damage Approach)	F3c E1a	Test Method	12/31/2011	TTI
13	Continuum Damage Permanent Deformation Analysis for Asphalt Mixtures	E1a	Test Method	9/30/2011	TTI
14	Characterization of Fatigue and Healing Properties of Asphalt Mixtures Using Repeated Direct Tension Test	E1a	Test Method & Data Analysis Program	9/30/2011	TTI
15	Nondestructive Characterization of Tensile Viscoelastic Properties of Undamaged Asphalt Mixtures	E1a	Test Method & Data Analysis Program	Completed	TTI
16	Nondestructive Characterization of Field Cores of Asphalt Pavements	E1a	Test Method & Data Analysis Program	9/30/2011	TTI
17	Self-Consistent Micromechanics Models of Asphalt Mixtures	E1a	Analytical Model & Data Analysis Program	6/30/2011	TTI
18	Nondestructive Characterization of Anisotropic Viscoelastic Properties of Undamaged Asphalt Mixtures under Compressive Loading	E1a	Test Method	Completed	TTI
19	Mix Design for Cold-In-Place Recycling (CIR)	E1c	Practice	12/31/2011	UNR
20	Mix Design for Cold Mix Asphalt	E1c	Practice	3/31/2012	UNR
21	Evaluation of RAP Aggregates	E2b	Practice	4/30/2011	UNR
22	Identification of Critical Conditions for HMA mixtures	E2c	Practice	12/31/2011	UNR
23	Thermal Stress Restrained Specimen Test (TSRST)	E2d	Test Method	9/30/2011	UNR
24	HMA Thermal Stresses in the Intermountain Region	E2d	Model	3/31/2012	UNR

Table TD3.1 continued. Summary of mid- and long-term technology development products.

25	Dynamic Model for Flexible Pavements 3D-Move	VP3a	Software	3/31/2011	UNR
26	Bitumen Bond Strength Test (BBS)	M1a	Test Method	Completed	UWM
27	Elastic Recovery – DSR	F2a	Test Method	12/31/2010	UWM
28	Linear Amplitude Sweep (DSR)	F2e	Test Method	Completed	UWM
29	Binder Yield Energy Test (BYET)	F2e	Test Method	Completed	UWM
30	Rigden Voids for fillers	F2e	Test Method	9/30/2011	UWM
31	Binder Lubricity Test – DSR	E1c	Test Method	12/31/2010	UWM
32	RAP Binder PG True Grade Determination	E2b	Test Method / Software	3/31/2011	UWM
33	Single Edge Notch Bending	E2d	Test Method	5/31/2011	UWM
34	Binder Glass Transition Test	E2d	Test Method	5/31/2011	UWM
35	Asphalt Mixture Glass Transition Test	E2d	Test Method	5/31/2011	UWM
36	Planar imaging/ Aggregate Structure	E1b	Test Method/ Software	3/31/2011	UWM
37	Gyratory Pressure Distribution Analyzer (GPDA)	E1c	Test Method	Completed	UWM
38	Improved Oxygen and Thermal Transport Model of Binder Oxidation in Pavements	F1c	Methodology , Publication	3/31/2011	TAMU
39	Field Validation of an Improved Oxygen and Thermal Transport Model of Binder Oxidation in Pavements	F1c	Methodology , Publication	3/31/2011	TAMU
40	Validation of an improved Pavement Temperature Transport Model for use in an Oxygen and Thermal Transport Model of Binder Oxidation in Pavements	F1c	Methodology , Publication	3/31/2011	TAMU
41	Pavement Air Voids Size Distribution Model for use in an Oxygen and Thermal Transport Model of Binder Oxidation in Pavements	F1c	Methodology , Publication	3/31/2011	TAMU

Table TD3.1 continued. Summary of mid- and long-term technology development products.

42	Improved Understanding of Fast-Rate, Constant-Rate Binder Oxidation Kinetics Mechanism through the Effects of Inhibitors	F1c	Publication	3/31/2011	TAMU
43	Improved Understanding of Fatigue Resistance Decline with Binder Oxidation	F1c	Publication	3/31/2011	TAMU
44	Micromechanical Properties of Various Structural Components in Asphalt using Atomic Force Microscopy (AFM)	F2d	Test and Analysis Method	3/31/2011	TAMU

Work Element TD4: Develop Mid-Term and Long-Term Products (Years 3, 4, and 5) (AAT, TTI, UNR, UW-M, WRI)

Work continued on the development of the mid-term and long-term products. Responses to the product rating request issued to the ETGs by the FHWA were compiled by the research team and included in the progress report for last quarter. These responses are being considered by the research team in selecting the effort that will be expended on each of the mid- and long-term products.

Work Planned Next Quarter

The research team will continue with the development of the mid- and long-term technology development products.

Significant Problems, Issues and Potential Impact on Progress

None.

PROGRAM AREA: TECHNOLOGY TRANSFER

CATEGORY TT1: OUTREACH AND DATABASES

Work element TT1a: Development and Maintenance of Consortium Website (Duration: Year 1 through Year 5) (UNR)

Work Done This Quarter

The ARC website was maintained and updated. The ARC quarterly technical progress report, April 1- June 30, 2011, was uploaded to the ARC website. The ARC newsletter (Vol. 5, Issue 2) was uploaded to the website. The following references and files were updated:

- List of Publications and Conference Proceedings under the “Publications” webpage.
- List of Presentations and Posters under the “Outreach” webpage.

The 3D-Move Discussion Group Forum was also maintained.

Significant Results

None

Significant Problems, Issues and Potential Impact on Progress

None

Work Planned Next Quarter

Continue maintaining and updating the ARC website. Update the list of Publications and Conference Proceedings. Update the list of Presentations and Posters and the list of Theses and White Papers. Post information and new releases for 3D-Move. Maintain the 3D-Move Discussion Group Forum.

Work element TT1b: Communications (Duration: Year 1 through Year 5) (UNR)

Work Done This Quarter

Published the ARC Newsletter Vol. 5, Issue 2: “New design tool helps ensure quality in mixes that include high percentages of recycled asphalt pavement.”

Significant Results

None

Significant Problems, Issues and Potential Impact on Progress

None

Work Planned Next Quarter

Prepare and publish the tenth ARC Newsletter.

Work element TT1c: Prepare Presentations and Publications (All)

Presentations

Advanced Asphalt Technologies, A presentation was made to the Models Expert Task Group describing Work Element E2e, Design Guidance for Fatigue and Rut Resistance Mixtures, September 2011.

Bahia, H.U., and A. Golalipour, Analysis of MSCR variability workability, *Presentation made to Expert Task Group Meeting on Asphalt Binders*, September 2011.

Bahia, H., H. Tabatabaee, and R. Velasquez, Thermal Stress Build-Up and Glass Transition of Asphalt Mixtures Development of Asphalt Thermal Cracking Analyzer (ATCA), *Presentation made to the Expert Task Group Meeting for Asphalt Mixtures and Construction*, September 2011.

Cui, Yuanchen, Xin Jin, Rongbin Han, and Charles J. Glover. "Introduction to a New, Fast, Binder Aging Test," presented at the 48th Annual Petersen Asphalt Research Conference, July 13, 2011.

Derek D. Li and Michael L. Greenfield(*), "Next Generation Molecular Models of Well-Characterized Asphalts," presentation made at the Petersen Asphalt Research Conference, July 11-13, 2011, Laramie, WY.

Hajj, E.Y., and Ekedahl, M., ARC Database Status Report and Presentation, Presentation made to the Expert Task Group meeting for Asphalt binder, Fall River, Massachusetts, Sep. 23, 2011.

Hajj, E.Y., and Ekedahl, M., 3D-Move Analysis Software Status, Presentation made to the Expert Task Group meeting for Fundamental Properties and Advanced Models, Fall River, Massachusetts, Sep. 20, 2011.

Hajj, E.Y., and Ekedahl, M., ARC Database Status Report and Presentation, Presentation made to the Expert Task Group meeting for Fundamental Properties and Advanced Models, Fall River, Massachusetts, Sep. 20, 2011.

Hajj, E.Y., Sebaaly, P.E., Loria, L., Kass, S. and Liske, T., Impact of High RAP Content on the Performance Characteristics of Asphalt Mixtures in Manitoba, Presentation made at the Transportation Association of Canada Conference, Edmonton, Alberta, Sep 11-14, 2011.

Han, Rongbin, Yuanchen Cui, Xin Jin, and Charles J. Glover. "A Comprehensive Model of Binder Oxidation in Pavements," presented at the 48th Annual Petersen Asphalt Research Conference, July 13, 2011.

Pauli, Troy, Asphalt Microstructure Modeling, Presentation made at the Fundamental Properties and Advanced Models ETG, September 19-20, 2011, Fall River, MA.

Tabatabaee, H., R. Velasquez, and H. Bahia, Predicting Physical Hardening of Asphalt binders and Mixtures, *Presentation made to the US National Congress on Computational Mechanics*, 2011, Minneapolis, MN.

Publications

Alavi, M., E. Hajj, A. Hanz, and H.U. Bahia, "Evaluating Adhesion Properties and Moisture Damage Susceptibility of Warm Mix Asphalts Using Bitumen Bond Strength (BBS) and Dynamic Modulus Ratio (ESR) Tests." Submitted to the 91st Annual Meeting of the Transportation Research Board. *Transportation Research Board of the National Academies*, Washington D.C., 2012.

Bahia, H., H. Tabatabaee, and R. Velasquez, Effect of Bitumen Physical Hardening on Asphalt Thermal Stress Buildup and Relaxation, *Submitted to the 5th Eurobitume Congress*, June 2012, Istanbul, Turkey.

Bahia, H., H. Tabatabaee, and R. Velasquez, Asphalt Thermal Cracking Analyzer, *Submitted to the 7th International Conference on Cracking in Pavements*, June 2012, Netherlands.

Bahia, H.U., N. Tabatabaee, C. Clopotel, and A. Golalipour, Evaluation of Using the MSCR Test for Modified Binder Specification, *Accepted at the Annual meeting of the Canadian Technical Asphalt Association*, November 2011.

Donald W. Christensen, Jr. and Ramon F. Bonaquist, "Modeling Fatigue Damage Functions for Hot Mix Asphalt," submitted to the Association of Asphalt Paving Technologists.

Donald W. Christensen, Jr. and Ramon Bonaquist, Analysis of FHWA ALF Fatigue Data Using a Continuum Damage Approach, submitted to the Association of Asphalt Paving Technologists.

Frigio, F., D. Swiertz, N. Tabatabaee, and H. Bahia, Estimating the Effect of RAP, RAS and Warm Mix Additives on the High Temperature Viscosity of Blended Binders. Submitted for publication in the *Transportation Research Record: Journal of the Transportation Research Board*, 2011.

Greenfield, Michael L., 2011, Molecular Modelling and Simulation of Asphaltenes and Bituminous Materials. *Int. J. Pavement Eng.*, 12, 325-341.

Hajj, E. Y., Loria, L., and Sebaaly, P.E., Estimating Effective Performance Grade of Asphalt Binders in High Rap Mixtures Using Different Methodologies: Case Study, submitted to the 91st Annual Transportation Research Board Meeting, January 22-26, 2012, Washington DC.

Hajj, E. Y., Thushanthan, P., Sebaaly, P. E., and Siddharthan, R., Influence of Tire-pavement Stress Distribution, Shape and Braking on Asphalt Pavement Performance Predictions, submitted to the 91st Annual Transportation Research Board Meeting, January 22-26, 2012, Washington DC.

Hajj, E. Y., Sebaaly, P.E., West, R. Morian. N., and Loria, L., Recommendations for the Characterization of RAP Aggregate Properties Using Traditional Testing and Mixture Volumetrics, submitted to the 87th Annual Meeting and Technical Sessions, April 1-4, 2012, Austin, TX.

Han, Rongbin, Xin Jin, and C.J. Glover, 2011, Modeling Pavement Temperature for Use in Binder Oxidation Models and Pavement Performance Prediction. *Journal of Materials in Civil Engineering*, 23(4), 351-359.

Han, R., X. Jin, X., and C.J. Glover, "Oxygen Diffusivity in Asphalts and Mastics," *Petroleum Sci. and Technol.*, in press.

Hanz, A., G. Andreoni, and H.U. Bahia. "Evaluation of the Effects of Reduced Binder Aging on Performance for WMA Using a Simple Thin Film Aging Method." Submitted to the 91st Annual Meeting of the Transportation Research Board. *Transportation Research Board of the National Academies*, Washington D.C., 2012.

Miller, T., "FHWA Equipment Loan Program Summary." Internal report submitted to Applied Asphalt Technologies for incorporation into annual report for FHWA, 01 September 2011.

Miller, T., D. Swiertz, L. Tashman, N. Tabatabaee, and H. Bahia, "Characterization of Asphalt Pavement Surface Texture." *Publication submitted to the Transportation Research Board Annual Meeting*, 2012.

Moraes, R., R. Velasquez, and H. Bahia, *Using Bond Strength and Surface Energy to Estimate Moisture Resistance of Asphalt-Aggregate Systems*. Full paper submitted to AAPT 2012 Annual Meeting and Technical Sessions, Austin, Texas, April 1 - 4, 2012.

Moraes, R., R. Velasquez, and H. Bahia, *The Effect of Bitumen Stiffness on the Adhesive Strength Measured by the Bitumen Bond Strength Test*. Full paper submitted to 5th Eurasphalt and Eurobitume Congress, Istanbul, Turkey, 13th to 15th June, 2012.

Moraes, R., R. Velasquez, and H. Bahia, *Selección de Materiales para Mezclas Asfálticas Resistentes al Daño por Humedad Utilizando el Método de La Gota Sésil*. Paper accepted for XVI CILA – Congresso Ibero-Latino Americano do Asfalto, Rio de Janeiro, Brazil, November 20th - 25th, 2011.

Moraes, R., A. Hanz, G. Andreoni, and H. Bahia, *Verification of Warm Mix Asphalt (WMA) Moisture Susceptibility Using the Bitumen Bond Strength Test (BBS)*. Abstract submitted to ISAP 2nd International Symposium on Asphalt Pavements & Environment, Fortaleza, Brazil, October 1st – 3rd, 2012.

Porras, J., Hajj, E. Y., Sebaaly, P.E., Kass, S., and Liske, Y., Performance Evaluation of Field-Produced WMA Mixtures in Manitoba, submitted to the 91st Annual Transportation Research Board Meeting, January 22-26, 2012, Washington DC.

Stimilli, A., C. Hintz, Z. Li, R. Velasquez, and H. Bahia, Effect of Healing on Fatigue Law Parameters of Asphalt Binders. *Submitted for presentation and publication to Transportation Research Record, Journal of the Transportation Research Board*, Washington D.C., 2012.

Swiertz, D., P. Johannes, L. Tashman, and H. Bahia, Evaluation of Laboratory Coating and Compaction Procedures for Cold Mix Asphalt. Submitted for publication in the *Journal of the Association of Asphalt Paving Technologists (AAPT)*, 2012.

Tabatabaee, H., R. Velasquez, and H. Bahia, Modeling Thermal Stress in Asphalt Mixtures Undergoing Glass Transition and Physical Hardening, *Submitted to the 91st Annual Transportation Research Board Meeting*, January 22-26, 2012, Washington DC.

Teymourpour, P., L. Tashman, and H.U. Bahia, “Critical Considerations in Mixture Design Warm Mix Asphalt.” Submitted to the 91st Annual Meeting of the Transportation Research Board. *Transportation Research Board of the National Academies*, Washington D.C., 2012.

Ulloa, A., Hajj, E. Y., Siddharthan, R., and Sebaaly, P. E., Establishing Equivalent Loading Frequencies In Static Multilayer Analyses To Simulate Dynamic Responses In Asphalt Layer, submitted to the 91st Annual Transportation Research Board Meeting, January 22-26, 2012, Washington DC.

Work element TT1d: Development of Materials Database (Duration: Year 2 through Year 5) (UNR)

Work Done This Quarter

The following list describes the work items completed or in progress this quarter:

- Continued training and usability feedback
- Bug fixes and performance enhancements
- File Management System (File Upload form)
- File Management System (Manage Keywords form)
- File Metadata form
- Public User Interface
 - Public account request form

- Public account approval form
- Forgot Password form
- File Download form

Significant Results

Continued training and usability feedback

Work continued to improve the user interface based on user feedback. Selected consortium members are meeting roughly each month to discuss the database status, usability, and new features that would be helpful. The following list describes suggested feature improvements:

- The File Upload and File Download forms should have additional filters so as to filter files by owner, organization, material type, date, metadata and file groups.
- The original File Grouping form prototype has proved to be useful. Development will continue and bug fixes completed. Presently the file grouping form does not apply filters.
- Presently, it is only possible to assign work elements by their respective subtask. It should also be possible to link files by work element and select all subtasks for a particular work element.
- Provide the ability to link files and materials.

See Work Planned for Next Quarter for an additional discussion of these items.

Bug Fixes and Performance Enhancements

Last quarter, several changes were made to improve the performance of various pages. As mentioned in last quarter's report, we proposed upgrading the ARC system to IIS version 7.5. This task was completed. Because of internal changes, this upgrade should serve to further improve database performance.

Coinciding with the upgrade to IIS version 7.5, the ARC database was also upgraded to version 4.0 of the .NET Framework from version 3.5. This change should also serve to improve performance slightly due to improvements in the process and threading model. Note that this change was also necessitated by the implementation of the new Silverlight control. This change has no visible impact to end users.

The site map diagram on the home page had incorrect links and a few items were out of date. The site map diagram was revised to include additional icons. Site map links along the bottom of the page were also updated. The updated site map diagram has been uploaded to the production database.

Comments were made by Elie Hajj related to selected tables suggesting records be sorted in a different order. These changes were made, as necessary.

File Management System – File Upload Form

Last quarter, a revised file management system was deployed that allowed users to select multiple files for upload. However, the HTML limitation persisted that required that each file scheduled for upload be selected individually. User feedback indicated that this limitation was not acceptable. One restriction imposed on the ARC system was that ARC users should not be required to download any software to their computer. The FHWA relaxed this restriction allowing us to use a client Silverlight control to upload files. This change allows users to select any number of files simultaneously in a single dialog box, thereby simplifying the upload process. Figure TT1d.1 shows the File Upload control with the new Silverlight user interface.

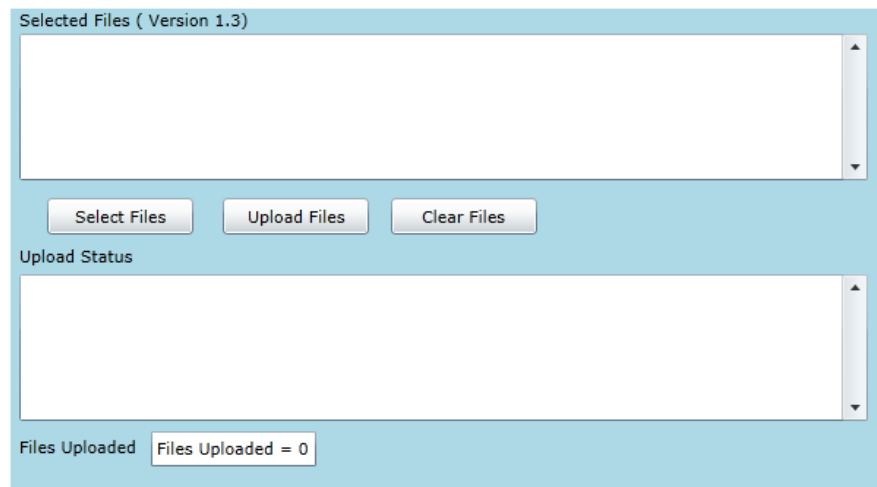


Figure TT1d.1. Silverlight control.

As shown in figure TT1d.1, users first select files for upload. When the Upload Files button is clicked, all selected files are uploaded at once, and any default values (metadata) records are recorded to the database. Status information appears on the lower box. A count of uploaded files is also maintained.

In addition to the Silverlight control, the file upload implementation was modified so that extremely large files could also be uploaded. Other than time, there is no limitation to the size of a file that can be uploaded. The implementation required that a custom HTTP handler be created that works in conjunction with the Silverlight control. The Silverlight control and corresponding HTTP handler work together to upload files in fixed-size chunks. These fixed-size chunks are reassembled on the server to create a completed uploaded file.

File Management System – Manage Keywords Form

A hierarchical keyword list was mentioned last quarter that would be used to replace the arbitrary keyword system that was initially implemented. This hierarchical keyword list has been fully implemented. UNR created an initial list of keywords. This keyword list was sent to consortium members for initial review. The review was completed and the keyword system was

redesigned and implemented. An additional administrative form was created allowing authorized users to create keywords and sub keywords. Figure TT1d.2 shows the Manage Keywords form.

Manage Keywords

MESSAGES

▲ ▼

KEYWORDS

	Keyword ID	Keyword Name
Select Delete	1	Accelerated Testing
Select Delete	2	Additive
Select Delete	3	Aggregate
Select Delete	4	Asphalt Binder
Select Delete	5	Distresses
Select Delete	21	Field Testing Devices
Select Delete	6	LabTest/Material Property
Select Delete	7	Mixture
Select Delete	8	Modeling/Vehicle-Pavement Interaction
Select Delete	13	Other
New		<input style="width: 90%;" type="text"/>
12		

SUB KEYWORDS

	Keyword ID	Sub Keyword	Sub Keyword Name
Delete	1	1	ALF
Delete	1	2	APT
New			<input style="width: 90%;" type="text"/>

Figure TT1d.2. Manage Keywords form.

Help files were implemented for the above form. UNR has added the keywords and sub-keywords to the ARC database. In addition to the above changes and based on our last monthly conference call, the following work items were discussed to further improve the file upload user interface:

- Associate files with material properties when uploading with defaults.
- Enhance the default attribute subsystem so that defaults could be reapplied to previously uploaded files.
- Complete the File (report) grouping prototype form.

We expect the following implementation changes to be completed this quarter. (See Work Planned for Next Quarter.)

File Metadata form

Pursuant to discussions with Eric Weaver (FHWA), it was determined that the ARC system should be able to associate additional descriptive data (metadata) with uploaded files. This metadata includes the following:

- File extension

- File type (binary, word, ANSI standard, bitmap, ...)
- Software used to create the file
- Equipment model used to create specific data files
- Equipment description
- Additional descriptive information about the file or machine
- A structured XML data type (unused at present)

This form has been completed and appears in figure TT1d3. Note – At present, only administrative users can edit file metadata.

File Metadata

MESSAGES

[Help](#)

	Extension	File Type	Software	Equip. Model
Select	*.TIF	Tagged Image File Format		
Select	*.TIFF	Tagged Image File Format		
Select	*.txt	Text/Plain	Notepad	
Select	*.vic	Vicar Picture File	Vic-2D	Vic-2D
Select	*.wp	Corel WordPerfect Document	Corel WordPerfect	
Select	*.wpt	Corel WordPerfect Template	Corel WordPerfect	
Select	*.xls	MS Excel	Microsoft Office Excel	
Select	*.xlsx	MS Excel	Microsoft Office Excel 2007	
Select	*.z2d	Vicar Picture File	Vic-2D 2009	Vic-2D 2009
12345				

SELECTED METADATA TYPE

Field	Value
Metadata ID:	45
File Ext.	*.z2d
File Type	Vicar Picture File
Software	Vic-2D 2009
Description	
Equip. Model	Vic-2D 2009
Equipment Desc.	Digital Image Correlation System
Material	

Figure TT1d.3. File Metadata form.

Public User Interface

Much of this quarter’s work efforts concentrated around the public user interface. The following features and enhancements were made to the public user interface based on the work in progress for the last quarter:

- The prototype public user application form has been completed after feedback from the FHWA about the required fields was gathered. Changes to the form included drop-down boxes for state and country. These values were taken from the LTPP defaults.

Requirements for telephone numbers were removed. A standard disclaimer was added to all login forms and request for account forms.

- An administrative form was created to approve or reject public user requests.
- A form was added to allow users to recover forgotten login and password information based on their e-mail, secret question and answer.

The public user application form is complete. At this point, users have been using the form to request accounts. Figure TT1d.4 shows the finalized public user application form.

The screenshot shows a web form titled "New User Registration" under the "Asphalt Research Consortium" header. The form is divided into two main sections. The top section, labeled "MESSAGES", contains a text input field and a "Help" button. The bottom section, labeled "COMPLETE REQUIRED ACCOUNT INFORMATION", includes a note that "Required fields are denoted with an *". The fields in this section are: "User Name (Login): *", "E-mail address: *", "Password: *", "Confirm Password: *", "Secret Password Question: *", "Secret Password Answer: *", "Title:", "First Name: *", "Last Name: *", "Address:", "City: *", "State / Province: -- None --", "Zip (Post) Code:", "Country: * -- None --", "Affiliation: *", and "Notes:". Each field is represented by a text input box, and the dropdown menus for "State / Province" and "Country" are currently set to "-- None --".

Figure TT1d.4. New User Registration form.

It was decided that public users should not be automatically granted access to the ARC system. Instead, after public users requested an account, they would be put into an approval queue for later activation by a database administrator. The administrative approval form for public users is available for use. Figure TT1d.5 shows the Approve Public Users form.

As shown in Figure TT1d.5, the user name and e-mail address appear. A check box allows the administrator to approve requests one-by-one, or approve all requests. Once a public user has been authorized by the administrator, an e-mail is automatically sent to the user indicating that the account is active.

Approve Public Users

MESSAGES

APPROVE PUBLIC USERS

User Name	First Name	Last Name	E-mail	
joe1234	joe	beets	ekedahl@unr.edu	<input checked="" type="checkbox"/>
bmorge	Bruce	Morgenstern	bruce.morgenstern@wyo.gov	<input type="checkbox"/>
turg1cur	Curt	Turgeon	curt.turgeon@state.mn.us	<input type="checkbox"/>
chuckws	Charles	Schwartz	schwartz@umd.edu	<input type="checkbox"/>
masoori	Mohammad	Masoori	mohammad.masoori@gmail.com	<input type="checkbox"/>
lwangvt	Linbing	Wang	wangl@vt.edu	<input type="checkbox"/>
whao992011	Hao	Wang	whao992011@gmail.com	<input type="checkbox"/>
archiksm	Sun-Myung	Kim	archiksm@neo.tamu.edu	<input type="checkbox"/>
rplye	Roger	Pyle	rplye@pineinst.com	<input type="checkbox"/>
Griffier	Beth	Griffin	Elizabeth.r.griffin@usa.dupont.com	<input type="checkbox"/>

[12](#)

Figure TT1d.5. Approve Public Users form.

As of September 30, 2011, all public users who have requested an account have been activated. Note, an additional feature will be added that allows the administrator to select a user and display all of the user’s application information. This suggested feature provides ease of use as all user information is available on the general user application form.

A final form, which is under development, allows users who forgot their credentials to obtain them by supplying their e-mail and the answer to their secret question. This user interface is made up of two dialog boxes as shown in figure TT1d.7 and TT1d.8. As shown in part 1, the first form requests the user’s email. The e-mail is authenticated and the security question is displayed and an answer requested as shown in part 2.

Figure TT1d.7. Forgot Account form – Part 1.

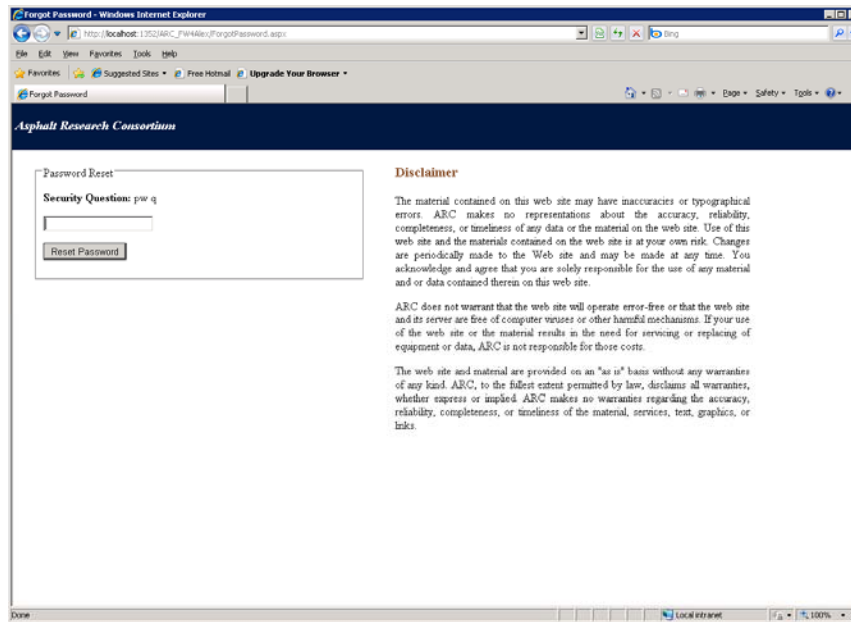


Figure TT1d.8. Forgot Account form – Part 2.

If the security answer is correct, the account password is reset and the user is notified via e-mail.

Public users should not have privileges to write data to the database. Additionally, access to some forms should be restricted. This quarter, Elie Hajj provided a preliminary list of publically accessible forms. Based on this information, the following implementation has been completed:

- Publically accessible forms have been modified so that all user interface elements to add, change, or delete records have been disabled or made invisible to general users.
- The site map structure of the ARC software has been modified to generate two separate site maps. One site map is seen by public users and the other is seen by consortium users. The result is that public users see a limited menu system in which non-applicable forms do not appear.

The File Download form does allow users to select a file or report for download. However, single-file downloads will become impractical when users download many related files. In addition, a file download feature will be most often used by public users. A prototype form has been created to satisfy this need having the following characteristics:

- Users should be able to select files for download using filters similar to those found on the File Upload page and others. This implementation is partially complete and should be finished this quarter.
- Users should be able to download large numbers of files so that the downloaded files are compressed into a single zip file. Users can then unzip the downloaded archive on the client computer. This facility was suggested by Eric weaver. (This implementation is complete.)

- Users should be able to control how the .zip archive is created. (Not completed)

Figure TT1d.9 shows the file download form.

The screenshot shows a web interface for the Asphalt Research Consortium. The main heading is "Download Files and Reports". On the left is a navigation menu with items like "Home Page", "Materials", "Properties", "Measurements", "Validation Sites", "Files / Reports", "Admin Functions", "Users", and "Help". The main content area has a "MESSAGES" section with a "Help" button. Below that is a "SEARCH FILES" section with checkboxes for "Filter By Subtask", "Filter By Folder", and "Filter By Keyword". A "SELECTED FILES" section contains a table with the following data:

ID	File Name	Description	Date Finalized	Internal URL	Download
Select 146	83r107a3.ddx		6/23/2011	/Manitoba/83R107/83r107a3.ddx	<input type="checkbox"/>
Select 147	83R107A3.F20		6/23/2011	/Manitoba/83R107/83R107A3.F20	<input type="checkbox"/>
Select 148	83R107A3.F25		6/23/2011	/Manitoba/83R107/83R107A3.F25	<input type="checkbox"/>
Select 149	83R107A3.mdb		6/23/2011	/Manitoba/83R107/83R107A3.mdb	<input type="checkbox"/>
Select 150	83r108a1.ddx		6/23/2011	/Manitoba/83R108/83r108a1.ddx	<input type="checkbox"/>
Select 151	83R108A1.F20		6/23/2011	/Manitoba/83R108/83R108A1.F20	<input type="checkbox"/>
Select 152	83R108A1.F25		6/23/2011	/Manitoba/83R108/83R108A1.F25	<input type="checkbox"/>
Select 153	83R108A1.GPX		6/23/2011	/Manitoba/83R108/83R108A1.GPX	<input type="checkbox"/>
Select 154	83R108A1.mdb		6/23/2011	/Manitoba/83R108/83R108A1.mdb	<input type="checkbox"/>
Select 155	83R108A1.WPT		6/23/2011	/Manitoba/83R108/83R108A1.WPT	<input type="checkbox"/>

Below the table is a "SELECTED FILE" section with the text "No record selected."

Figure TT1d.9. File Download form.

Help System

Work continues on the Help system as modifications are made to existing forms and new forms are created. During this quarter, all of the data definition forms were modified to reflect changes to the database structure and to include several new database tables.

Significant Problems, Issues and Potential Impact on Progress

None

Work Planned for Next Quarter

- Continue with bug fixes and user-interface enhancement, and database documentation.
- Modify work tasks so that all subtasks can be selected based on a parent work element, work category, or program area.
- Complete an enhanced filtering system for uploaded files so that files and reports can be searched by organization, user, date, material, and other database characteristics.

- Optimize the Upload files form to refresh only on demand and optimize scrolling. Enhance the default attribute subsystem so that defaults could be reapplied to previously uploaded files.
- Complete filtering implementation for the file download form.
- Continue obtaining user feedback on the public user interface and work on improvements to this interface.
- Design and develop a data import subsystem to import UWM data and possibly use this subsystem as a prototype to import other data. (This work item was planned for this quarter but was deferred allowing UWM to complete the data set and restructure the data format so as to increase the compatibility with the ARC system).

In addition, selected ARC members will continue to hold Web meetings roughly every five weeks to monitor status.

Work element TT1e: Development of Research Database (Duration: Year 2 through Year 5) (UNR)

Work Done This Quarter

Uploaded the quarterly technical progress report and the ARC newsletter to the ARC website. Updated the “Publications” and “Outreach” web pages.

Significant Results

None.

Significant Problems, Issues and Potential Impact on Progress

None.

Work Planned Next Quarter

Upload the ARC quarterly technical progress report to the ARC website. Publish the ARC newsletter on the ARC website.

Work Element TT1f: Workshops and Training (UNR lead)

Work Done This Quarter

None

Significant Results

None

Significant Problems, Issues and Potential Impact on Progress

None

Work Planned Next Quarter

None

TABLE OF DECISION POINTS AND DELIVERABLES FOR TECHNOLOGY TRANSFER

Name of Deliverable	Type of Deliverable	Description of Deliverable	Original Delivery Date	Revised Delivery Date	Reason for Changes in Delivery Date
TT1a: Development and Maintenance of Consortium Website (UNR)	Progress report	Upload quarterly progress report and newsletter	07/11	Complete	N/A
	Newsletter	Upload newsletter	07/11	Complete	N/A
	Progress report	Upload quarterly progress report and newsletter	10/11	N/A	N/A
	Newsletter	Upload newsletter	11/11	N/A	N/A
	Progress report	Upload quarterly progress report and newsletter	01/12	N/A	N/A
	Newsletter	Upload newsletter	03/12	N/A	N/A
	Progress report	Upload quarterly progress report and newsletter	04/12	N/A	N/A
TT1b: Communications (UNR)	Newsletter	Publish newsletter	07/11	Complete	N/A
	Newsletter	Publish newsletter	11/11	N/A	N/A
	Newsletter	Publish newsletter	03/12	N/A	N/A
TT1d: Development of Materials Database (UNR and All)	Workshop	Training for “super users” and “sub users” on how to use the materials database and validation section and to evaluate the potential errors, bugs and the ease of use of the database system.	04/11	Complete	N/A
	Database	Materials database software	03/12	N/A	N/A
TT1f: Workshops and Training (UNR and All) (TAMU)	Workshop	Training for “super users” and “sub users” on how to use the materials database and validation section and to evaluate the potential errors, bugs and the ease of use of the database system.	04/11	Complete	N/A
	Workshop	PANDA software training	8/11	4/13	N/A

Technology Transfer Year 5




	Year 5 (4/2011-3/2012)												Team
	4	5	6	7	8	9	10	11	12	1	2	3	
(1) Outreach and Databases													
TT1a: Development and Maintenance of Consortium Website													UNR
TT1b: Communications													UNR
TT1c: Prepare presentations and publications													UNR
TT1d: Development of Materials Database													UNR
TT1d-1: Identify the overall Features of the Web Application													
TT1d-2: Identify Materials Properties to Include in the Materials													
TT1d-3: Define the Structure of the Database													
TT1d-4: Create and Populate the Database													
TT1e: Development of Research Database													UNR
TT1e-1: Identify the Information to Include in the Research Database													
TT1e-2: Define the Structure of the Database													
TT1e-3: Create and Populate the Database													
TT1f: Workshops and Training													UNR

Deliverable codes

D: Draft Report
 F: Final Report
 M&A: Model and algorithm
 SW: Software
 JP: Journal paper
 P: Presentation
 DP: Decision Point

Deliverable Description

Report delivered to FHWA for 3 week review period.
 Final report delivered in compliance with FHWA publication standards
 Mathematical model and sample code
 Executable software, code and user manual
 Paper submitted to conference or journal
 Presentation for symposium, conference or other
 Time to make a decision on two parallel paths as to which is most promising to follow through

 Work planned
 Work completed
 Parallel topic

Technology Transfer

	Year 2 (4/08-3/09)				Year 3 (4/09-3/10)				Year 4 (04/10-03/11)				Year 5 (04/11-03/12)				Team
	Q1	Q2	Q3	Q4	Q1	Q2	Q3	Q4	Q1	Q2	Q3	Q4	Q1	Q2	Q3	Q4	
(1) Outreach and Databases																	
TT1a: Development and Maintenance of Consortium Website																	UNR
TT1b: Communications																	UNR
TT1c: Prepare presentations and publications																	ALL
TT1d: Development of Materials Database																	UNR
TT1d-1: Identify the overall Features of the Web Application																	
TT1d-2: Identify Materials Properties to Include in the Materials Database																	
TT1d-3: Define the Structure of the Database																	
TT1d-4: Create and Populate the Database								SW, v, β	SW								
TT1e: Development of Research Database																	UNR
TT1e-1: Identify the Information to Include in the Research Database																	
TT1e-2: Define the Structure of the Database																	
TT1e-3: Create and Populate the Database																	
TT1f: Workshops and Training																	UNR

Deliverable codes

D: Draft Report
 F: Final Report
 M&A: Model and algorithm
 SW: Software
 JP: Journal paper
 P: Presentation
 DP: Decision Point

Deliverable Description

Report delivered to FHWA for 3 week review period.
 Final report delivered in compliance with FHWA publication standards
 Mathematical model and sample code
 Executable software, code and user manual
 Paper submitted to conference or journal
 Presentation for symposium, conference or other
 Time to make a decision on two parallel paths as to which is most promising to follow through

 Work planned
 Work completed
 Parallel topic